2015

Long Term Blood Oxygenation Membranes

Joseph V. Alexander
University of Kentucky, joseph.v.alexander@uky.edu

STUDENT AGREEMENT:

I represent that my thesis or dissertation and abstract are my original work. Proper attribution has been given to all outside sources. I understand that I am solely responsible for obtaining any needed copyright permissions. I have obtained needed written permission statement(s) from the owner(s) of each third-party copyrighted matter to be included in my work, allowing electronic distribution (if such use is not permitted by the fair use doctrine) which will be submitted to UKnowledge as Additional File.

I hereby grant to The University of Kentucky and its agents the irrevocable, non-exclusive, and royalty-free license to archive and make accessible my work in whole or in part in all forms of media, now or hereafter known. I agree that the document mentioned above may be made available immediately for worldwide access unless an embargo applies.

I retain all other ownership rights to the copyright of my work. I also retain the right to use in future works (such as articles or books) all or part of my work. I understand that I am free to register the copyright to my work.

REVIEW, APPROVAL AND ACCEPTANCE

The document mentioned above has been reviewed and accepted by the student's advisor, on behalf of the advisory committee, and by the Director of Graduate Studies (DGS), on behalf of the program; we verify that this is the final, approved version of the student's thesis including all changes required by the advisory committee. The undersigned agree to abide by the statements above.

Joseph V. Alexander, Student

Dr. Eric A Grulke, Major Professor

Dr. Abhijit Patwardhan, Director of Graduate Studies

LONG TERM BLOOD OXYGENATION MEMBRANES

DISSERTATION

A dissertation submitted in partial fulfillment of the
requirements for the degree of Doctor of Philosophy in the
College of Engineering
at the University of Kentucky

By

Joseph Victor Alexander

Lexington, Kentucky

Co-Directors: Dr. Eric Anderson Grulke, Professor of Chemical and Materials Engineering
and Dr. Joseph Bertram Zwischenberger, Professor of Surgery, Lexington, Kentucky

ABSTRACT OF DISSERTATION

LONG TERM BLOOD OXYGENATION MEMBRANES

Hollow fiber membranes are widely used in blood oxygenators to remove carbon dioxide and add oxygen during cardiopulmonary bypass operations. These devices are now widely used off-label by physicians to perform extracorporeal blood oxygenation for patients with lung failure. Unfortunately, the hollow fiber membranes used in these devices fail prematurely due to blood plasma leakage and gas emboli formation.

This project formed ultrathin (~100nm) polymer coatings on polymer hollow fiber membranes. The coatings were intended to "block" existing pores on the exterior surfaces while permitting high gas fluxes. This coating is synthesized using surface imitated control radical polymerization.

The coating was durable and did not peel or degrade. Fibers modified using this coating technique did not substantially degrade the mechanical properties of the membrane. This coating technique prevented blood plasma leakage and gas emboli formation. The coating permitted blood oxygenation and carbon dioxide removal from in a mock circulation module.

Coating formation on polymeric hollow fiber membranes using surface initiated controlled radical polymerization allows for the formation of membranes that have the potential for long term blood oxygenation. This coating technique would allow these long term blood membranes to be produced more inexpensively than currently existing membranes used for long term use.

KEYWORDS: Hollow Fiber Membrane, Surface Initiated Polymerization, Atom Transfer Radical Polymerization, Long Term Blood Oxygenation, Extra Corporeal Membrane Oxygenation, Polymer Surface Modification

_____Joseph Victor Alexander____
Student's Signature

_____
Date

LONG TERM BLOOD OXYGENATION MEMBRANES

By

Joseph Victor Alexander

_____Dr. Eric A. Grulke
Co-Director of Dissertation

Dr. Joseph B. Zwischenberger
Co-Director of Dissertation

_____Dr. Abijit Patwardhan
Director of Graduate Studies

_____
Date

To the family, friends and mentors that made this possible

ACKNOWLEDGMENTS

The following dissertation, while an individual work, benefited from the insights and direction of several people. First, I would like to acknowledge my gratitude to my Dissertation Co-Chairs, Dr. Eric Grulke, PhD and Dr. Joseph Zwischenberger, MD. Dr. Grulke's ridged requirements for experimental analysis and reporting exemplify high quality scholarship. Dr. Zwischenberger's enthusiasm, energy and openness to new ideas are an inspiration to all. I would like to sincerely thank both of these accomplished gentlemen for the freedom and independence they granted me. It has truly been a privilege to learn from both.

Next, I wish to thank the complete Dissertation Committee, and outside reader, respectively: Dr. David Puleo, Dr. Thomas Dzuibla, Dr. Zhakary Hilt, Dr. Hainsworth Shin and Dr. Thomas Balk Each individual provided insights that guided and challenged my thinking, substantially improving the finished product.

In addition to the technical and instrumental assistance above, I received equally important assistance from family and friends. Outside mentors provided me with the wisdom and knowledge to not only earn my PhD but to develop my learning and scientific abilities to the level at which I could independently devise and employ engineering solutions. My mother, Paula Alexander, instilled in me, from an early age, the desire and skills to obtain the Ph.D.

Table of Contents

LIST OF TABLES

LIST OF FIGURES

CHAPTER 1 INTRODUCTION

Currently, the vast majority of blood oxygenators use hollow fiber membranes. These hollow membranes permit sufficient blood gas diffusion in a small volume due to the large surface area and high permeability of these fibers. The high permeability of hollow fibers is due to the porous walls that comprise the membrane. This porosity allows oxygen traveling through the lumen of the fiber to come in direct contact with blood surrounding the fiber at the surface of the pores.

Although the open, porous network permits very high blood gas permeability of the hollow fiber wall, it is responsible for problems that limit the time that current membrane oxygenators may be used. These include blood plasma leakage and gaseous emboli formation.

Upon contact with blood, equilibrium is established between the forces of the surface tension and pressures acting on the blood. This equilibrium results in the formation of an interface between the blood plasma and sweep gas across the opening of the membrane's pore. This interface allows the superior gas exchange encountered in hollow fiber oxygenators. However, phospholipids in the blood act as a surfactant and disrupt the surface tension equilibrium. [1]The hydrophobic portion of these molecules adhere to the wall of the micropore, leaving the hydrophilic portion oriented toward the middle of the pore. This action allows the plasma/sweep gas interface to advance in the direction of the center of the fiber. The interface between blood plasma and sweep gas then moves through the length of the pore until it reaches the inner surface of the fiber. At this point the lung is "wetted out" and is no longer capable of exchanging sufficient amounts of blood gasses with the blood flow on the outer surface of the fiber due to impaired diffusion through liquid filled micropores.

Gaseous emboli formation occurs when the pressure difference between blood on the outer surface of the fiber and sweep gas on the inner surface is sufficient enough to change the force equilibrium at the blood plasma/sweep gas interface. If the interface is driven to the outside of the fiber by sufficiently high sweep gas pressures or low pressures on the blood side of the membrane, emboli may be formed. These bubbles, if transported into the body have the potential to cause serious harm by forming an embolism. Disruptions of blood flow into the oxygenator, resulting in low pressures on the outside of the fiber, are the most common cause of this dangerous condition.

The introduction of polymethylpentene hollow fiber membranes has greatly reduced the problem of blood plasma leakage. Oxygenators incorporating these fibers are now used off-label for extended periods of time in human patients. However, there remains some danger of plasma leakage and these devices are capable of producing blood gas emboli if not carefully monitored. As a result, patients connected to polymethylpentene based oxygenators must be carefully monitored in an ICU setting.

In addition to wetting and emboli formation, thrombus formation limits the use and longevity of current hollow fiber oxygenators. Upon contact with foreign surfaces, components of the blood coagulation systems are activated and a powerful signaling cascade is initiated, ultimately leading to thrombus formation. Although systemic anticoagulants are administered during the use of any blood oxygenation device, clot formation within the oxygenator remains an issue that may cause failure.

In order for an artificial lung to become a reality, oxygenators capable of extended use, safely, must be developed. These devices must be immune to blood plasma leakage, blood gas emboli

formation and resistant to the initiation of blood coagulation. With medical costs a center of national focus, long term oxygenators must be as inexpensive as possible - particularly if they are to be exchanged at regular intervals.

The development of long term blood oxygenators, safe enough to attain regulatory approval for this purpose, would provide clinicians a potent treatment option for patients with acute and end-stage pulmonary disease. An oxygenator impervious to blood plasma leakage, gas emboli formation, as non-thrombogenic and non-blood activating as possible may allow many patients with lung failure to exercise, or possibly leave the hospital for extended periods.

Our team has investigated and developed a technique to form hollow fiber membrane modules with the potential for long term use at the University of Kentucky. This technique involves forming ultrathin (~100 nm) coatings on the exterior surface of polymeric hollow fiber membranes contained within membrane modules. These coatings are formed using surface initiated atom transfer radical polymerization. (s-ATRP)

Chapter 2 provides a description of the current state of blood oxygenator development. The current situation regarding treatments and outcomes for end stage and acute lung failure are described. Side effects, outcomes and current clinical practice regarding long term blood oxygenation are reviewed. Also presented is the current state of membrane science regarding polymeric membranes and the use of surface initiated atom transfer radical polymerization.

Chapter 3 describes the mechanical strength of hollow fiber membranes after functionalization. Chapter 4 measures the amount of contamination on polymer hollow fiber membranes. In chapter 5 the pathway of functionalizing and forming s-ATRP formed layers using only aqueous solvents. Chapter 6 s-ATRP is used to form composite hollow fiber membrane within a membrane module. Chapter 7 describes the algorithm that was developed to determine the yield point of tensile testing data. This body of work is summarized in chapter 8. Appendix A contains the MATLAB program that was used to determine the mechanical properties of the hollow fiber membranes from tensile testing data.

CHAPTER 2 BACKGROUND

2.1 Introduction

Currently, the vast majority of devices used for blood oxygenation use hollow fiber membranes. These hollow membranes permit sufficient blood gas diffusion in a small volume due to the large surface area and high permeability of these fibers. The high permeability of hollow fibers is due to the porous walls that comprise the membrane. This porosity allows oxygen traveling through the lumen of the fiber to come in direct contact with blood surrounding the fiber at the surface of the pores.

Although the open, porous network permits very high blood gas permeability of the hollow fiber wall, it is responsible for problems that limit the time that current membrane oxygenators may be used. These include blood plasma leakage and gaseous emboli formation.

Upon contact with blood, equilibrium is established between the forces of the surface tension and pressures acting on the blood. This equilibrium results in the formation of an interface between the blood plasma and sweep gas across the opening of the membrane's pore. This interface allows the superior gas exchange encountered in hollow fiber oxygenators. However, phospholipids in the blood act as a surfactant and disrupt the surface tension equilibrium. [1]The hydrophobic portion of these molecules adhere to the wall of the micropore, leaving the hydrophilic portion oriented toward the middle of the pore. This action allows the plasma/sweep gas interface to advance in the direction of the center of the fiber. The interface between blood plasma and sweep gas then moves through the length of the pore until it reaches the inner surface of the fiber. At this point the lung is "wetted out" and is no longer capable of exchanging sufficient amounts of blood gasses with the blood flow on the outer surface of the fiber due to impaired diffusion through liquid filled micropores.

Gaseous emboli formation occurs when the pressure difference between blood on the outer surface of the fiber and sweep gas on the inner surface is sufficient enough to change the force equilibrium at the blood plasma/sweep gas interface. If the interface is driven to the outside of the fiber by sufficiently high sweep gas pressures or low pressures on the blood side of the membrane, emboli may be formed. These bubbles, if transported into the body have the potential to cause serious harm by forming an embolism. Disruptions of blood flow into the oxygenator, resulting in low pressures on the outside of the fiber, are the most common cause of this dangerous condition.

In addition to wetting and emboli formation, thrombus formation limits the use and longevity of current hollow fiber oxygenators. Upon contact with foreign surfaces, components of the blood coagulation systems are activated and a powerful signaling cascade is initiated, ultimately leading to thrombus formation. Although systemic anticoagulants are administered during the use of any blood oxygenation device, clot formation within the oxygenator remains an issue that may cause failure.

Various attempts have been undertaken to create hollow fiber membranes capable of long term blood oxygenation. These approaches involve coatings applied to existing, porous membranes and the production of non-porous membranes. Although substantial progress has been made recently, no hollow fiber membrane based blood oxygenator is approved for long term use by the United States Food and Drug Administration.

Each of the approaches and techniques of developing long term blood oxygenation membranes has advantages and drawbacks. A disadvantage of each coating technique previously explored is the

reliance on a very specific chemistry to form the coating. The reaction of human blood to foreign surfaces is very complex, for a composite long term blood oxygenation membrane to be viable the surface chemistry of this fiber must be as non-activating as possible.

Another drawback involves the lack of strong chemical bonds anchoring the coating to the exterior surface of the fiber. A common failure mechanism of medical coatings is delamination and undesired degradation and leaching, all of which are unacceptable during long term blood oxygenation.

In section 2.2 the development of blood oxygenators is reviewed until the present. Section 2.3 describes the current and expanding use of extra corporeal membrane oxygenation (ECMO). Section 2.4 reviews the current state of lung transplantation. Section 2.5 reviews acute respiratory distress syndrome (ARDS), particularly current treatments involving ECMO. Section 2.6 describes the current state of long term respiratory support using blood oxygenators in off-label uses. Section 2.7 reviews muscular atrophy occurring as a result of prolonged bed rest. Reviewed in this section is the effect of diaphragm atrophy during prolonged ECMO use. Section 2.8 describes advances in the development of artificial lungs, particularly fully implantable devices and long term oxygenator designs not incorporating hollow fiber membranes. In section 2.9 surface initiated atom transfer radical polymerization is discussed and reviewed. Following this, in section 2.10, membrane modification using s-ATRP is discussed.

2.2 Blood Oxygenator Development

Successful blood oxygenator began in 1953 when Gibbons performed the first cardiopulmonary bypass surgery.[2] This device used a rotating screen to produce a thin film of blood that is contacted with oxygen to facilitate gas exchange. These devices were large, bulky and required a large priming volume. As a result, they were difficult to sterilize.[3]

Rotating screen type oxygenators were quickly replaced by the end of the 1950's by rotating disk oxygenators. This device was prone to hemolysis and the production of blood foam.[4] Like the rotating screen device, it oxygenated blood by exposing it to an oxygen atmosphere. This action is known to causes extensive activation of the thrombogenic and contact immune activation processes within the blood.

This phenomenon was decreased significantly with the introduction of bubble oxygenators in the late 1950's.[3] These devices introduced small bubbles of oxygen into the blood as it flowed through the oxygenator. After oxygenation, the blood then passed into a defoaming chamber in which silicone lined surfaces caused the small gas bubble to coalesce into larger bubbles.[5] These oxygenators dominated the cardiopulmonary bypass market between 1960 and 1980. They were used in approximately 90% of open heart surgeries worldwide in 1976.[3]

In 1963 Kolobow introduced the first oxygenator in which a patient's blood did not directly contact the air. His device used a spirally wound silicone rubber membrane. Blood gasses were then exchanged across this membrane. This oxygenator was the first to be used for the treatment of acute respiratory distress syndrome.[6] (ARDS) This device was used for the first neonatal ECMO case in 1975.[7]

The first hollow fiber membrane oxygenator was introduced in 1972 by the Terumo Corporation. It quickly achieved 60% of the oxygenator market share.[3] Oxygenators of this type use porous, polymeric hollow fibers to exchange blood gasses. Due to their simplicity of use and disposability, they remain the

standard oxygenator for cardiopulmonary bypass to the present. A major shortcoming of oxygenators incorporating microporous hollow fiber membranes is the tendency to leak blood plasma. Various coatings and solid hollow fibers have been explored to allow hollow fiber membrane oxygenators to be used for extended periods.

One of the most successful advances in long term blood oxygenation membranes was the introduction of hollow fibers spun using poly-1-methyl pentene.[8] These fibers are much less porous than the previously used polypropylene. As a result, oxygenators incorporating polymethylpentene fibers have been used to provide extracorporeal blood oxygenation for periods beyond 60 days.[9] Although a vast improvement, oxygenators utilizing polymethylpentene hollow fibers are not FDA approved for periods longer than 4-6 hours. These fibers do contain areas of exposed porosity, allowing limited blood plasma leakage and gas emboli formation. As a result, patients attached to these devices during ECMO procedures must be carefully and constantly monitored in an ICU setting.

2.3 Lung Transplantation – Targets for Long Term Blood Oxygenator

In 2010 the number of lung transplants worldwide was 3,200 with approximately 1,200 of these performed in the USA. Of these transplants, at any given time 1,700 patients are on lung transplant waiting lists. Of these waitlist patients, 14% will expire before a suitable transplant becomes available.[10]

The prognosis for patients with end stage lung failure fortunate enough to qualify for lung transplantation is not promising. Only some 80% of lung transplant patients survive one year after transplantation. After 5 years post-transplant, the survival rate is 50%.[10]

2.3.1 Research Challenges

The introduction of a blood oxygenator capable of safe, long term use would allow patients with end stage lung failure to maintain or increase their overall fitness levels before the transplant operation. Most end-stage lung failure patients are unable to move significantly or exercise. As a result, their muscle tone degrades rapidly. Some studies have shown significant loss of muscle tone after one week of sedation. This weakness may last up to two years after discharge.[11]

Many physicians are now requiring critically ill patients on ventilation to undergo modest physical exertion, particularly walking.[12] The development of a blood oxygenator safe enough for reliable long term use would allow ECMO and end-stage lung failure patients to maintain a much higher level of muscle fitness during extracorporeal blood oxygenation and would significantly increase outcomes after discharge.

2.5 Atom Transfer Radical Polymerization

Atom transfer radical polymerization is a form of controlled radical polymerization in which the rate of polymerization is controlled through the concentration ratio of a transition metal redox pair that are chelated within an appropriate ligand molecule. The lower oxidation state transition metal is capable of removing certain halogen atoms from a carbon-halogen bond, leaving a free radical. This free radical is then capable of polymerizing double bond containing monomers, particularly those with a resonance stabilized olefin group. The higher level oxidation state transition metal ion acts as a deactivator and may place a halogen on an exposed free radical. [13]

This activation/deactivation process allows for careful control of the rate and extent of polymerization. Through this process, the reaction process may be stopped and started at will.

Both of these transition metals are chelated within an appropriate ligand. The ligand contains multiple functional groups with available lone pairs of electrons. These lone pairs are able to complex the transition metal ions within the ligand molecule.

ATRP is a particularly attractive technique of controlled radical polymerization as unlike alternate methods, it can be performed at room temperature in aqueous conditions, with a variety of monomers and solvents.

Recent advances in the use of ATRP form polymers has produced systems in which the transition metal catalyst concentration has been dramatically reduced. This reduces or mitigates the need for removal of these transition metal catalysts post polymerization.[14]

Additional improvements include the development of ATRP techniques that may be performed with regeneration of the catalyst. As a result, ATRP reactions may be performed without the extensive oxygen removal previously necessary.[15]

Further developments now allow ATRP be initiated and controlled via light and electrically.[16]

2.5.1 Research Challenges

Limitations and potential research targets concerning the ATRP reaction particularly concern the development of ligands capable of chelating transition metal catalysts at low ph. Ligands used in ATRP reactions contain multiple lone pairs necessary to chelate transition metals. At low pH conditions these lone pairs become protonated and can no longer chelate transition metal. This condition sets a limit on the acidity in which an ATRP reaction may be performed.[15]

Similarly, the polymerization of charged or electrically active monomers is a challenge.[17] This is due to the oxidation or reduction of redox pair. If the ratio of the lower oxidation state transition metal ions to the higher oxidation state ions is increased substantially, the polymerization will not be controlled but more free radical in nature. If this ratio is decreased low initiation will substantially slow or stop the polymerization process.

2.6 Surface Initiated Atom Transfer Radical Polymerization

ATRP has been performed using surface bound halogen atoms as initiators to form polymer films. Due to the wide variety of monomers and solvents that may be used, as well as the controllability of the reaction, s-ATRP is an attractive method of forming polymer thin films. S-ATRP allows for much higher chain density per unit area of surface compare to other grafting techniques.[18] This is due to very low termination and efficient initiation.

The persistent radial effect must be taken into account when performing s-ATRP reactions. This phenomenon occurs when two neighboring free radicals from a bond via disproportionation. As a result, the heads of propagating chains are linked by a carbon bond, preventing further polymerization. Without control of the persistent radical effect, high rates of termination will limit the maximum thickness that may be obtained.[19, 20]

The kinetics of S-ATRP is an area of active investigation. To minimize the amount of termination and increase the thickness of the polymer film the number of actively growing chains must be minimized. This is accomplished through the use of a higher amount of deactivator complexes and a lower concentration of transition metal catalysts.[21]

2.6.1 Research Challenges

Current research challenges concerning the formation of polymer films via s-ATRP involve increasing the thickness of the completed film. This is accomplished by minimizing termination of the growing polymer chains.

The other main obstacle to the wide scale adoption of s-ATRP to form polymer coatings involves the surface bound initiator necessary for coating growth. The usual initiator molecule contains secondary or tertiary halogen. Bromoisobutrylbromide and other air and water sensitive reagents are widely used for this purpose. The employment of aqueous reagents for this purpose would allow for inexpensive and straightforward attachment of halogens to surfaces to be functionalized from s-ATRP

2.7 Membrane Modifications with s-ATRP

Development of coated and modified porous membranes by ATRP has been investigated by a few researchers. ATRP coatings on ceramic membranes, particularly alumina have been fabricated. They have shown that very thin (<50nm) coatings can be synthesized by ATRP and that complete occlusion of the pores is possible.[22] These researchers also confirmed that these ATRP synthesized coatings are permeable to oxygen and carbon dioxide.[22]

Porous membranes have been modified using s-ATRP to produce non-fouling or anti-bacterial surfaces.[23] Investigators have demonstrated that gas selective and gas permeable polymer coatings may be deposited on the surface of porous structures using s-ATRP.[22]

2.7.1 Research Challenges

The route previous investigators functionalized porous structures or formed composite membranes using polymer layers via s-ATRP is not amenable to scale up and industrial production. These approaches typically involved the use of ozone gas in the functionalization process. Ozone does not uniformly functionalize the polymer surfaces and quickly degrades the underlying hollow fiber. Additionally, the halogenation emplacement procedure typically involved the use of an air and water sensitive acyl halide such as bromoisobutryl bromide. Finally, the s-ATRP reaction itself used organic solvents such as tetrahydrofuran. These solvents will dissolve the plastic components of most membrane modules, preventing deposition of the polymer coating within the module.

The purpose of this work is to develop a reaction sequence and approach that will allow composite hollow fiber membranes to be formed within membrane modules using s-ATRP.

CHAPTER 3 MECHANICAL STRENGTH OF HOLLOW FIBER MEMBRANES AFTER SURFACE FUNCTIONALIZATION

This chapter is based on work published as: Joseph V. Alexander, James W. Neely, Nathan McKee, Eric A. Grulke, Journal of Polymer Science: Polymer Physics.

Keywords: Tensile Test, Burst Strength, Ozone, Persulfate, Polypropylene Hollow Fiber Membranes

3.0 Abstract

Chemical treatment of polymeric hollow fiber membranes is used to prepare their exterior surfaces for coatings. Typical treatments can cleave both C-C and C-H bonds of polypropylene, leading to lower mechanical strength of the fibers. This study evaluated the yield strength, maximum strain, ultimate tensile strength, and burst strength of hollow fiber membranes treated with each of three common oxidizing reagents: ozone as a gas phase system, aqueous solutions of potassium persulfate, and ammonium persulfate for liquid phase systems. The yield strength and ultimate tensile strength of hollow fiber membranes decreased continuously with increasing ozonation time. Batch treatments with aqueous oxidizing systems showed limiting values of the yield and ultimate tensile strengths with time. Swelling the hollow fibers with methanol prior to oxidation caused less reduction of the mechanical properties after persulfate treatment. Fibers pretreated with methanol showed lower losses of mechanical properties strength with aqueous oxidation systems.

3.1 Highlights

- Persulfate treatments allow for hydroxylation of the surface of PP HFMs with minimal degradation of mechanical properties.
- Ozone treatments rapidly decrease the mechanical strength of PP HFMs.
- Neither ozone or persulfate treatments affect the gas transport properties of HFMs in a significant manner
- Pretreatment of PP HFMs with methanol immersion to allow water to impregnate the pores decreases the degradation of mechanical properties during persulfate treatments.
- Extended fiber treatments with persulfate do not decrease the burst strength of the fibers to a value of less than 160 psig.

3.2 Introduction

Polymeric hollow fiber membranes (HFMs) are currently widely used in a variety of applications including blood oxygenation, hemodialysis, industrial fluid filtration, gas separation, and bioreactors. In each of these applications, the physio-chemical properties of the membrane surface are critical to its performance. However, common hollow fiber membrane materials, such as polypropylene and poly(1-methyl pentene), may not have optimal surface properties for all possible applications. Therefore, hollow fiber membranes surfaces are often modified to change the hydrophillicity, to alter the surface electrical properties or to deposit a coating.[24, 25] The first step in a modification process often is the generation of surface groups on the surface of the polymer. Common reagents include ozone[23, 26, 27], ammonium persulfate[28], potassium persulfate[29, 30]. These oxidizing agents can cleave both carbon-carbon and carbon-hydrogen bonds, leading to lower mechanical strength of the polymeric material.

Aqueous potassium persulfate has shown to be an effective method of hydroxylating polypropylene hollow fiber membranes.[31] The decomposition of potassium persulfate, first elucidated by Bartlett et.al.[32] is strictly first order and is not influenced by the presence of other radicals. Potassium persulfate decomposes into two sulfate radicals that are capable of reacting with water, forming hydroxyl radicals. Hydroxyl radicals are highly reactive and are capable of abstracting hydrogen atoms bonded to carbon, leaving a carbon radical. A hydroxyl group is then formed at this carbon radical by an interaction between an additional hydroxyl radical or sulfate radical – which is subsequently hydrolyzed by water to form the final hydroxyl group.[31] The hydrogen abstraction reaction is much faster than the reaction between the sulfate radical and water. It is also independent of ph.[30]

Reactions between the persulfate ion and the carbon backbone of the polypropylene inevitably cause scissions of the polymer chain.[31] As a result, the mechanical strength of the polypropylene hollow fiber membrane will be decreased. This can negatively impact the membrane's performance, setting limits on the operation conditions in the application.[30, 33] For example, membrane-based gas separation operations are more efficient when performed at the highest pressure economically possible. Increasing the inlet pressure of the feed stream generally increases the gas flux per unit area. The selectivity ratio cannot exceed the pressure ratio for these applications.[34]

Ozone has been extensively reported in the literature for the modification of polypropylene hollow fiber membranes and to prepare them for surface modification.[23, 26, 27, 35] This reaction involves hydrogen abstraction from a tertiary carbon. A radical is then left on this carbon which reacts with another ozone molecule, forming a peroxide. Further reaction of the peroxide with the polymer backbone leads to chain scission, followed by formation of carbonyl, carboxylic acid or hydroxyl groups.

Although gaseous ozone is able to penetrate into porosity within the wall of the hollow fiber membrane, aqueous potassium persulfate or ammonium persulfate may not be able to do so. These aqueous solutions form an interface at the pores on the exterior surfaces of the hollow fibers. Surface tension can prevent these aqueous solutions from entering into the wall pores. As a result, without pretreatment, hollow fiber membranes may not be functionalized on the interior surface within the walls of these fibers. The hydroxyl groups or carboxylic acid groups will be confined to the exterior surfaces.

Due to its lower surface tension, methanol will penetrate into the porosity within the walls of hollow fibers after immersion. The surface tension of methanol in air is 22.5 mN/m, approximately 1/3 that of water (surface tension of 72.9 mN/m). Subsequent immersion of the fibers into water will replace the methanol. Afterward, exposure to reactive aqueous solutions will allow these reagents to penetrate into the porosity of the membrane.

The mechanical integrity of the membranes affects blood oxygenation and hemodialysis applications. For a membrane-based long term artificial lung to be possible, hollow fibers will need to be capable of withstanding cyclic loading for a month or more.

There have been few reports on the effects of chemical treatments on the mechanical properties of HFMs. Mechanical properties with relevance for membrane applications include yield strength, ultimate tensile strength, maximum strain, and burst strength. Physic-chemical properties that relate to membrane performance include crystallinity and permeability. This study evaluated the effects of common oxidizing agents; ozone, potassium persulfate or ammonium persulfate, on the mechanical properties of HFMs was evaluated. These data provide a basis for the development of chemical functionalization processes for hollow fiber membranes.

3.3 Experimental

3.3.1 Materials

Polypropylene x30-240 hollow fiber membranes and Oxyplus™ polymethylpentene (PMP) fibers were purchased from Celgard, U.S.A. Reagent grade ammonium persulfate (APS) (lot# MKBK5725V, 98%) was purchased from Sigma-Aldrich, U.K. Reagent grade potassium persulfate (KPS) (lot# BCBH2552V, ≥99.0%) was purchased from Sigma-Aldrich, U.K. Ultra high purity grade argon was purchased from Scott-Gross Co., Inc., U.S.A. Ozone was produced from an A2Z Ozone generator (model# A2ZS-6G). Deionized ultra-filtered (DIUF) water was used during the APS and KPS functionalization trials. Reagent grade methanol was purchased from Fischer Scientific. These reagents were used as delivered without further purification.

3.3.2 Hollow Fiber Preparation

3.3.2.1 Fiber Cleaning

The polypropylene hollow fiber membranes were thoroughly cleaned before use in order to remove contaminants remaining from manufacture of the fiber. The polypropylene fibers were placed in a Soxhlet extraction apparatus using acetone and refluxed for 24 hours. Once clean, the fibers were placed under vacuum for 24 hours to remove residual acetone.

3.3.2.2 Wetting of Fibers with Solvent

To determine the effect of functionalization within the porous walls of the HFMs, a portion of the membranes was immersed in methanol for at least one hour before subsequent exposure to potassium peroxydisulfate or ammonium peroxydisulfate. After immersion in methanol, the fibers were immediately immersed in argon purged water for one hour. They were then removed and immersed in an additional bath of deionized water before exposure to ammonium peroxydisulfate or potassium peroxydisulfate.

3.3.3 Fiber Oxidation

3.3.3.1 Potassium Persulfate

400 mL of deionized (DI) ultrapure water was sparged with argon for one hour to rid the water of oxygen. The water was then placed in a 500 mL reaction flask with an attached condenser and the sample of HFM was added. The reaction flask was sealed with a rubber stopper and heated to 80oC. The water was continually sparged throughout the heating process. Once the water reached the desired temperature, 10 weight/volume % of potassium persulfate (3.7x10-4 M) was added to the water without introducing oxygen by using a syringe. [33] The solid potassium persulfate was placed into a syringe and the plunger was then replaced and a 6 inch needle added. This needle was then used to pierce the rubber septum on the reaction flask containing the fiber bundle immersed in boiling water. The plunger was then withdrawn, pulling boiling water into the syringe without exposure to oxygen. After the persulfate was dissolved, the plunger was used to pump the persulfate solution into the reaction flask. The KPS solution and boiling water were continually kept under argon during the procedure.

At the predetermined time, the fibers were removed from the potassium peroxydisulfate solution, rinsed with DI water, and set aside. Samples were taken for reaction times ranging from one to 180 minutes.

This procedure was repeated using the fibers impregnated with wate0r as described in the previous section.

3.3.3.2 Ammonium Persulfate

400 mL of deionized ultrapure water was sparged with argon for one hour to rid the water of oxygen. The water was then placed in a 500 mL reaction flask with an attached condenser. The reaction flask was sealed with a rubber stopper and heated to 80^{o}C. The water was continually sparged with argon throughout the heating process. Once the water reached the desired temperature, 10 weight/volume % of ammonium persulfate (4.38x10-4 M) was added to the water. Once thoroughly mixed, the HFM sample was added to the reaction flask and immersed for a predetermined amount of time. The ammonium persulfate solution was continually kept under argon during the procedure.

3.3.3.3 Ozone

Another series of fibers were treated using ozone. After undergoing the same cleaning and preparation procedures, the fibers were placed in a dry 500 mL reaction vessel. The vessel was sealed and ozone (6 g/h) was pumped through the reaction vessel at 3 L/min. This trial was repeated and samples were taken for ozone exposure times ranging from one minute to 180 minutes.

3.3.4 Mechanical Testing

3.3.4.1 Yield Strength, Ultimate Tensile Strength and Maximum Strain

Tensile strength and elongation at break of the hollow fibers were measured by an Instron 4442 tensile test machine with a load cell of 50 kN at a constant elongation velocity of 2.5 mm/min. The initial distance between the clamps was 25 mm. The clamp attachments used to grip the fibers were Instron CAT# 2710-004 with a maximum load of ±500 N. The Instron tensile test machine worked in collaboration with the Instron computer software program (Instron Series IX Version 7.50.00 / Merlin Version 3.3) running on Microsoft Windows 95 operating system. For each tensile test, a single fiber was clamped into position using the aforementioned Instron clamps and sandpaper for extra grip. Each trial stretched the given fiber through inelastic deformation and proceeded until fracture. For each sample, ten fibers were removed from the woven matt and tested.

3.3.4.2 Analysis of Tensile Testing Data

To determine the yield point in a repeatable manner, an algorithm was developed that defined the yield point as the point of inflection occurring at the linear region's end. This point is known as the proportional limit. At this point in the stress-strain data, the fiber's deformation is no longer elastic and becomes plastic.

The inflection point was determined by calculating the cumulative moving average of Ei' (modulus prime) at each point, starting at the initiation of the linear region of deformation. The modulus prime is equal to the force at each point divided by the corresponding elongation. The difference between the cumulative moving average of the modulus prime (how many points included in the moving average) and the value of the modulus prime at each point was then determined. The point of elongation at which the difference between the cumulative moving average of the modulus prime and the value of the modulus prime reached a minimum was determined to be the yield point.

$$E_i' = \frac{F_i}{L_i} \quad \text{Eq. 3.1}$$

$$CA_i = \frac{\sum_1^i E_i'}{i} \quad \text{Eq. 3.2}$$

$$i_{yield} \cong min\{(CA_i - E_i')^2\} \quad \text{Eq. 3.3}$$

i – index of point in series

E_i' – Modulus Prime at point i

F_i – Force at point i

L_i – Elongation of fiber at point i

CA_i – Cumulative average of E_i' at point i

i_{yield} – Index of point where yielding point occurs

Calculations were performed without regard to cross sectional surface area due to the non-uniform porosity within hollow fiber membranes. For this reason a force/elongation parameter – modulus prime, was used to calculate membrane mechanical characteristics.

In order to eliminate the errors from clamp slippage, the first 50 points were discarded from analysis.

This approach produces a yield point that is conservative compared to other methods, notably the 0.2% offset approach.[29]

To efficiently determine the yield points of the hollow fiber membrane a MATLAB program was created incorporating the previously described algorithm. This also determined the strain at break and ultimate tensile force.

The ultimate tensile strength was determined as the maximum load on the fibers. Maximum elongation was determined as the largest extension occurring on the fiber before break.

3.4.3 Burst Strength

To determine the maximum bore pressure that may be applied to a hollow fiber membrane sample, a custom built apparatus was constructed as shown in Figure 3.2.

HFM samples were embedded in a castable polyurethane resin. After this resin had hardened the samples were placed in the membrane testing apparatus and gas pressure was applied through the port on the top of the chamber, thus applying the pressure to the bore of the membrane. The port at the bottom of the chamber, which collected gas diffusing across the membrane, was connected to an electronic mass flow controller (MKS 1179A12CS1BV). This mass flow controller measured the gas flow rate. The maximum pressure used was 160 psig.

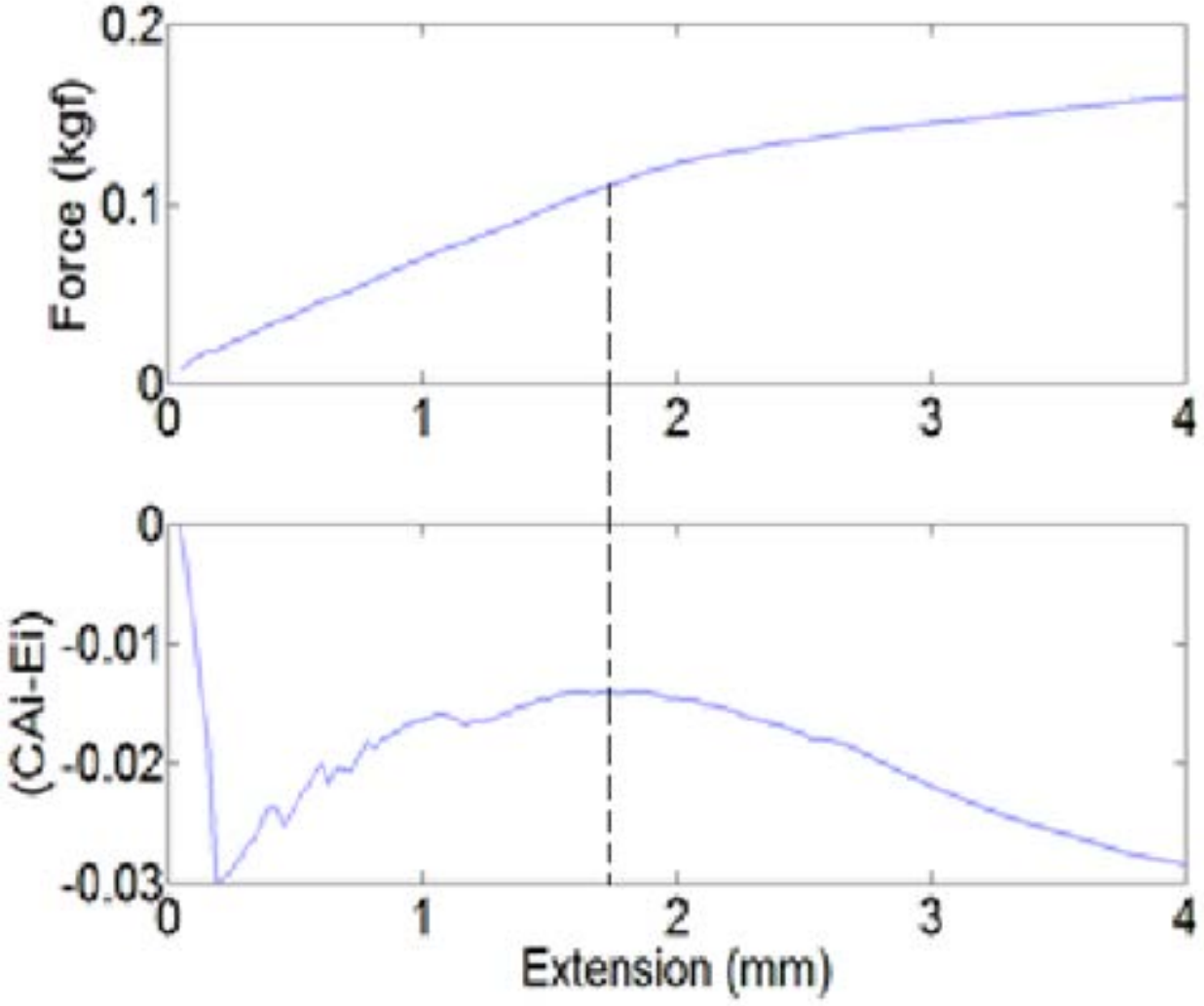

Figure 3.1; (top) Force vs extension of polypropylene HFM. (bottom) Difference between cumulative average of modulus and modulus.

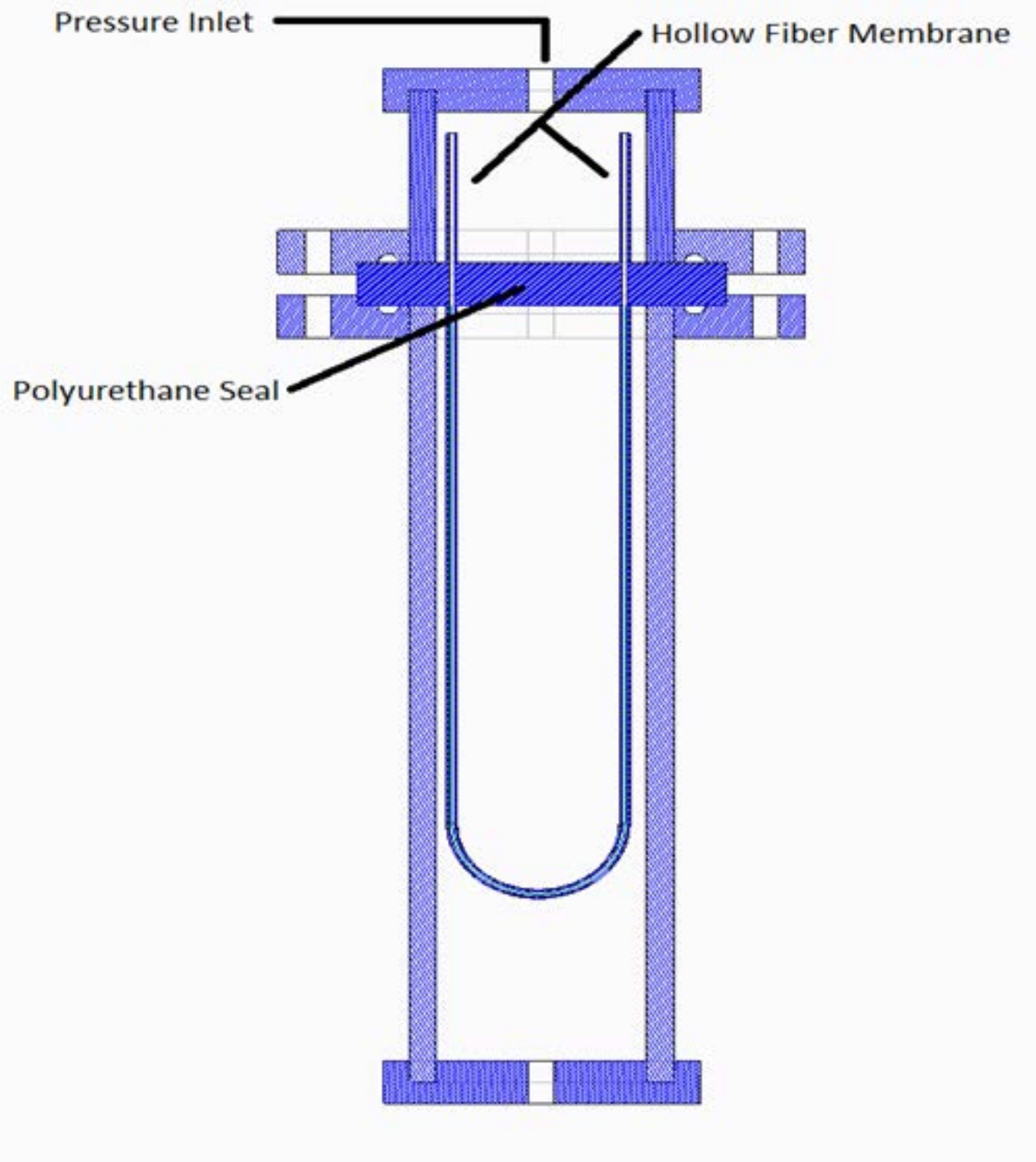

Figure 3.2; Half sectional drawing of membrane testing apparatus.

3.3.5 Physio-Chemical Properties

3.3.5.1 X-Ray Diffraction

To determine the effects of exposure to the functionalization agents on the crystalline structure of the polypropylene HFMs, X-Ray diffraction patterns of the treated PP HFMs was compared to those of the virgin material. A Siemens Diffraktometer™ using copper Kα radiation was used for this analysis.

Before analysis, the bundle of the fiber to be analyzed was placed upon a slide made from amorphous glass. The X-Ray diffraction machine measured and stored the amplitude of the diffracted peaks with respect to the diffraction angle. Diffraction peaks between 5 and 30 degrees were determined. Refracted X-ray intensities were measured every 0.01 degree.

3.3.5.2 *Permeability*

Membrane permeability was tested in the membrane testing apparatus (Fig. 6.2). After securely sealing in the testing vessel, gas pressure was applied and then increased at intervals of 10psi. At each point, the gas flux through the fibers was measured. The pressure was held steady for at least one minute at each step to ensure the gas flow rate had stabilized.

The flow rate was then plotted against the inlet pressure for each sample. These data were then fitted with a linear best fit line. This best fit line's slope was the averaged ratio of flow rate with pressure across all data points within a sample. The permeability was then determined by normalizing the slope of the best fit line with the surface area of each sample. The permeability of each membrane sample was determined by equation 3.4.

Equation 3.4; $Permeability = \frac{\dot{Q}}{t*SA*P}$

where $\dot{Q} - Gas\ Flux$ (ml),

$t - Time\ (seconds)$,

$SA - Surface\ Area\ (nm^2)$,

$P - Pressure\ (cmHg)$

3.3.5.3 Statistical Analysis

The influence of pretreatment on the mechanical properties was determined by comparison using the one way ANOVA. This one-way ANOVA was performed using SigmaPlot™. Significance was determined between two data points using at least five measurements at each point.

ANOVA was used to determine the impact of impact of pre-impregnation with methanol of PP HFM on subsequent surface treatments with ammonium persulfate or potassium persulfate. Independent data sets - HFMs pre-wetted using the methanol immersion method and dry, virgin HFMs were compared. Both sets were treated under the same reaction conditions before measurement.

ANOVA was used as well to determine the repeatability of persulfate treatments. Data sets were then compared between fiber samples treated for the same periods at different times.

3.4 Results and Discussion

3.4.1 Tensile Testing of PP HFM Exposed to Aqueous Potassium Persulfate

Figures 3.3 through 3.5 show the yield stress, the ultimate tensile stress, and the maximum strain for polypropylene HFMs treated with potassium persulfate. The yield force, tensile force and maximum strain were higher for samples immersed in methanol prior to exposure to the potassium persulfate. These differences were larger at longer functionalization times.

It should be noted that with the samples, the yield force, ultimate tensile force and ultimate tensile strain decrease much less than with fibers treated with ozone.

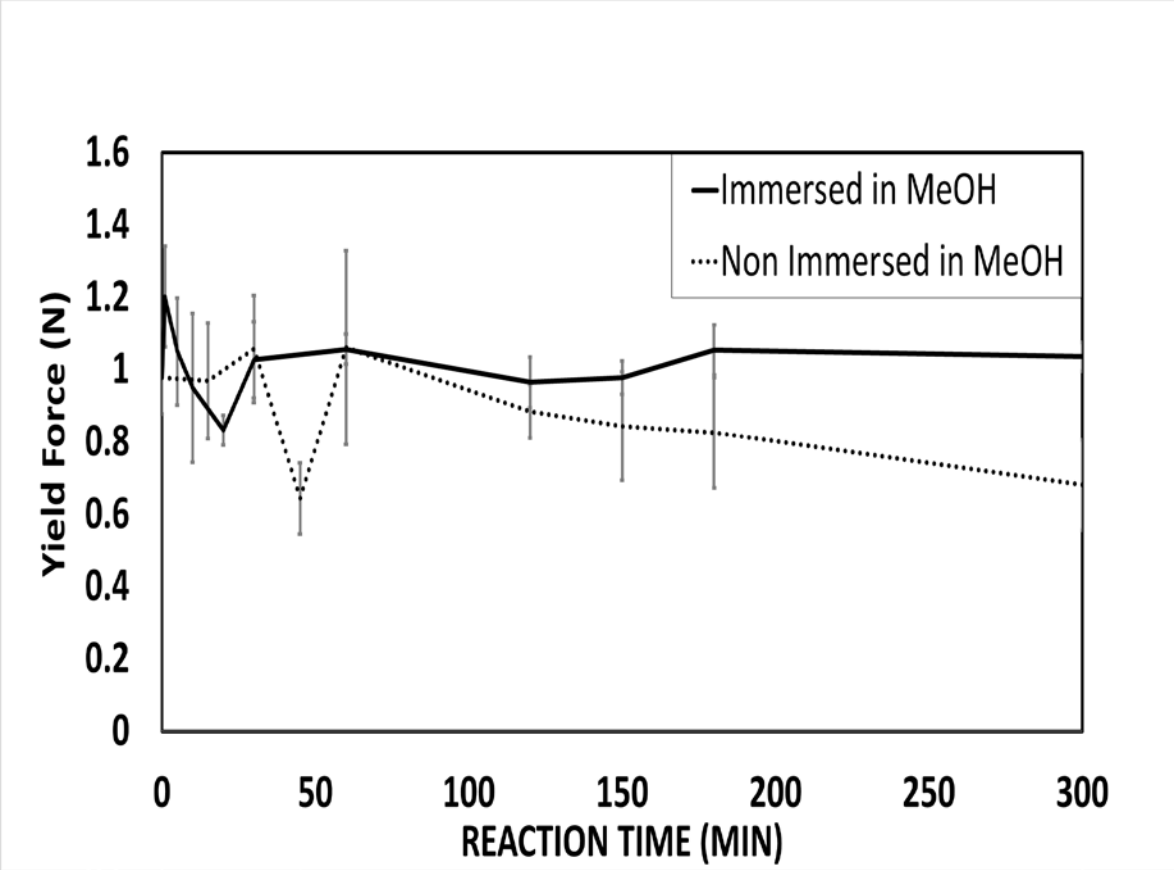

Figure 3.3. Yield force of PP HFM, treated with KPS

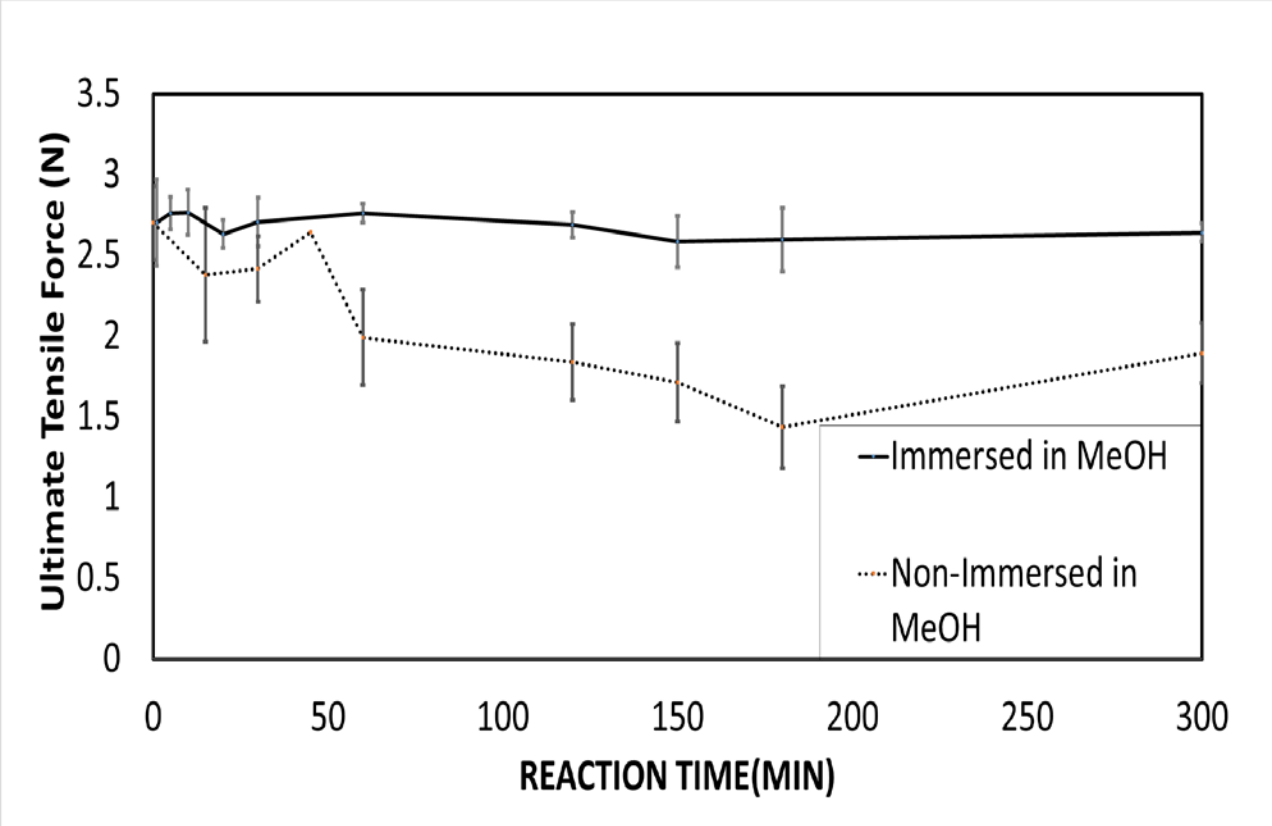

Figure 3.4. Ultimate tensile force of PP HFM, treated with KPS.

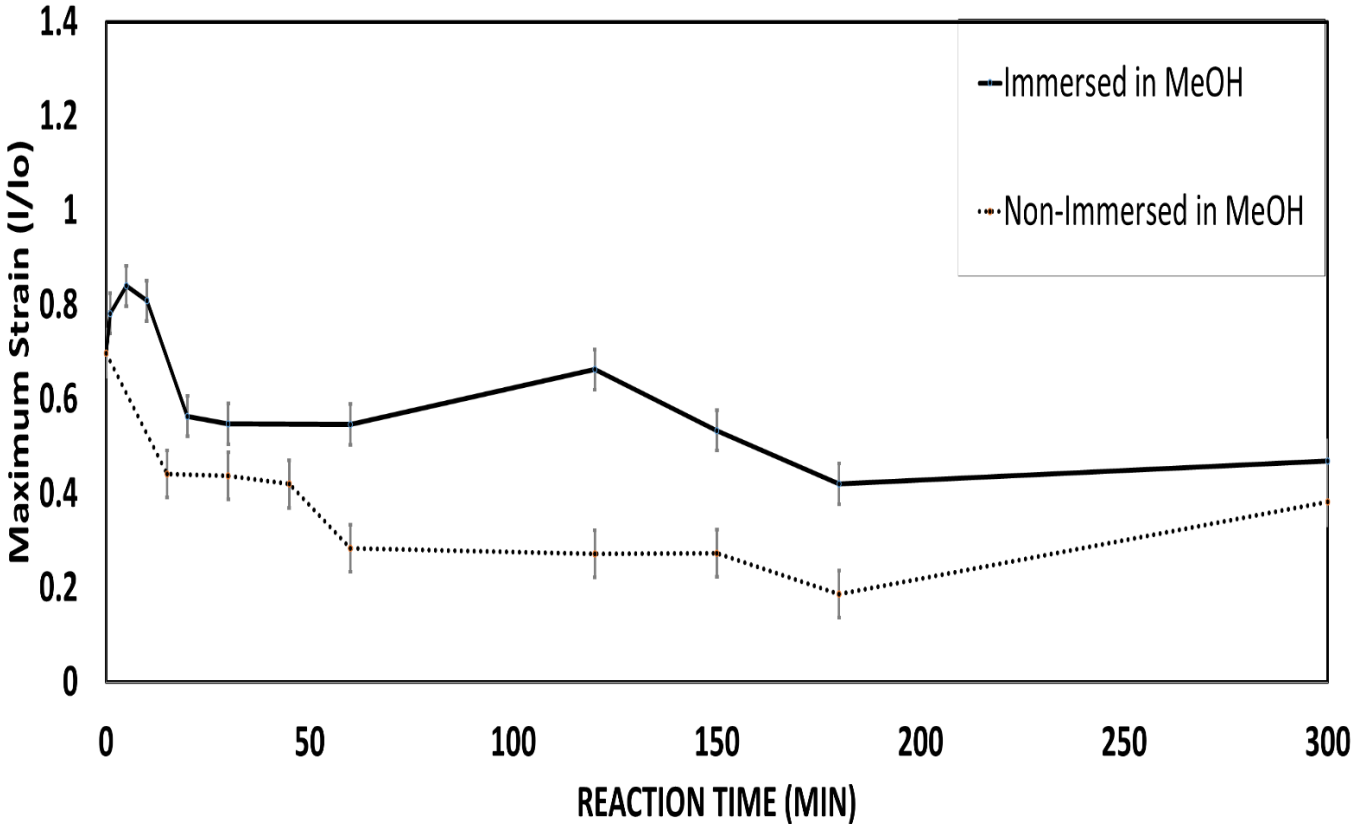

Figure 3.5: Maximum strain PP HFM, treated with KPS.

3.4.2 Ammonium Persulfate Pretreatment

The results from mechanical testing of polypropylene hollow fiber membranes functionalized with ammonium persulfate are displayed in figures 3.6 through 3.8. The yield strength, ultimate tensile strength and ultimate tensile all approached horizontal asymptotes. Fibers pre-impregnated using the methanol immersion method maintained their mechanical strength with extended treatment times.

3.4.3 Ozone Gas Pretreatment

Figures 3.9 through 3.11 yield stress, ultimate tensile stress, and maximum strain for fibers pretreated with ozone gas The yield force of the PP HFM treated with ozone did not decrease appreciably over thirty minutes. After this time period, the yield force decreased by half between thirty minutes and one hour of exposure time. The ultimate tensile strength and ultimate tensile strain however, decreased dramatically after initial exposure. The ultimate tensile strength decreased in a linear fashion with exposure time. The ultimate tensile strain decreased by approximately 50% after one minute of exposure to 5% ozone.

3.4.4 Statistical Analysis of Tensile Testing Data from Treated Membranes

Tensile testing data obtained from PP HFMs treated with aqueous potassium persulfate and ammonium persulfate yielded an unexpected observation that was not observed in HFMs treated with ozone. The mechanical properties PP HFMs treated with either type of persulfate decreased immediately upon contact with the functionalizing reagent. After a predetermined time period, the rate of this decrease slowed substantially and appeared to approach a horizontal asymptote. The magnitude of this asymptote appeared to be strongly influenced by the pretreatment of the fibers.

This asymptote was larger for PP HFMs immersed in methanol prior to exposure to the aqueous functionalization agent. This behavior held for HFMs treated subsequently with potassium persulfate or ammonium persulfate. Pretreatment with methanol and then subsequently water allows the aqueous functionalization agent to penetrate into the porosity within the walls of the membrane. The higher magnitude of this horizontal asymptote associated with methanol pretreatment is unexpected as a larger decrease in mechanical strength was predicted for fibers exposed to the functionalization agent over a significantly larger portion of their available surface area compared to fibers that were dry when immersed in the persulfate solutions.

Pretreatment using the methanol impregnation method followed by water displacement showed a significant impact on the final mechanical properties of the fiber. The impact of this became more significant with time for KPS treated fibers. The p value comparing samples immersed in methanol and then water with those that were dry before subsequent exposure to aqueous potassium persulfate decreased dramatically with exposure time to the potassium persulfate across all measures of mechanical strength. Pretreatment with the methanol immersion method appears to have the most dramatic effect on the yield strength of the fiber as compared to other mechanical properties.

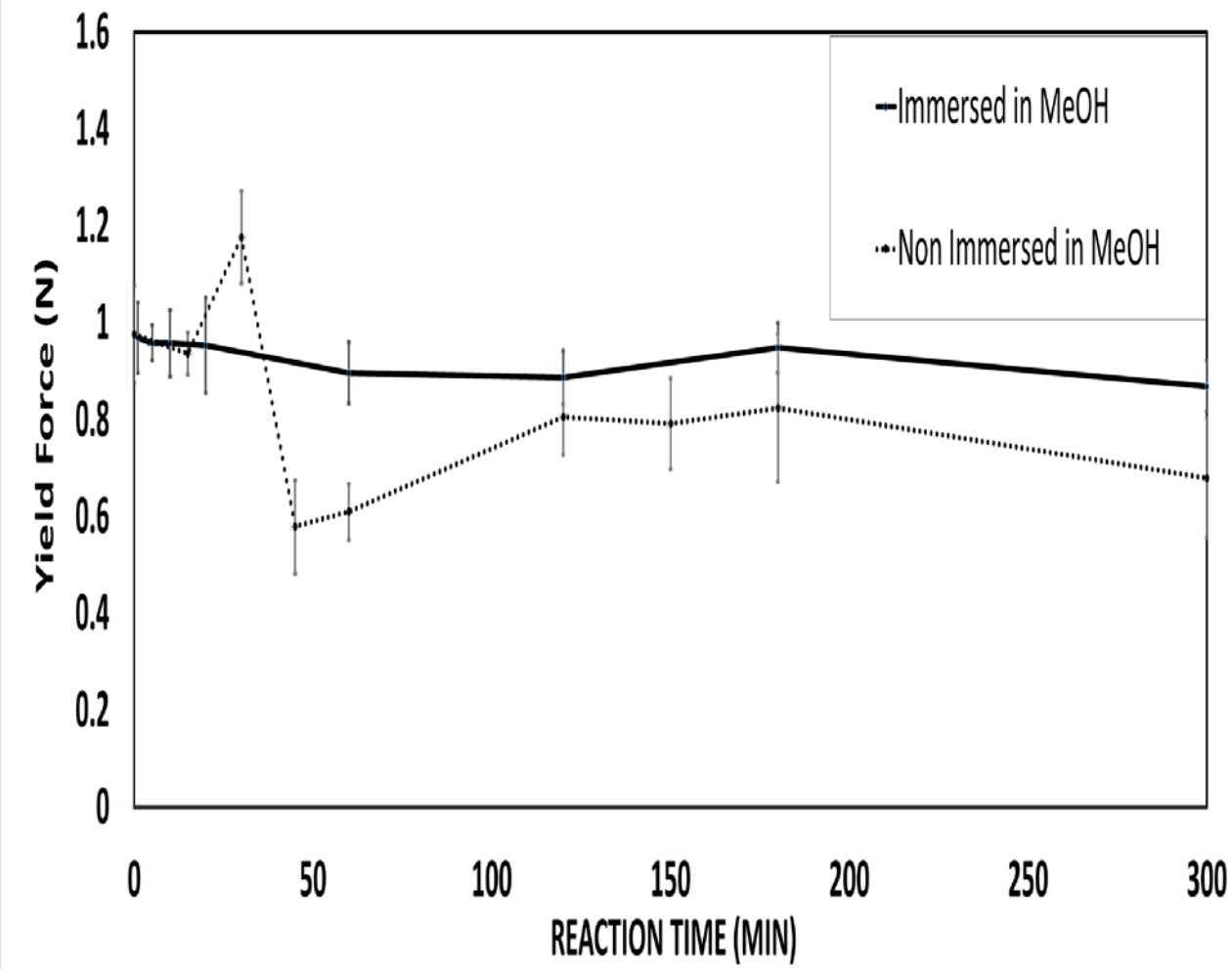

Figure 3.6. Yield force of PP HFH, treated with APS.

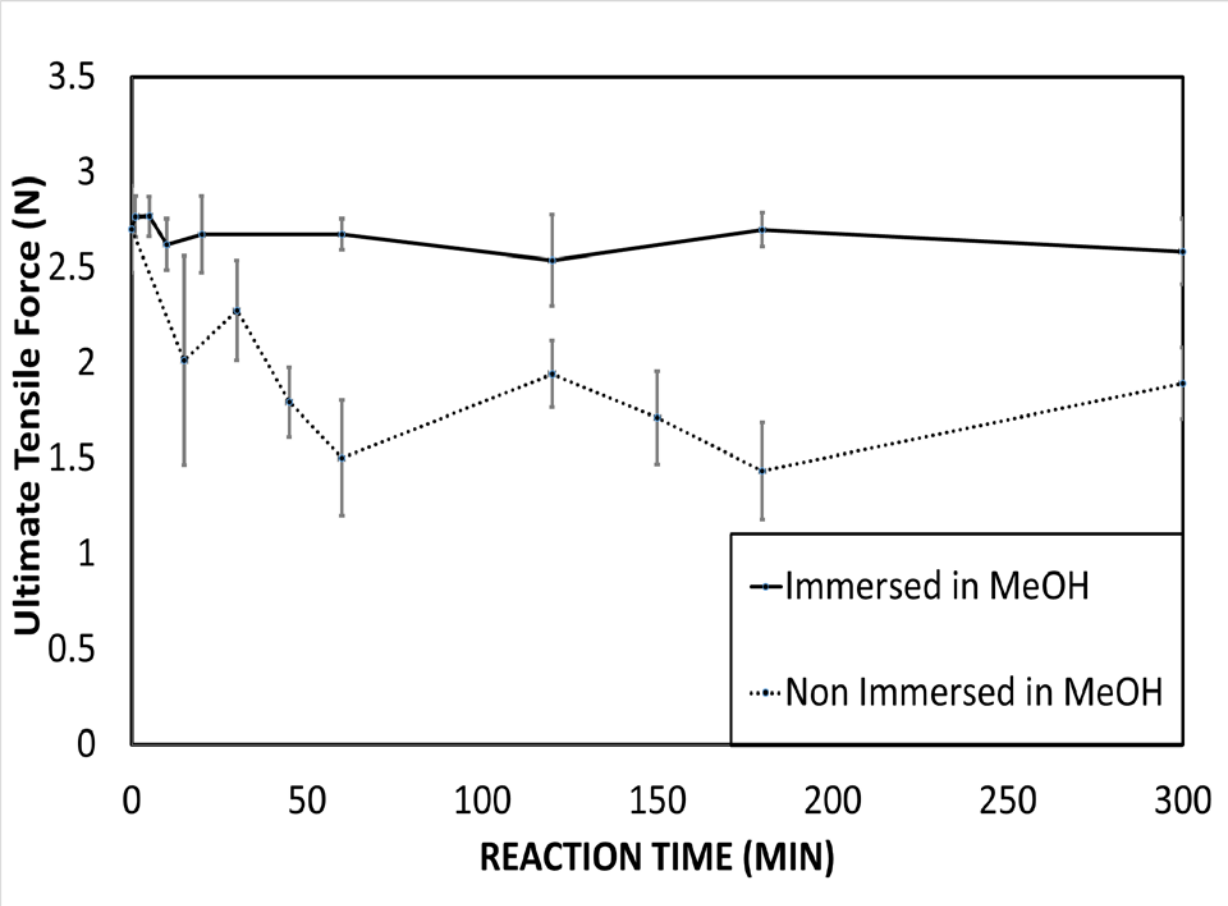

Figure 3.7. Ultimate tensile force of PP HFM, treated with APS.

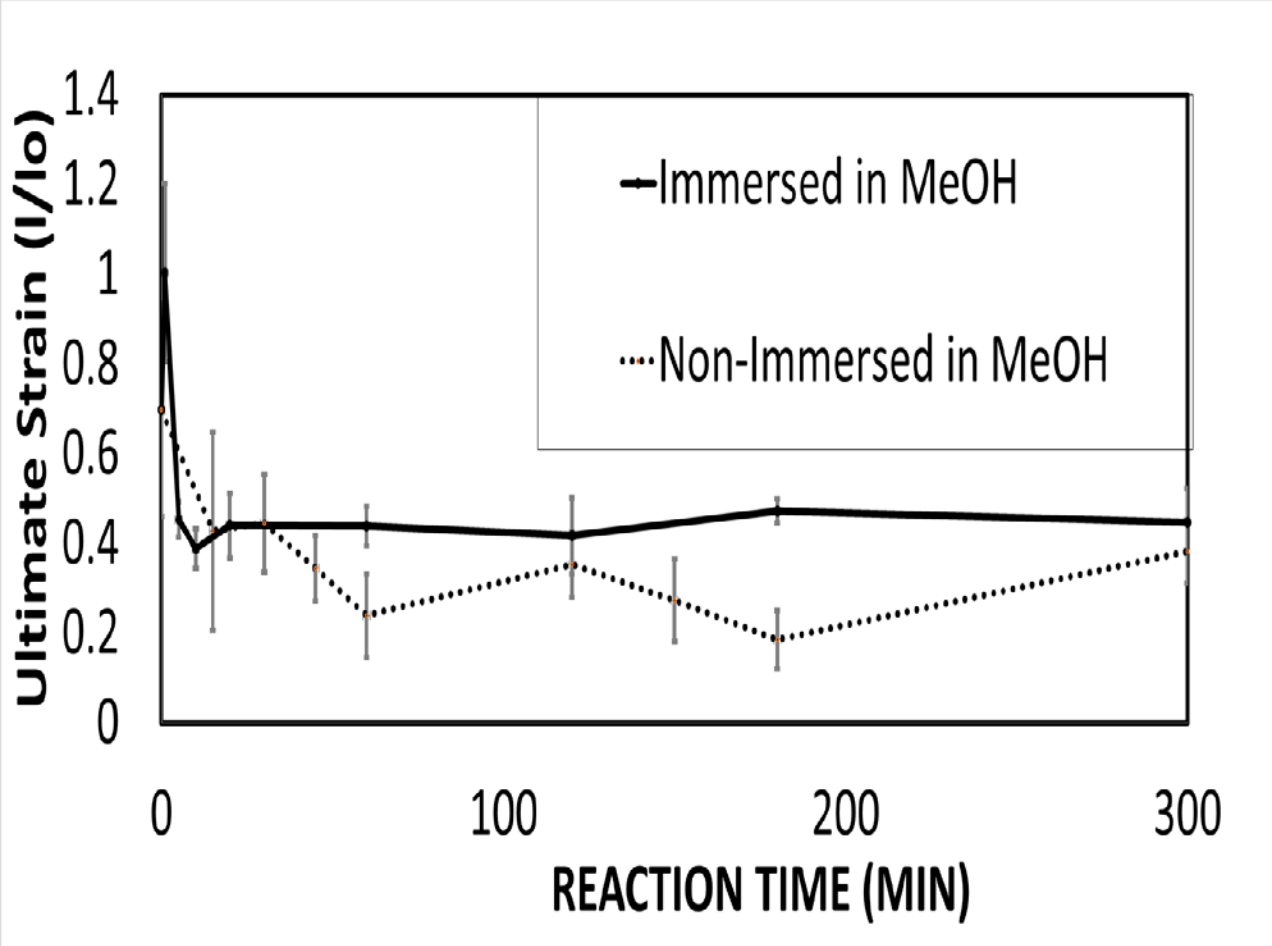

Figure 3.8. Strain at failure of PP HFM, treated with APS.

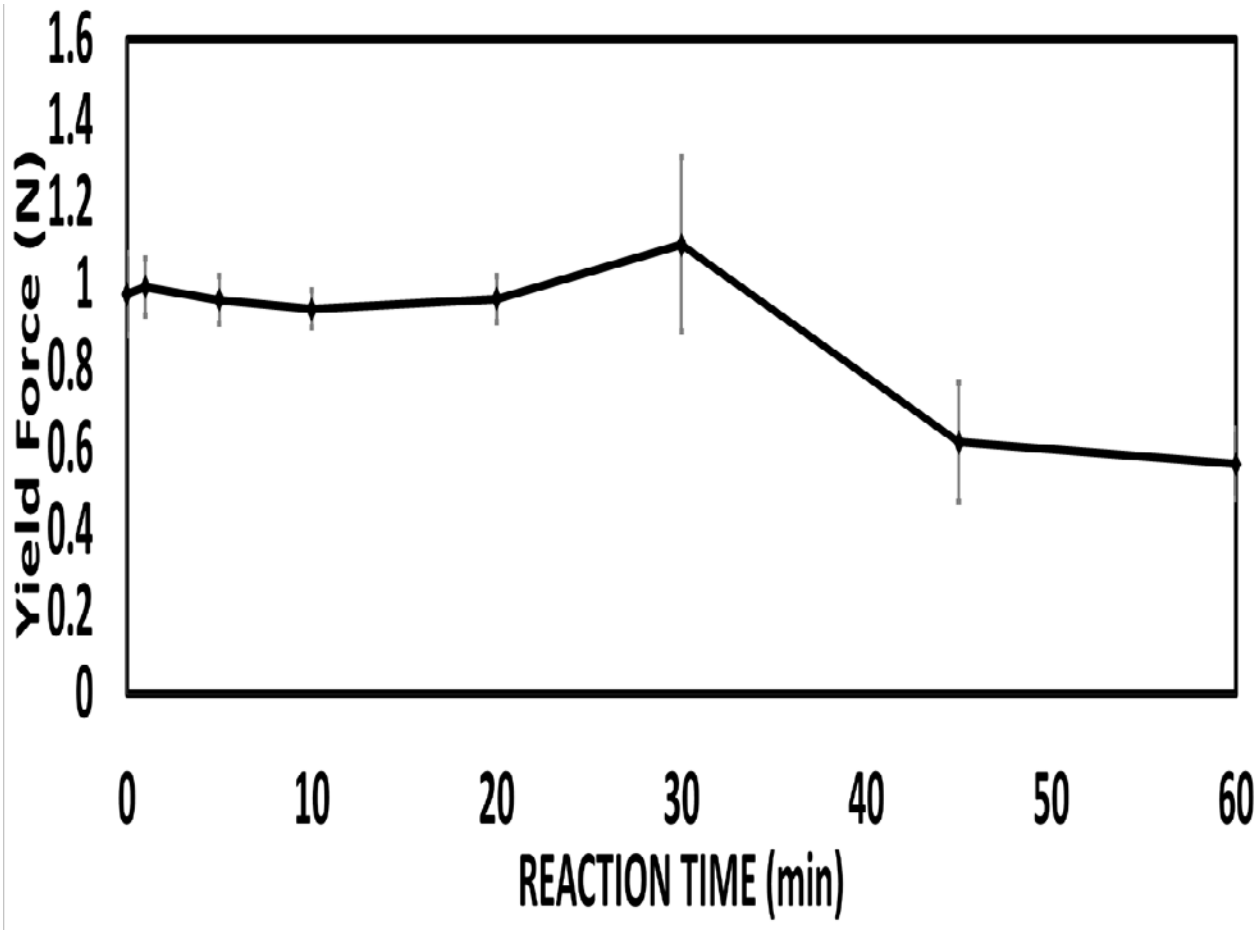

Figure 3.9. Yield force of PP HFM, ozone treatment

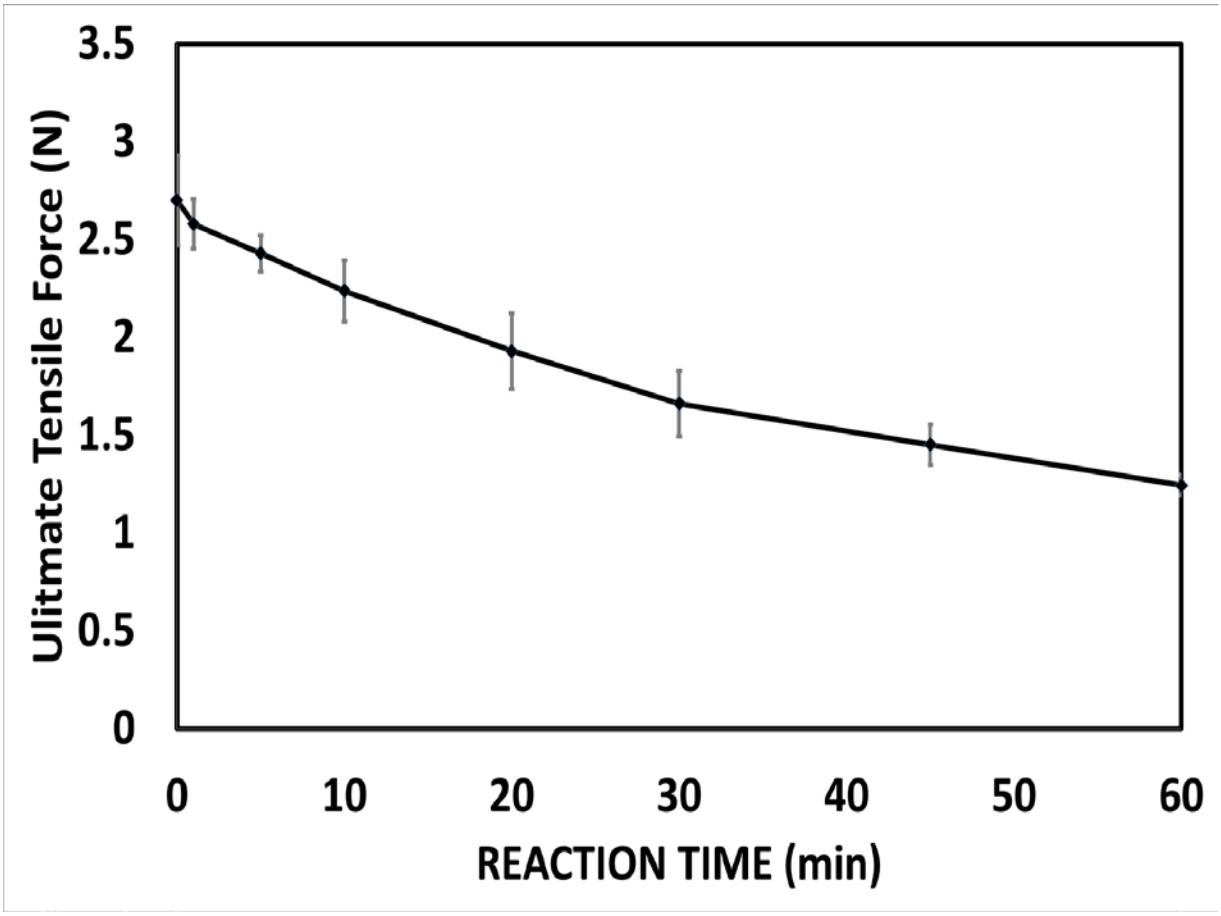

Figure 3.10: Ultimate tensile force of PP HFM, ozone treatment

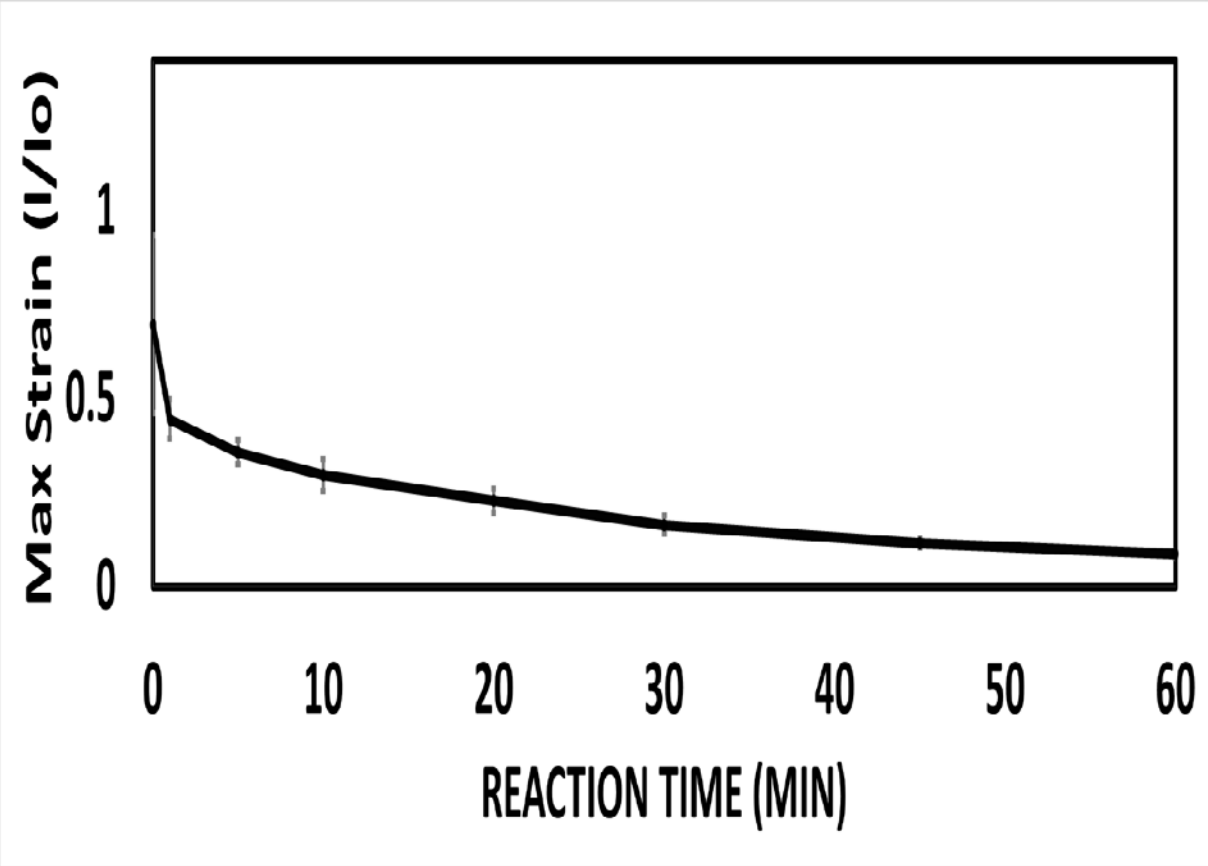

Figure 3.11. Strain at failure of PP HFM, ozone treatment

Table 3.1. P value between groups of PP HFM treated with KPS. Significance of water impregnation prior to treatment.

	P value		
KPS Treatment Time (min)	**Yield Strength**	**UTF**	**Elongation At Break**
30	0.637	0.324	0.324
60	0.477	0.082	0.082
120	0.053	0.1	0.1
150	0.021	0.051	0.051
180	0.007	0.039	0.039
300	<0.001	0.048	0.048

Table 3.2. P value between repeated groups of PP HFM treated with APS to determine variability. Significance of water impregnation prior to treatment.

	P Value		
APS Treatment Time (Min)	**Yield Strength**	**UTF**	**Elongation At Break**
60	<0.001	0.192	0.342
120	0.019	0.068	0.363
180	0.05	0.044	0.068
300	<0.001	0.018	0.085

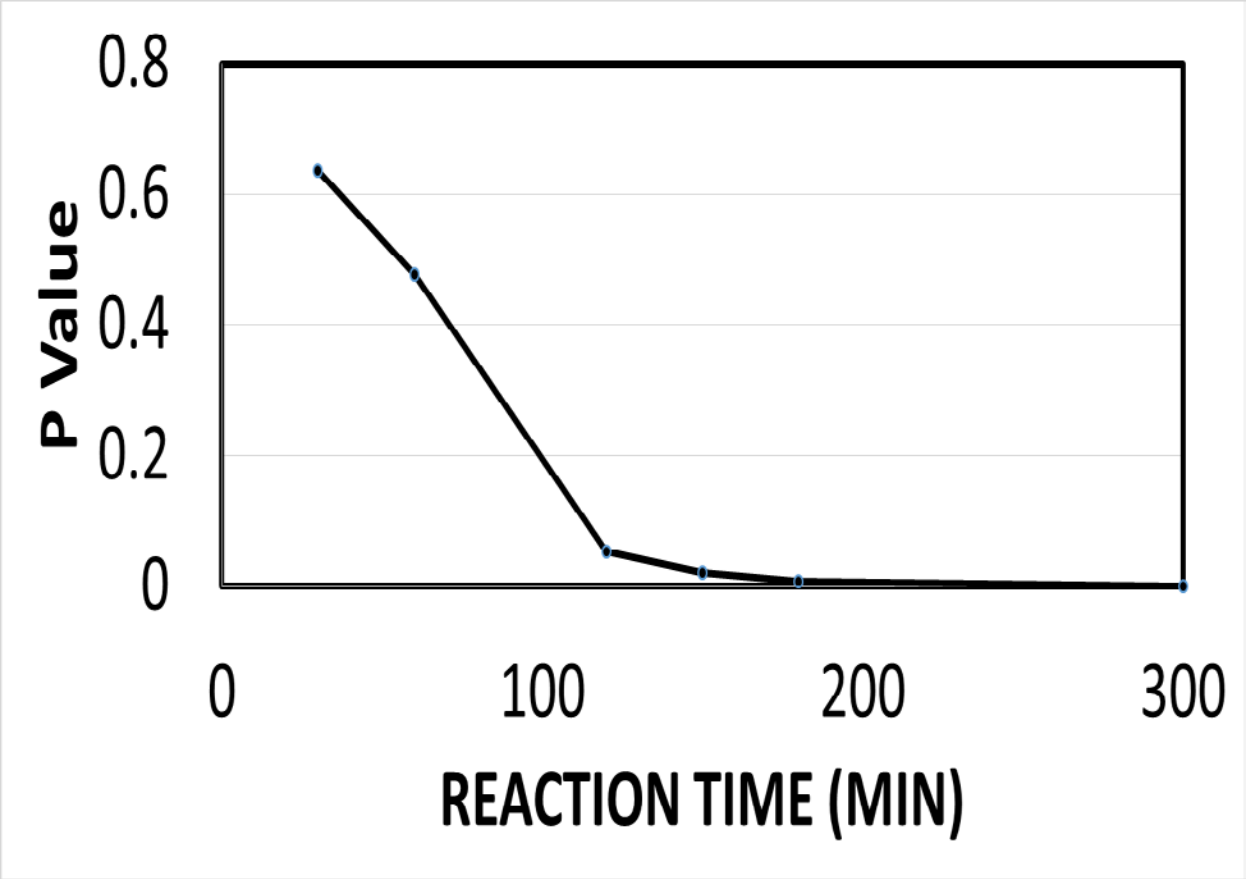

Figure 3.12. P value of yield strength with treatment time of KPS. Significance of water impregnation method before reaction.

Pretreatment of the HFMs with the methanol impregnation method had a significant impact as compared to those that were previously dry before immersion in aqueous ammonium persulfate. The degree of the significance when comparing yield strength is very pronounced at all time periods and is independent of the reaction time. Pretreatment with methanol resulted in an approximate increase of 17% in the yield force and caused a 37% increase in the ultimate tensile force.

The attenuation of the mechanical property degradation of PP HFMs treated by either potassium persulfate or ammonium persulfate previously treated by the methanol impregnation method is believed to be the result of two possible influences or from a contribution of the two.

Within the first proposed mechanism, during the methanol immersion process, methanol diffuses into the bulk to the hollow fiber. After removal from the methanol and immersion in a series of water baths to remove the liquid methanol within the porosity, the methanol diffused into the bulk of the PP HFM remains. During subsequent reaction with either potassium persulfate of ammonium persulfate, the dissolved methanol acts as a buffer that reacts with a portion of the persulfate ions that dissolve into bulk. The persulfate ion is known to react very quickly with methanol.[32] Therefore, as the persulfate ion diffuses into the bulk it is neutralized by the methanol molecules contained within the bulk of the fiber. This phenomenon would limit cleavage of the polypropylene backbone by reaction with the persulfate ions to the surface of the fiber.

The second proposed mechanism involves the formation of crosslinks in the polymer chain by reaction of the persulfate ion. The reaction between polypropylene and a persulfate ion is known to produce a radical on the chain of the polypropylene[29]. If such radicals are produced in the same vicinity, a crosslinking reaction is likely, increasing the strength of the polymer. Similar reaction schemes using the Fenton reaction have been used to cross link molecules.[36] This phenomenon may explain the observed increase in yield and ultimate tensile force of the PP HFMs briefly treated with potassium persulfate and those fibers treated with ammonium persulfate.

3.4.5 Repeatability of Aqueous Treatments

To ensure that the variation between separate functionalization procedures is not significant, separate repetitions were performed using the X30-240 PP HFM matts. Ten fibers were removed from each of these mats and analyzed using tensile testing.

The statistical significance between the original and repeated samples was analyzed using 1-Way ANOVA.

Table 3.3: Variance in mechanical measurements as measured between two samples of polypropylene hollow fiber membrane treated separately for two hours with potassium persulfate.

	P Value Between Repeated Samples
Sample	**2hr KPS (non-immersed)**
Yield force	0.496
Extension	0.92
UTS	0.225
Extension at break	0.01

3.4.6 X-Ray Diffraction of Polypropylene Hollow Fibers after Reaction with Functionalization Reagents

Polypropylene hollow fiber membranes are highly crystalline due to the large degree of drawing that is performed during manufacture.[37] The stretching of the fibers induces the formation of crystalline lamellar structures oriented in the direction of drawing.[33]

Upon exposure to reactive chemicals, the non-crystalline portions of polymers are preferentially attacked due to the higher ring strain. Additionally, lower diffusivity of the reacting species within the crystalline portion of the polymer contributes to the preferentially chemical attack of the amorphous portions of the fiber.

X-Ray diffraction of the polypropylene hollow fiber membranes after they were exposed to reacting species was performed to determine the effect that the surface functionalization procedure would have on the crystalline structure of the polymer.

Well defined peaks were found at angle 2 theta of 14.2, 17.02 and 18.64. The amplitudes of these peaks was then measured on samples of polypropylene hollow fiber membrane treated with a surface functionalizing agent.

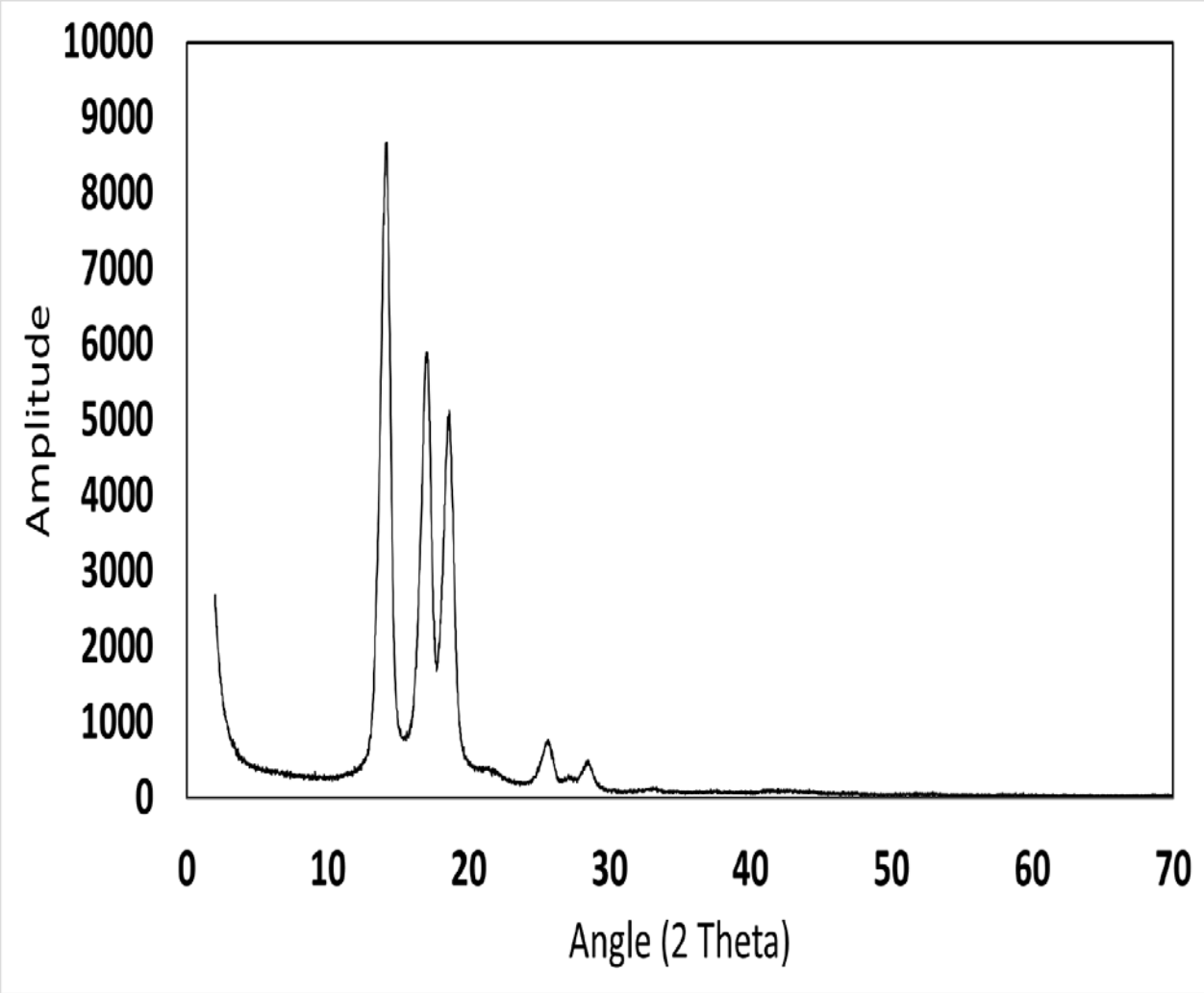

Figure 3.13. X-Ray diffraction scan of PP HFM

Table 3.4: Magnitude of XRD peak decrease after 1 hr reaction time.

	Decrease in Amplitude of X-Ray Diffraction Peaks From Virgin PP HFM (%)				
Angle (2Θ)	**Ozone**	**KPS (Immersed)**	**KPS (non-immersed)**	**APS (immersed)**	**APS (non-immersed)**
14.2	34.61	32.83	56.23	30.7	51.8
17.0	30.15	30.37	51.44	21.8	48.0
18.6	29.44	29.38	50.75	29.3	48.3
Average	31.40	30.86	52.81	27.3	49.4
Standard Deviation	2.80	1.78	2.98	4.8	2.1
Percent Error	8.92	5.76	5.65	17.4	4.3

The decrease in the magnitudes of the x-ray diffraction peaks of PP HFMs after treatment with functionalization reagents as compared to virgin PP HFMs was very consistent across the distinct peaks with a percentage error of less than 5% of the magnitude.

This decrease in peak height indicates that some crystallinity was lost as a result of each of the surface treatments. Thus, each surface treatment is penetrating into the bulk of the polymer and reacting. The immersed samples displayed a significantly lower peak reduction compared to the non-immersed samples (average of 22.25%). Thus, methanol pretreatment may be protecting the bulk of the polymer when methanol molecules, diffusing into this bulk react with the persulfate species, neutralize them and protect the bulk crystallinity from further attack.

The samples of PP HFM treated with the methanol immersion procedure before functionalization had a significantly smaller decrease in amplitude than those PP HFM samples that were dry before immersion in the ammonium persulfate or potassium persulfate aqueous solution.

An interesting result was consistent amplitude decreases between both immersed samples and between both non-immersed samples. The fibers immersed in methanol and subsequently a series of water baths and then treated with either ammonium peroxydisulfate or potassium persulfate both showed a decrease in the X-ray diffraction peaks of approximately 30%. The fibers, initially dry, treated with either ammonium persulfate or potassium persulfate both showed a decrease in the amplitude of their respective diffractions peaks of approximately 50%.

These results, combined with the tensile testing data, indicated that methanol immersion method to impregnate the porosity within the HFM walls protects the polymer chains to some degree from degradation.

3.4.7 Fiber Permeation/Burst Strength

3.4.7.1 Treated Polypropylene Hollow Fiber Membranes

The pressure at which a hollow fiber membrane bursts is a limiting factor for its use. Since bursting while employed in a blood oxygenator would cause immediate catastrophic failure this parameter was measured using a custom made pressure vessel. The vessel and technique are derived from that described by Shilton et. Al.[36]

The permeation of oxygen through treated and virgin fibers was determined by exposing the bores of these HFMs to this gas at increasing pressures and then measuring the flow rate. A structurally intact membrane's gas permeation rate will increase linearly with the gas's pressure. When the pressure exceeds the bursting point, the flow rate will sharply increase.

From inspection of figures 3.18, 3.19, 3.20 no samples reached their burst strength even at pressures as high as 160 psi. As blood oxygenators are connected to standard hospital supplies, which operate at 50 psi, no danger of catastrophic failure is present for HFMs, even for those treated for extended periods.

This sample permeation and burst strength analysis was attempted for PP HFMs treated with ozone for a period of 1 hr. However, these fibers proved to be too fragile to even perform the manipulations necessary for permeation and burst strength analysis.

This study indicates that treatment of polypropylene hollow fibers with potassium persulfate or ammonium persulfate, even for periods much longer than necessary to achieve the desired surface functionalization will not substantially degrade the burst strength to the point where failure is a concern.

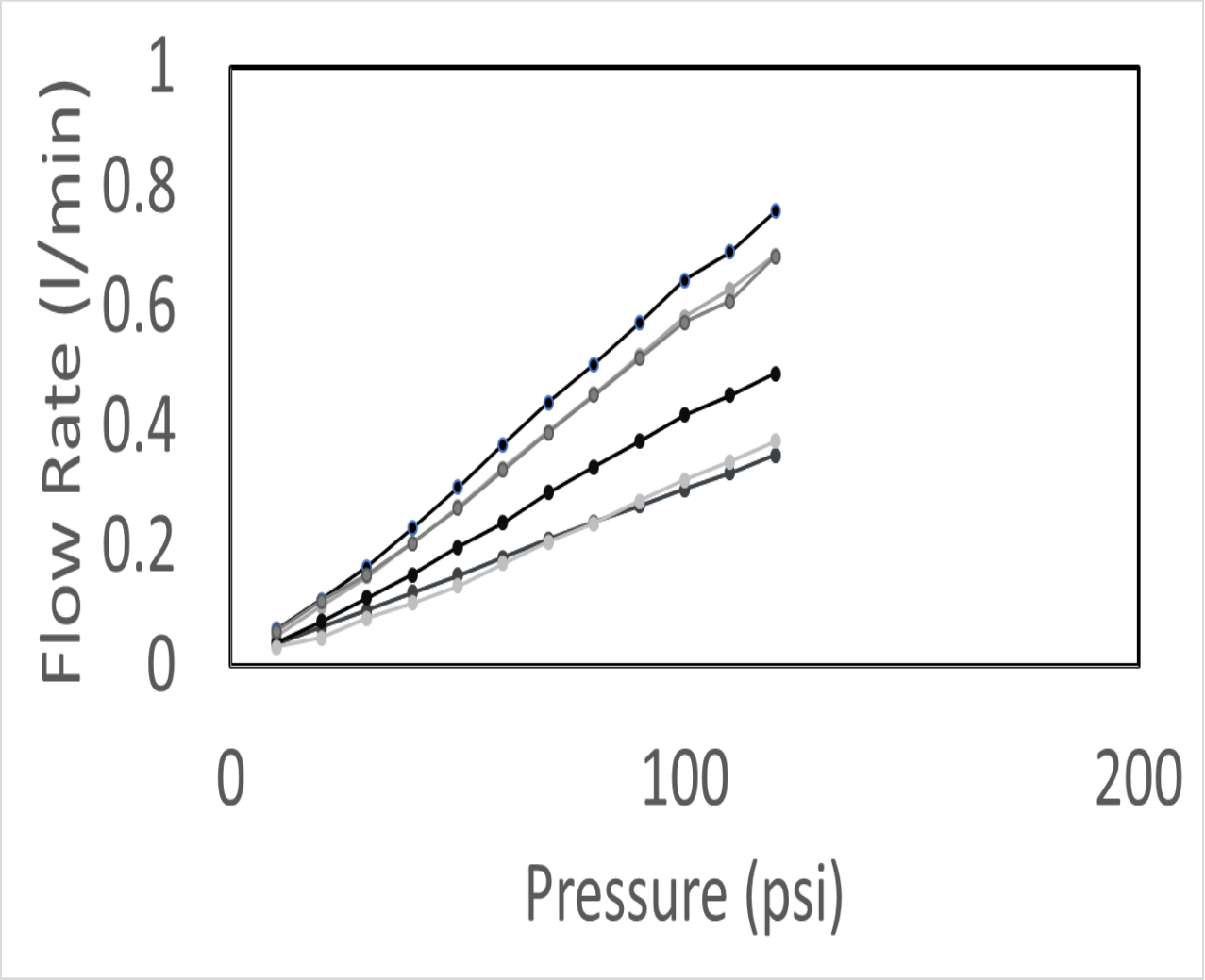

Figure 3.14; Flow rate of oxygen through virgin PP HFM, five samples.

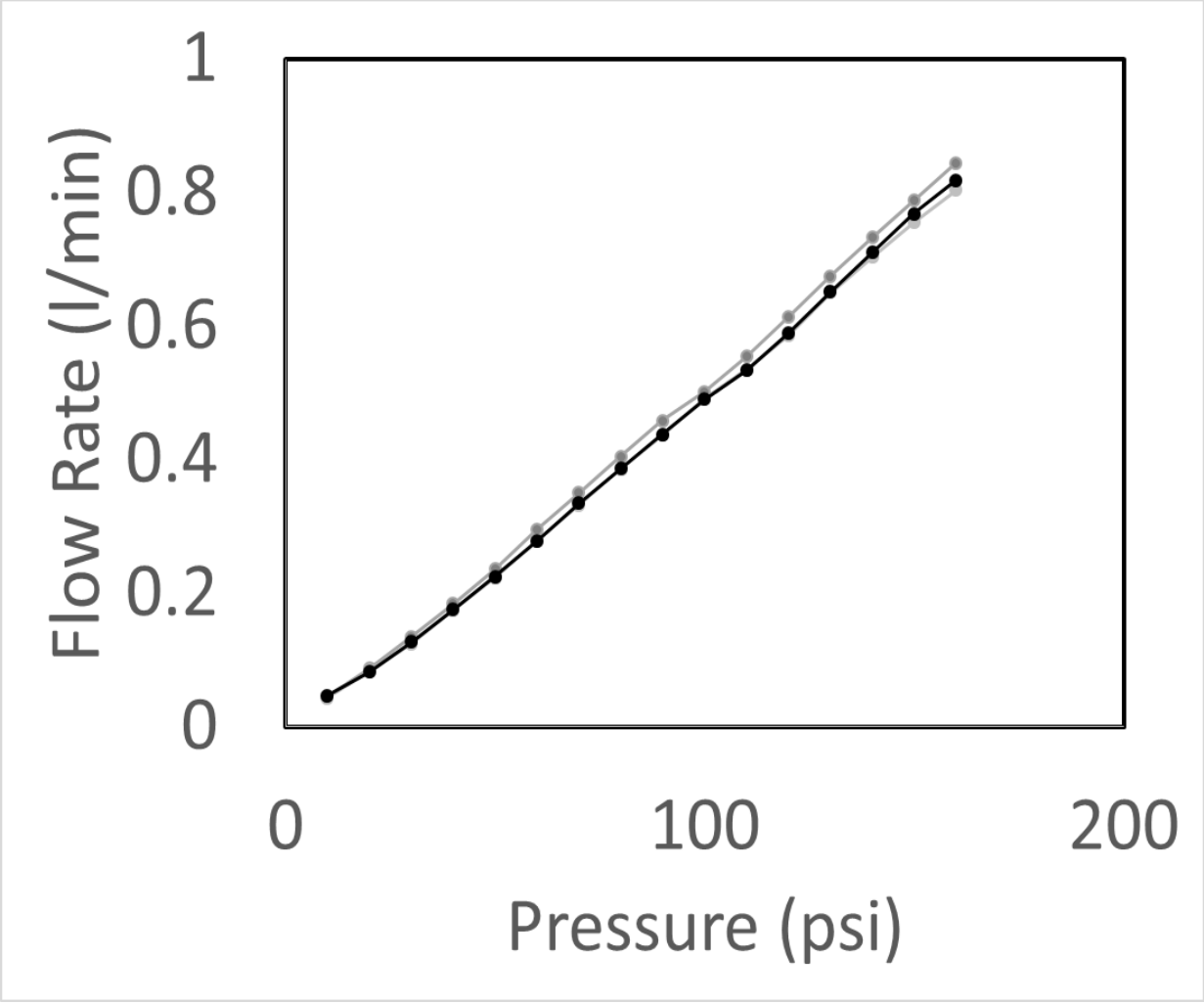

Figure 3.15; Flow rate of oxygen through polypropylene HFM reacted with KPS for 5hrs, three samples

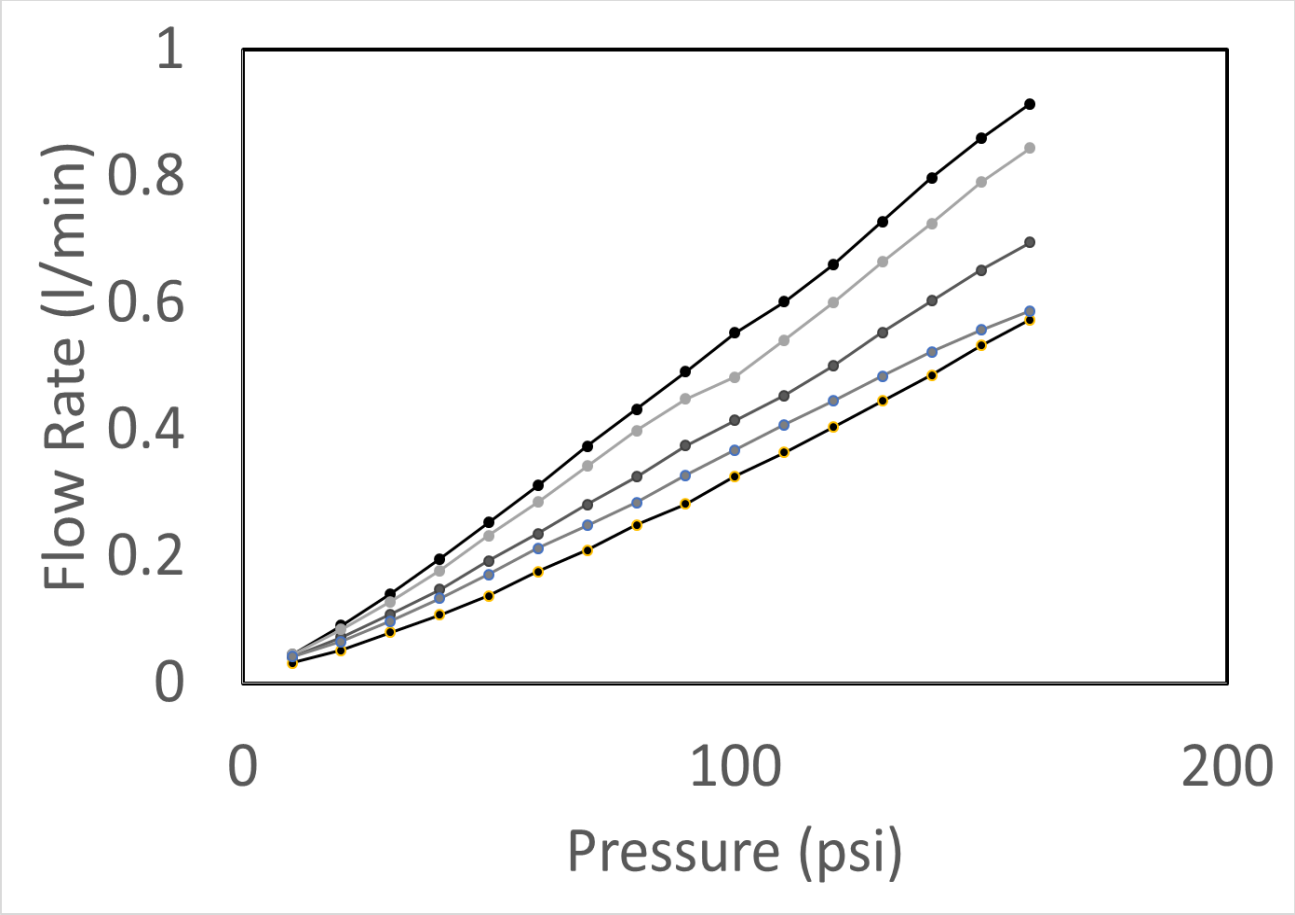

Figure 3.16; Oxygen flow rate through polypropylene HFM reacted with APS for five hours, five samples.

Table 3.5; Blood gas permeability of polymeric hollow fiber membranes used for blood oxygenation

	Permeability (ml/(s*cm^2*cmHg))			
Fiber Type	**O_2**		**CO_2**	
	Measured	**Literature[38]**	**Measured**	**Literature[38]**
PP	$1.74 \pm 0.54 \times 10^{-2}$	$1.77 \pm 0.01 \times 10^{-2}$	$2.10 \pm 0.71 \times 10^{-2}$	$1.62 \pm 0.01 \times 10^{-2}$
PMP	$7.38 \pm 3.90 \times 10^{-3}$	$1.08 \pm 0.09 \times 10^{-3}$	$1.47 \pm 0.72 \times 10^{-3}$	$1.40 \pm 0.08 \times 10^{-3}$

Table 3.6; Oxygen Permeability of Polypropylene after Surface Treatments

Treatment Type	Oxygen Permeability (ml/(s*cm^2*cmHg))
Polypropylene (X30-240)	$1.74 \pm 0.54 \times 10^{-2}$
Potassium Persulfate pretreatment	$1.54 \pm 0.36 \times 10^{-2}$
Ammonium Persulfate pretreatment	$1.56 \pm 0.33 \times 10^{-2}$
Ozone pretreatment	$2.45 \pm 0.07 \times 10^{-2}$

3.4.7.2 Membrane Burst Strength of PMP Fibers

Oxyplus™ PMP hollow fiber membranes were embedded into polyurethane and placed into the permeation apparatus shown in figure 3.2. The flow rates of oxygen and carbon dioxide at increasing pressures was then determined.

PMP fibers appeared to have a much lower burst pressure than polypropylene. Although one fiber burst catastrophically, failure of the remaining samples was determined through observation of a consistently increasing flow rate when held at static pressure. Across six samples, the average failure pressure, applied to the lumen was 113.3+15 psi. It should be noted that no PP HFM samples failed during testing. The highest pressure applied was 160 psi.

3.5 Conclusions

This study indicates that potassium persulfate and ammonium persulfate are capable of functionalizing polypropylene HFMs without significant attenuation of mechanical strength. Fibers functionalized by these reagents are then able to be modified or coated using a variety of techniques investigated by various authors. Additionally, these functionalized polypropylene HFMs are have a higher burst strength than PMP fibers which are currently used for blood oxygenation purposes.

CHAPTER 4 CONTAMINATION LEVELS OF COMMERCIALLY AVAILABLE POLYPROPYLENE HOLLOW FIBER MEMBRANES AND EFFECT ON SURFACE FUNCTIONALIZATION

This chapter is based on work that is being submitted to the American Society of Artificial Internal Organs for publication.

Keywords: Soxhlet Extraction, Hollow Fiber, Soybean Oil, Membrane, Contamination

4.0 Abstract

Attempts at functionalizing virgin polypropylene hollow fiber membranes as received did not produce satisfactory results. Large areas (tens of microns) were not sufficiently coated to occlude the underlying porosity. Extensive pre-cleaning via Soxhlet extraction with an acetone solvent allowed subsequent coating of the fibers with no exposed porosity.

4.1 Highlights

- A number of research teams are developing surface coatings for hollow fiber membrane (HFM) blood oxygenators to improve their biocompatibility and service life. Surface coating techniques can be quite sensitive to the presence of contaminants on the exterior surface of the hollow fibers.
- Large amounts of residual oils associated with several commercial HFMs, i.e., as much as 2.5 to 7.5 wt%.
- When using a surface-initiated atom transfer radical polymerization (s-ATRP) of poly(ethylene glycol-methacrylate), as-received hollow fiber membranes had exterior surfaces with areas over 100 μm^2 devoid of coatings.
- After extraction of residual oils, s-ATRP coatings were uniform and continuous across the hollow fibers.
- Removal of residual material should be considered prior to applying coating technologies to commercial HFMs.

4.2 Introduction

Long term extracorporeal support of lung failure patients with blood oxygenators is now routine[9]. The oxygenators use polymeric hollow fiber membranes (HFM), many of which are based on either polypropylene (PP) or polymethylpentene (PMP) [39-41] [42]. Surface modification of HFMs to form coated (or composite) membranes is an intense area of study and has been the subject of several reviews. Most, if not all, of these coating strategies would perform best when the exterior membrane surface has no contamination or extraneous materials. The presence of a surface contaminant could potentially interfere with covalent bonds, surface associations, or wetting between the HFM exterior surface and the applied material.

Hollow fiber membranes are usually manufactured using thermally-induced phase separation (TIPS) processes. The phase separating agent typically dissolves in the polymer at extrusion temperatures but phase-separates from the polymer at lower temperatures, creating porosity in within HFM walls. In the cases of commercial PP and PMP hollow fibers, soybean oil or mineral oil are often used as the phase separating agent[43]. In some cases, the phase separating agent is removed from the membrane by extraction with solvents such as 1,1,1-trichloroethane or isopropyl alcohol.[44, 45]

Residual oil on the surface of fibers may cause problems with post-synthesis coatings, including poor interfacial adhesion and/or incomplete coverage of all fiber surfaces. The delamination of such coatings within blood oxygenators has the potential to severely injure or kill a patient.

Leaching of the phase-separation agent into blood during oxygenator used may cause some health problems. Soybean oil, a commonly used phase separating agent, is known to be toxic to leukocytes. Linoleic acid, a major component of soybean oil, has been shown to cause apoptosis of human T-cells[46]. Linoleic acid causes mitochondrial depolarization and the generation of reactive ion species within lymphocytes[47]. Oleic acid, a component of soybean oil, induced apoptosis by activation of capsase 3[47]. If leached from the large blood contacting surface area of modern blood oxygenators, soybean oil may cause suppression of the immune response, promoting infection. Consequently, the presence and amount of any substance leaching from these devices should be determined. Food-grade mineral oil has been approved by the FDA for direct or indirect contact with food, and is generally recognized as safe (GRAS). While it might be tolerated by the body, it could still impact post-synthesis coating processes. The objectives of this work were to: leach any residual agents from commercial hollow fiber membranes, identify the general category of the leached material, and evaluate the quality of an s-ATRP coating on unleached and leached hollow fibers with respect to complete surface coverage and gas leakage rate.

4.3 Experimental

4.3.1 Materials & Equipment

X30-240 PP HFM and Oxyplus™ PMP HFM were acquired from Celgard. Chromosolv HPLC grade acetone with purity of greater than 99.9% was purchased from Sigma-Aldrich. Poly(ethylene glycol) methacrylate (PEGMA) with molecular weight of 360 was purchased from Sigma-Aldrich, passed through inhibitor removal columns (Sigma) and stored in a refrigerator before use. NOCHROMIX was used to clean all glassware used in this study and was purchased from Sigma-Aldrich. Bromoisobutyryl bromide, 99.9% anhydrous tetrahydrofuran, triethylamine, copper (I) chloride, copper (II) chloride, 2-2’ bipyridine and technical grade sulfuric acid were purchased from Sigma-Aldrich. The castable resin used for embedding the fibers in the cylinder was WC-781 from BJB Industries.

4.3.2 Equipment

A Hitachi Primaide system with a Kinetex C-18 column (5 μm particles, 100 Å pores, 150x4.60 mm; Phenomenex™) was used to perform all HPLC measurements. The column size was 150x4.60 mm. A ChemGlass Soxhlet apparatus and condenser was for all extractions. Figure 1 is a sketch of the pressure cell used for determining the pore size of the hollow fiber membranes before and after s-ATRP coating. The pressure cell was comprised of a steel cylinder with diameter of 60 mm and length of 215 mm. A 12.7 mm section of steel was welded onto one end of the cylinder and a ½ inch NPT threaded hole was created. On the opposing end of the cylinder, a 127 mm diameter ring of thickness 12.7 mm was welded onto the 60 mm cylinder. A mating surface was created to accommodate the fiber samples embedded in a castable resin. The upper portion of the pressure cell was created in the same manner, however with a 37 mm long cylinder.

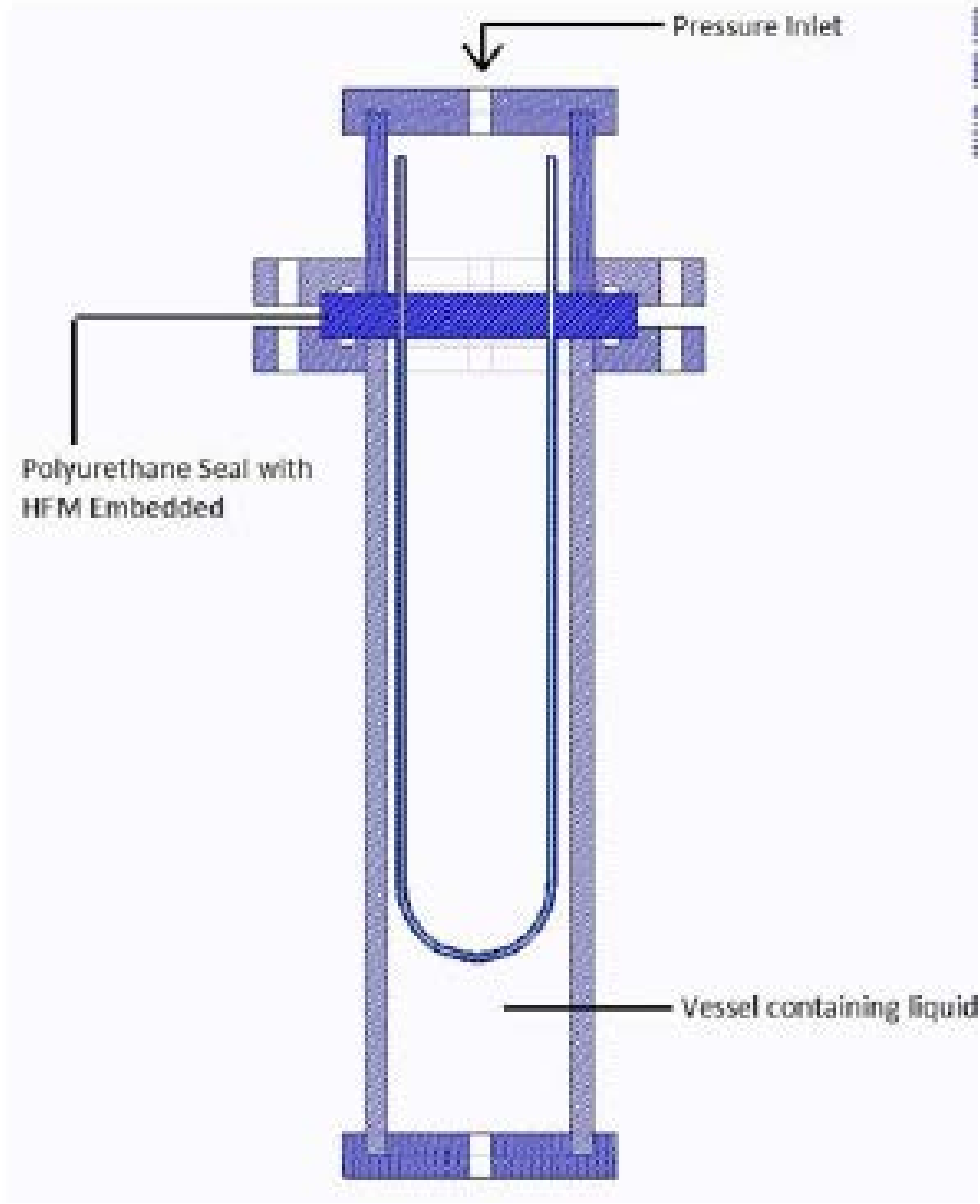

Figure 4.1 Pressure cell for bubble point and burst strength analysis

4.3.3 Procedures

4.3.3.1 Extraction of residual oils.

Approximately 2 grams of hollow fibers, either polypropylene or polymethylpentene, were wound around two wooden dowels of 0.5 inch diameter spaced at a distance of 30 inches. Sections of clean tantalum wire with length of two inches were weighed and then wrapped around each end of the fiber to create a bundle. These bundles were then weighed (compensating for the tantalum wire weight). Three bundles of each hollow fiber type were extracted to determine the weight fraction of residual oils.

The Soxhlet extraction apparatus and all glassware were cleaned by the following procedure. The glassware was immersed in a potassium hydroxide/isopropyl alcohol bath for a period of 24 hours. The glassware was then rinsed with deionized (DI) water and cleaned with a NOCHROMIX/sulfuric acid solution for 2 hours followed by rinsing with DI water and storage in an oven at 90^{o}C until use.

Each HFM bundle was individually placed into a Soxhlet extractor apparatus with a 500 ml round bottom flask as the solvent reservoir (500 ml solvent was used). CHROMOSOLV HPLC grade acetone (Sigma-Aldrich) with purity greater than 99.9% was used for all extractions. The extractor was run for 36 continuous hours. The key objective of this method was to remove all residual oils, so the leaching rate was not assessed. The acetone needed to be removed from the leachate in order to detect residual oils using HPLC.

4.3.3.2 HPLC analysis of extracted residue.

20 ml of acetone solvent used to extract the fibers were placed in flask at 80^{o}C to evaporate the solvent. Afterward, 2 ml of pure acetone was added to the flask to re-dissolve the residue. Afterward, this 2 ml of the remaining solvent was analyzed by HPLC. Samples (50 µl) were injected into the column with a gradient mobile phase and flow rate of 0.5 ml/min, with absorbance measurements of column effluent made at 254 nm.

Although previous literature reports used a water-to-acetonitrile solvent gradient to elute fatty acid peaks[48], we found that this gradient did not completely elute all of the unknown residue in the C18 column. For this reason, a second solvent gradient was added, acetonitrile-to-ternary solution, which contained acetonitrile, ethanol and hexane.[49] Table 4.1 shows the mobile phase composition vs. time for the HPLC runs. The initial elution solvent is very hydrophilic, so hydrophobic solutes will adsorb onto the packing. The adsorption and release of solutes from the C-18 column can be interpreted using Hansen solubility parameters.

Table 4.1. Mobile phase composition vs. time.

Elution time (min)	Solvent 1: Water + 0.1% Trifluoroacetic Acid	Solvent 2: Acetonitrile	Solvent 3: 40% Acetonitrile, 40% Ethanol, 20% Hexane
0	100%		
20	100%		
90		100%	
120		100%	
200			100%
230			100%

4.3.3.3 S-ATRP of Hollow Fiber Membranes

Using the protocol developed by Yao et al [50], a poly(ethylene glycol) methacrylate (PEGMA) coating was polymerized on the surface of isolated hollow fibers to a thickness of approximately 100 nm.

4.3.3.4 Gas leakage rate and average pore size determination.

Each fiber sample was embedded into the pressure cell, and the porosity of the polypropylene hollow fibers were then tested using ASTM Standard E128[51], modified for the measurement of pore size and distribution on the surface of hollow fiber membranes. DI water was used as the fluid for detecting bubble formation due to gas leaking through membrane pores. Nitrogen was then applied to the bore side of the fiber at increasing pressures until the first bubble broke from the surface of the fiber. This pressure was noted as the bubble point.

4.4 Results

4.4.1 HPLC chromatograms for soybean and mineral oils

Table 4.2 lists Hansen solubility parameter values for the individual solvents, solvent mixtures, and solutes in the HPLC separations. The starting solvent in the HPLC separations is water mixed with 0.1% trifluoroacetic acid, a strongly hydrogen-bonding solution. Since the stationary phase of the column packing is functionalized with ligands containing 18 carbons, either mineral oil components or soybean oil components should partition to the stationary phase. As the solvent phase composition changes during the HPLC separations, the continuous phase Hansen solubility parameters will change. When there is an adequate match between the solute and the solvent properties, the solute will desorb from the packing into the solvent, flow through the column, and be detected at the outlet.

Table 4.2. Values of Hansen solubility parameters for HPLC solvents and solutes [52]

	Hansen solubility parameters, $MPa^{1/2}$			
Solvent	**Dispersive, δ_d**	**Polar, δ_p**	**H-Bonding, δ_h**	**composite solubility parameter, δ**
Water	**15.5**	**16**	**42.3**	**47.8**
Trifluoroacetic acid	**15.6**	**9.9**	**11.6**	**21.8**
Acetonitrile	**15.3**	**18**	**6.1**	**24.4**
Ethanol	**15.8**	**8.8**	**19.4**	**26.5**
Hexane	**14.9**	**0**	**0**	**14.9**
1st elution mixture	**15.5**	**16.0**	**42.3**	**47.8**
2nd elution mixture	**15.3**	**18**	**6.1**	**24.4**
3rd elution mixture	**15.4**	**10.7**	**10.2**	**23.3**
Oleic Acid	**16.2**	**3.1**	**5.5**	**17.4**
Decane	**15.8**	**0**	**0**	**15.8**

For purposes of estimating differences between the Hansen solubility parameters of the target solute and the solvent mixture, oleic acid was used to represent soybean oil and decane was used to represent mineral oil. These differences are plotted for both the oleic acid-solvent and decane-solvent pairs versus elution time (Figure 4.2). All of the solvent-solute pairs have small differences between the disperse solubility parameters; the solvent changes do not affect the differences in Hansen dispersive components. During the change from solvent 1 to solvent 2, the differences between hydrogen-bonding values for the solute-solvent pair decrease significantly, while there is a 10% increase in the differences between the polar components of the solute-solvent pair. During the change from solvent 2 to solvent 3, the differences between the polar component of both pairs decrease, and the differences between the hydrogen-bonding component of both pairs increase.

Figure 4.3 shows the HPLC chromatogram for soybean oil in an acetone carrier. There is an initial solvent (acetone) peak at 5 minutes retention time. A few components are eluted near 50 minutes, but most of the sample is eluted between 140 and 190 minutes. This elution range corresponds to the region in which the differences between the polar components decrease from starting to decrease significantly. Soybean oil contains seven or more long chain fatty acids [53]. Figure 3 indicates the presence of multiple peaks of hydrophobic components.

Figure 4.4 shows the elution curve for mineral oil, which has appears between 60 – 80 minutes, followed by a slow release as the 3rd solvent is introduced (> 120 minutes). The first release coincides with the difference in the hydrogen-bonding components being reduced below 20 MPa$^{1/2}$. Material released beyond 120 minutes coincides with a slow reduction in the difference between the polar components. Figures 4.3 and 4.4 show that soybean oil and mineral oil can be distinguished by this particular HPLC protocol.

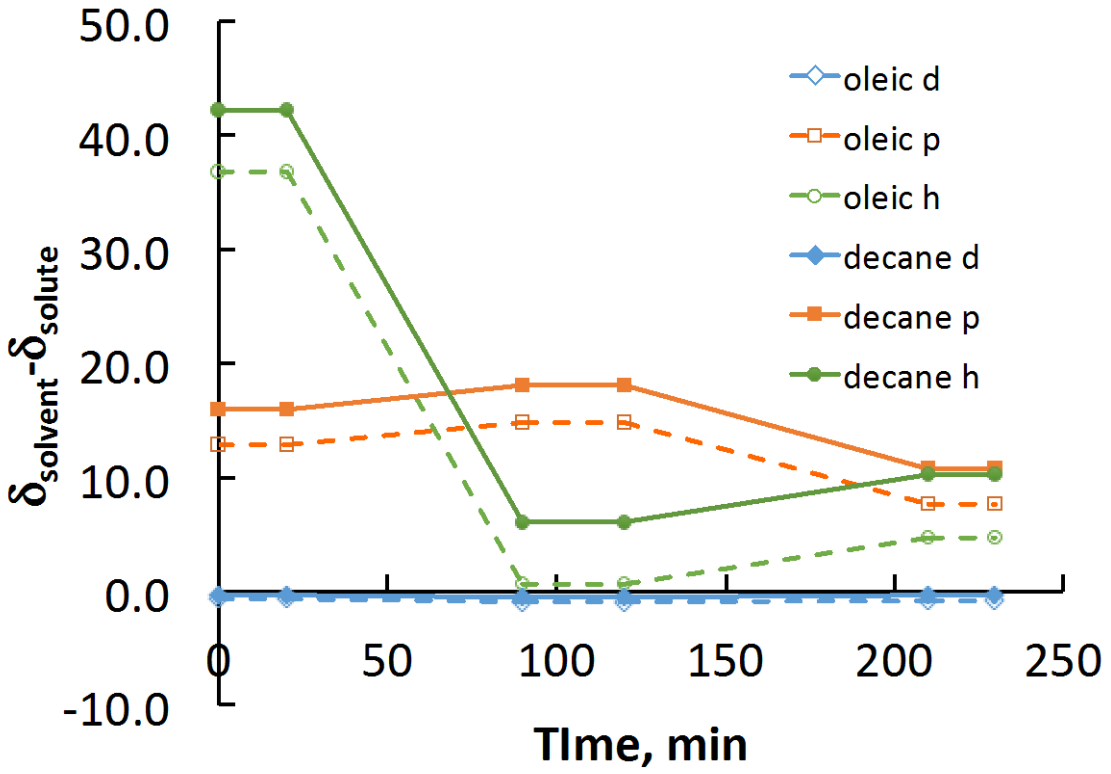

Figure 4.2. Estimated differences between the Hansen solubility parameter values of the HPLC mobile phase and a solute during elution. Dispersive forces = blue; polar forces = orange; hydrogen-bonding forces = green. Solid line = decane; dashed lines = oleic acid

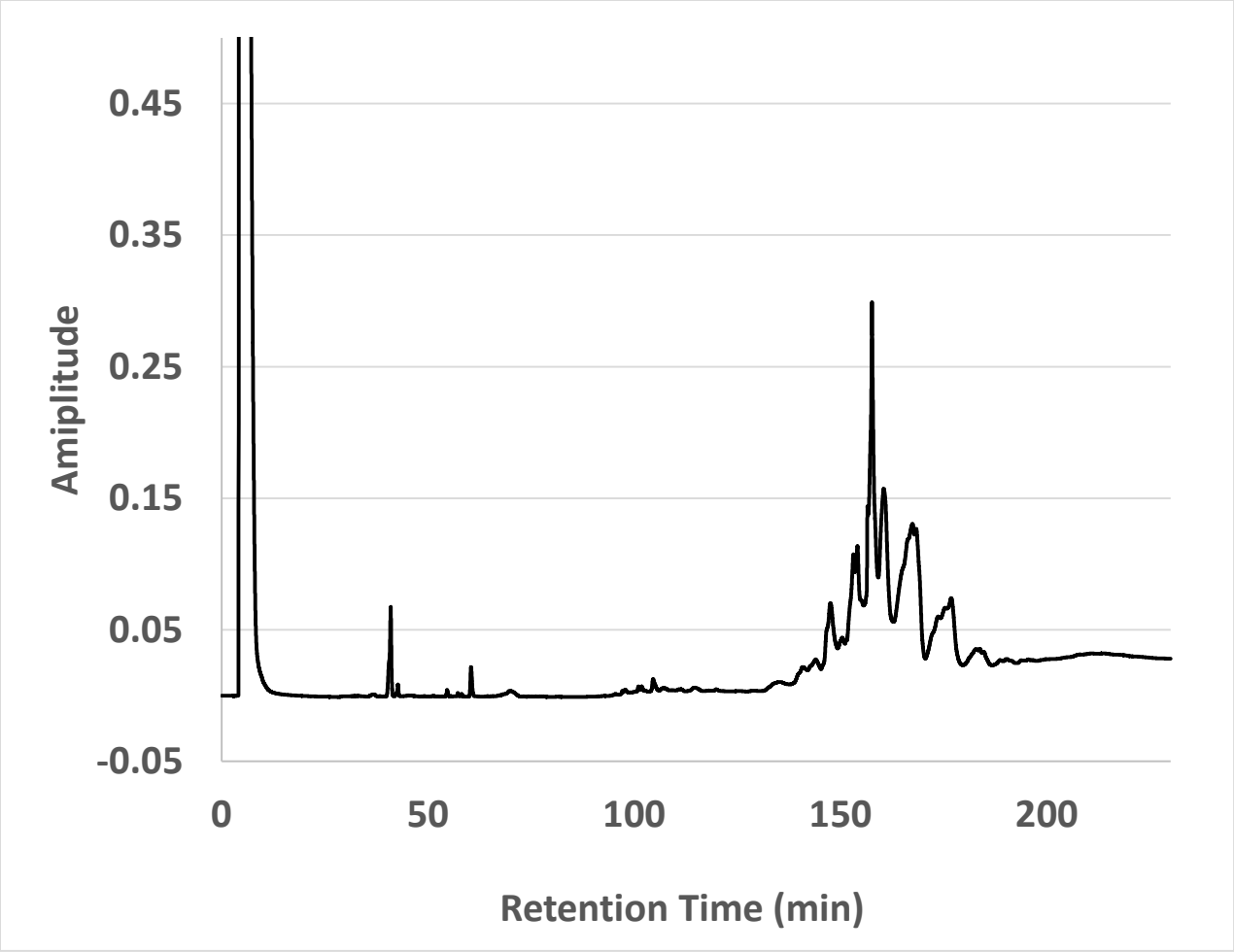

Figure 4.3. HPLC chromatogram of soybean oil

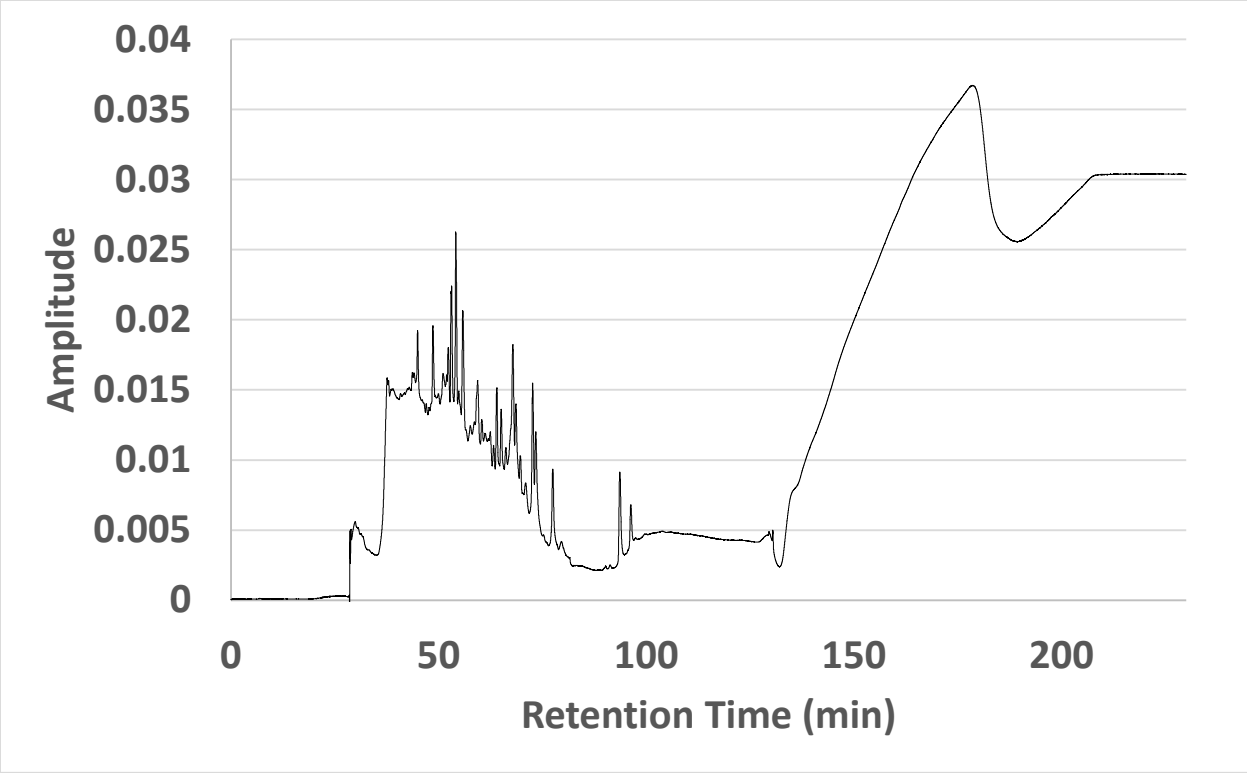

Figure 4.4. HPLC chromatogram of mineral oil

4.4.2 Residue Extracted from Hollow Fiber Membranes

The leachate from Soxhlet extraction was concentrated to enhance the signal from HPLC analysis. Concentration was accomplished by boiling the acetone (~ 56 ºC is the boiling point). Both soybean oil and decane have much higher boiling points (177 ºC and 174 ºC, respectively), so little of the solutes should have evaporated during the process. After evaporation of the acetone solvent, brown liquids remained. The HPLC chromatograms of the concentrated leachate residues are shown in Figures 4.5 and 4.6. Multiple peaks that elute as the mobile phase becomes more hydrophobic were observed. These multiple peaks, also observed in mineral oil and soybean oil (Figures 3 and 4), are determined to be hydrophobic oils.

The weight percent weight loss was 2.50±0.36% for PMP and 7.13±5.47% for PP after 36 hours of extraction with acetone. Our study indicates the presence of significant amounts of residue in HFMs used in blood oxygenators, both polypropylene and polymethylpentene. The presence of these oils remaining from manufacture of the HFMs may also interfere with the application of surface chemistry, coatings and molecular attachment schemes.

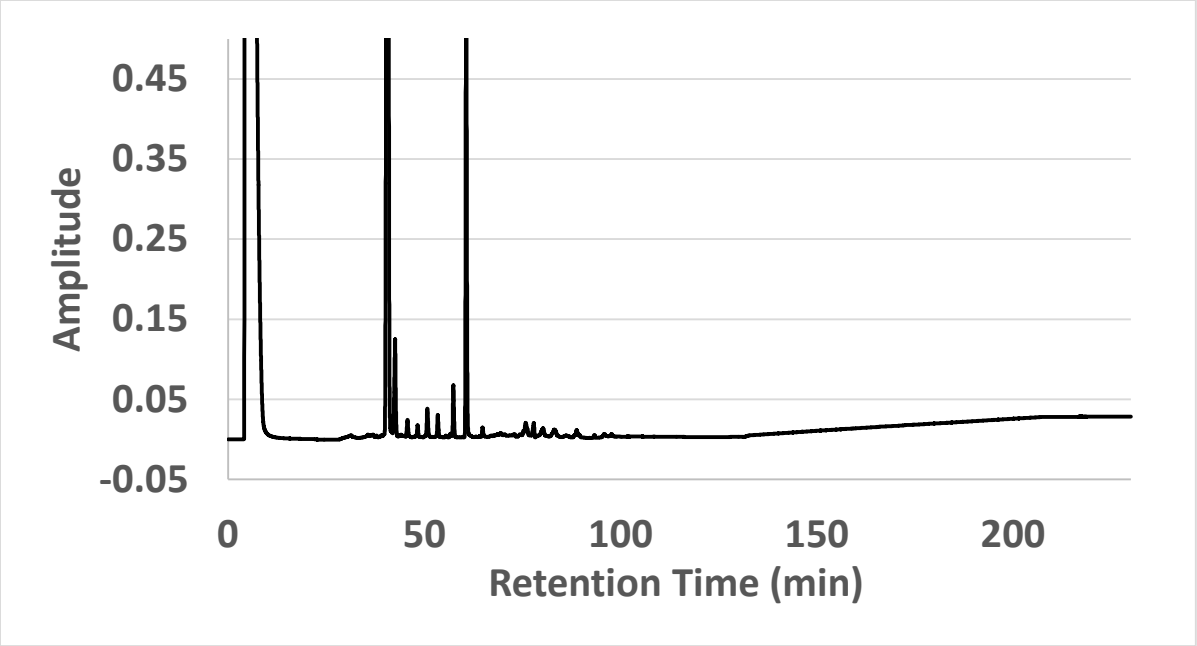

Figure 4.5. HPLC chromatogram of leachate from PMP hollow fibers

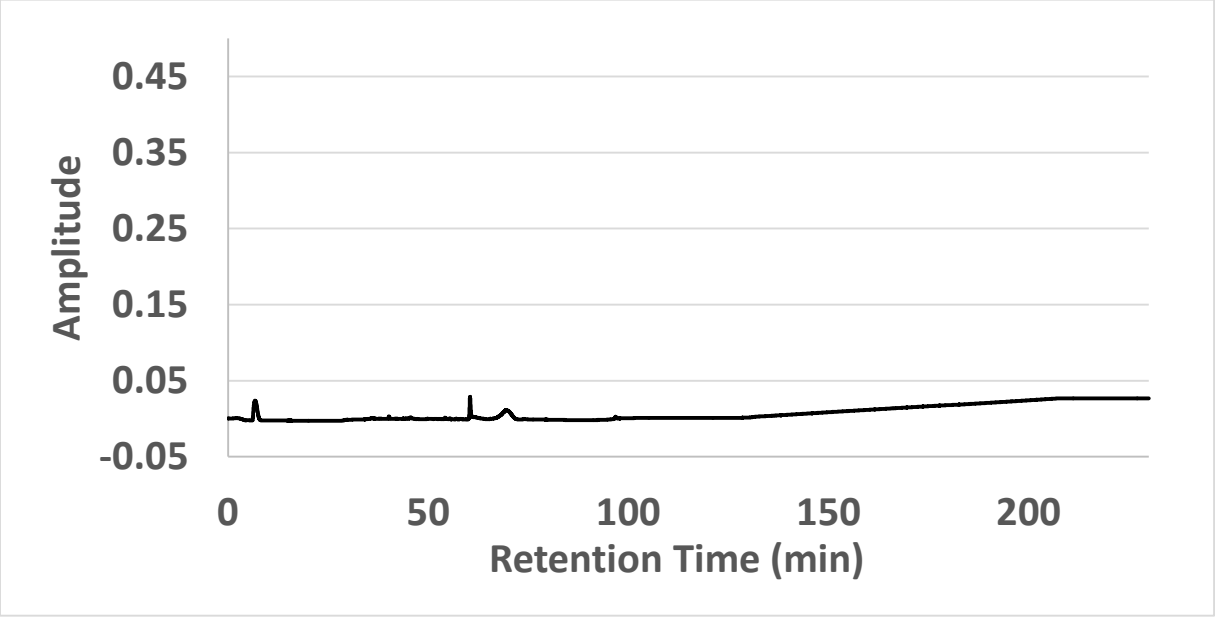

Figure 4.6. HPLC chromatogram of leachate from PP hollow fibers

4.4.3 PEGMA coatings on hollow fiber membranes

4.4.3.1 Scanning Electron Microscopy

Both as-received and leached hollow fiber membranes were modified with s-ATRP coatings. The procedure was designed to make uniform coatings of ~ 100 nm thickness on the hollow fiber membranes. Coated fibers were examined using scanning electron microscopy to evaluate the uniformity of the surface coatings. Fibers that were not cleaned and were coated as received showed large areas, on the order of 100 µm, over which no coating was present or the coating was incomplete. PP and PMP hollow fibers that were cleaned via leaching with acetone for 36 hours followed by functionalization by the s-ATRP process did not produce these discontinuities in the coating coverage.

Figure 4.7 shows selected surfaces of a polypropylene hollow fiber that was coated via the s-ATRP PEGMA process in the as-received state. Fibers that were not cleaned showed large areas, on the order of 100 µm, over which no coating was present or the coating was incomplete (Figure 4.7b). In these areas, the surface appears similar to that of the as-received fibers, with a series of pore openings present throughout the surface. Figure 4.7a shows an area on which PEGMA coating adhered; there are still some apparently open, but smaller, surface pores. Figure 4.8 shows the PEGMA coating on cleaned polypropylene hollow fibers. SEM evaluation of this sample showed no areas similar to those in Fig. 4.7a or 4.7b; the PEGMA-coated surface appeared to be continuous and complete.

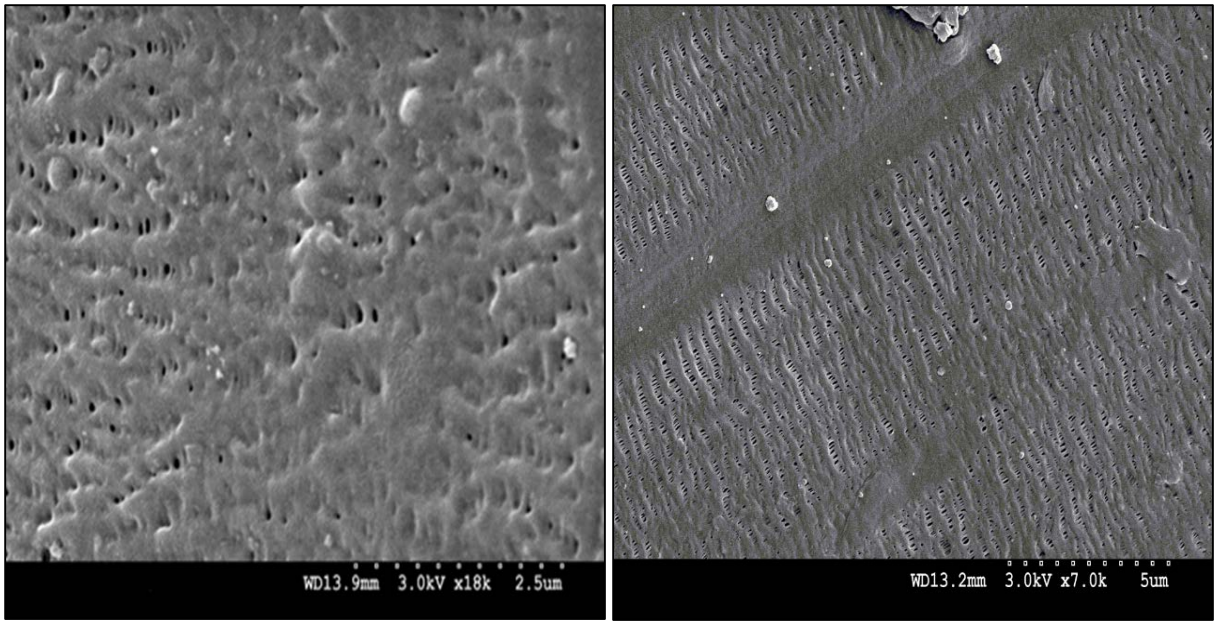

Figure 4.7. SEM images of as-received PP HFMs functionalized by 100 nm thick s-ATRP PEGMA coating. (a, *left*): Area with incomplete coating. (b, *right*) Area with no coating

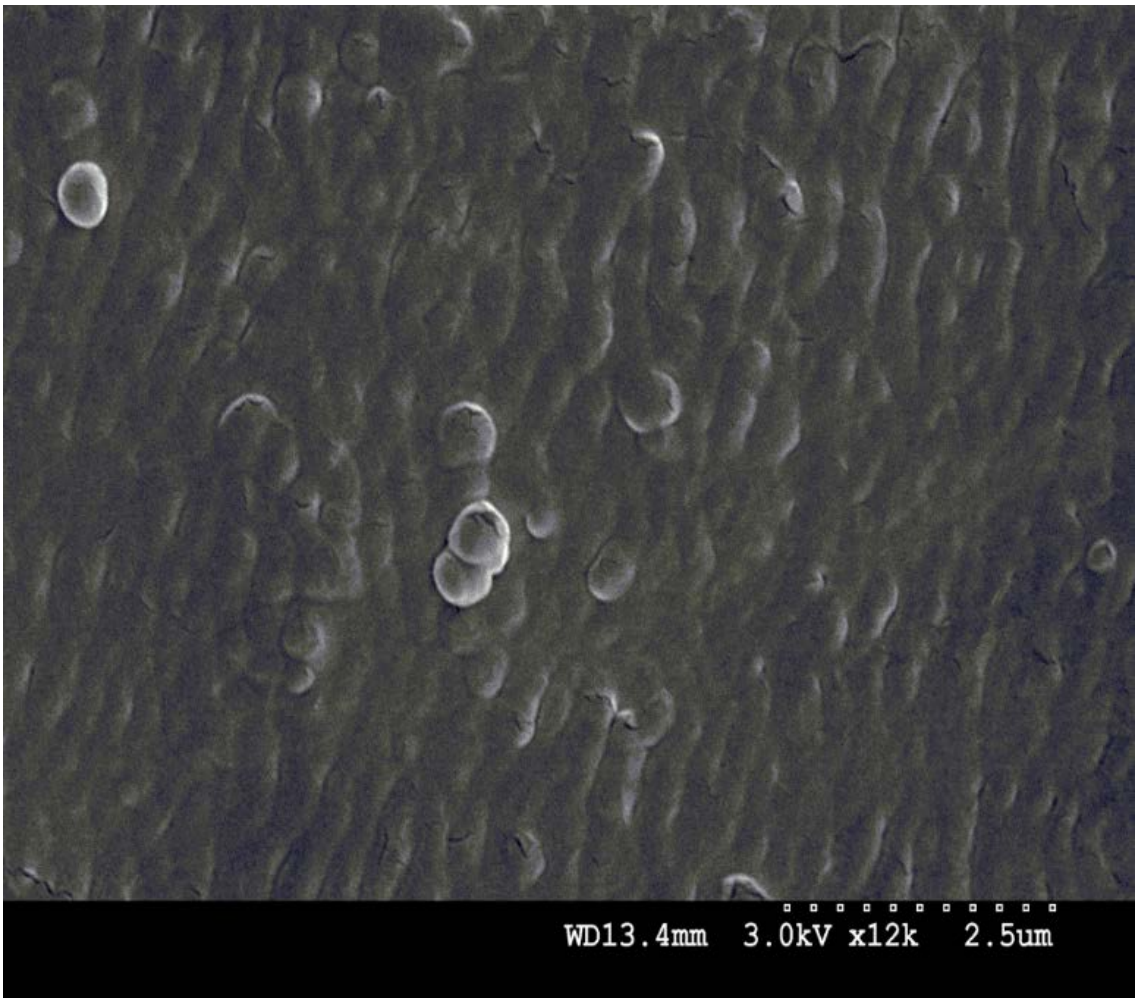

Figure 4.8. Continuous PEGMA coating formed by s-ATRP on surface PP HFM, cleaned by 36 hour extraction with acetone solvent prior to s-ATRP.

Table 4.3. Bubble point testing on PP hollow fibers before and after s-ATRP coatings.

Fiber Type	Bubble Pressure in water (psi)	Estimated Maximum Pore Size (μm)
Virgin X30-240	25	1.67
PEGMA coating (s-ATRP) on leached X30-240	> 160	< 0.26

4.4.4 Bubble point testing.

The presence of a continuous coating across the entire surface area of the PP HFM was further indicated by the pore size measurement by bubble point testing as shown in Table 3. The maximum pressure achieved in the pressure cell was 160 psi; at this point, no bubbles could be observed for fibers cleaned prior to coating deposition. The estimated maximum pore size for this pressure was 0.26 □m, although the actual maximum pore size must be smaller than this value. Therefore, the maximum pore size has decreased by at least 85% when residual oils are removed by leaching.

4.5 Discussion

This study illustrates that PMP and PP HFMs, both commonly used in blood oxygenation, contain significant amounts of an oily contaminant. Extensive Soxhlet extraction of these fibers with acetone caused them to lose between 2.5% to 7.5% of their initial weight. The HPLC chromatograms of the oily contaminants were compared to those of neat soybean oil and neat mineral oil.

Soybean oil showed two sets of elution peaks. The first set appears at elution times of ~ 40 and ~60 minutes. The two elution peaks are very sharp, suggesting that these might represent very specific compounds. During this time period, the hydrogen bonding difference between the solutes (decane or oleic acid) and the elution mixture is decreasing significantly. The second set of elution peaks appears over the time range, 140 to 190 minutes. During this time period, the polar component values of the solutes and elution mixtures solubility parameters are becoming more closely matched. Furthermore, there are a number of peaks, suggesting that multiple compounds are being released from the column, such as the many fatty acids that comprise soybean oil.

HPLC chromatograms of mineral oil showed two sets of elution peaks. The lower set, released over the time range of 40 to 90 minutes, showed multiple component peaks, consistent with the many alkane chain components of mineral oil. At higher elution times (t > 140 minutes), there is a slow change in the absorbance amplitude, but no definitive peaks.

The chromatograms of the residue leached from both PMP and PP HMFs showed two sets of components. The PMP elution curve appears to be more similar to that of mineral oil than soybean oil; it shows multiple peaks in the range, 40 to 90 minutes, with a slow, broad increase after 120 minutes. The chromatogram for the PP leachate shows lower levels of contaminants. However, it also shows a few sharp peaks at 60 and 70 minutes, followed by a gradual increase for times longer than 120 minutes. It appears that the residue leached from both of these hollow fibers is more similar to mineral oil than soybean oil. Since the fabrication protocols for both of these commercial hollow fibers are not generally known, we were unable to ascertain the phase-separating agent used for the production of either fiber type. However, both types of fiber release low molecular weight, oily residue on long term extractions. This could be caused by insufficient cleaning or the use of a polar solvent that unintentionally leaves the non-polar components of the co-solvent.

Removal of this residue was found to critical for the fabrication of a defect free, continuous coating on the entirety of the fiber's surface. Without extensive cleaning, s-ATRP derived polymer coatings left exposed surfaces on the order of 100 µm. s-ATRP coating fabrication performed on leached hollow fibers produced a continuous coating. The PEG coating also reduced the average pore size of the hollow fibers. Coated fibers had an estimated a maximum pore size of less than 0.26 µm, while uncoated fibers had a maximum pore size of 1.67 µm.

It is not clear what the effects of a leachable agent, like mineral oil, might be on the performance of as-received hollow fiber membranes in contact with blood. This would be a topic for further evaluation.

4.6 Conclusions

These data show that leachable residue is present in two commercial hollow fiber membranes. A covalently bound coating on unleached fibers left a number of open pores and was not uniformly applied across the whole exterior fiber surface. By contrast, the same coating applied to leached fibers appeared to be uniformly applied, and decreased the estimated maximum pore size by over a factor of five. The leachable residue appears to be more similar to mineral oil than soybean oil (these two oils have been reported as phase separation agents in the manufacture of hollow fibers).

CHAPTER 5 ULTRATHIN POLYMER FILMS ON POLYMERIC HOLLOW FIBER VIA AQUEOUS S-ATRP

Keywords: S-ATRP, Composite Membrane, Hollow Fiber Membrane, Aqueous ATRP

5.0 Abstract

Surface-initiated atom transfer radical polymerization (s-ATRP) allows the deposition of a of polymer coating securely to membrane surfaces with very precisely controlled thicknesses. This process suffers from many drawbacks, particularly the use of gaseous ozone to form active sites on the surface to be treated and the use of air and water sensitive reagents during surface halogenation. We have developed a technique to form ultra-thin surface initiated atom transfer radical polymerization (s-ATRP) coatings on the surface of polymeric hollow fiber membranes (HFMs) using completely aqueous procedures. The resulting porous membrane is coated with a thin, continuous and non-porous coating that was mechanically robust and durable. Virgin polypropylene hollow fiber membranes had a maximum pore size of 1.12 um. After deposition of the s-ATRP formed outer coating, the maximum pore size was below 0.25 um. The coating was continuous, non-porous, mechanically stable and resistant to degradation. The permeability of the composite hollow fiber membranes to oxygen and carbon dioxide is 9.40+2.17x10-4 and 9.83+2.65x10-4 ml/(s*cm2*cmHg), respectively.

5.1 Highlights

- Surface initiated atom transfer radical polymerization may be performed from the surface of polymeric hollow fiber membranes using only water soluble components
- This coating is resistant to delamination, peeling or degradation
- Significant pore size reduction may be realized by using surface initiated ATRP in an aqueous solvent
- The exterior polymer coating formed via aqueous s-ATRP does not penetrate into the pores of the membrane and is confined to the exterior.

5.2 Introduction

Due to their large number of industrial applications, surface modifications of hollow fiber membranes have been the subject of a great deal of investigation.

Surface initiated atom transfer radical polymerization (s-ATRP) has been explored within the last decade to modify membranes for a variety of purposes. These include the production of hollow fibers with anti-bacterial surfaces for water purification[23], non-fouling surfaces[54-57],to change the surface charge or hydrophillicity of these membranes[56] and to produce stimuli responsive membranes.[35, 58] Additionally, s-ATRP has been used to prepare membranes to improve biocompatibility.[59, 60]

s-ATRP has been explored as a technique to modify porous membranes to produce an ion exchange medium.[26] Using this same approach, commercially available hollow fiber membranes have been modified into absorbers for protein purification.[27] These protein purification membrane have shown dramatic improvements over previously available ion exchange media.

This approach to membrane modification was investigated to produce porous substrates coated with non-porous coatings to produce composite membranes.[22] These membranes are produced by

initiating the surface initiated atom transfer radical polymerization from an exterior surface of the porous support. The thickness of the non-porous layer can be carefully controlled through the polymerization time.

Each of the membrane modification approaches and techniques typically requires three steps. During the first step, the membrane's surface is functionalized with chemical groups, typically hydroxyls. The second stage involves the attachment of halogen atoms to the surface, usually through bonding of halogen containing molecules to the hydroxyls, often through ester bonds. The most commonly used molecule to produce a halogenated surface in this manner is bromoisobutyryl bromide. The last phase consists of growing the polymer film itself using s-ATRP to produce the non-porous polymer film itself.

Two major hindrances to the wider adoption of s-ATRP to membrane modification typically involve the wide use of ozone to functionalize the surface of polymer with hydroxyls as well as the use air sensitive reagents, such as bromoisobutryl bromide, to functionalize the surface of the membranes with the halogens necessary to initiate the s-ATRP reaction. During this halogenation step, the aprotic or non-polar solvents necessary to prevent side reactions the halogenation agent, will dissolve and attack many polymer components contained within the membrane module. Ozonation is typically non-uniform and over-exposure may quickly degrade a membrane's mechanical strength.

For composite membranes formed using s-ATRP to be commercially adopted, the coating must be able to be fabricated on large membrane surface areas. In particular, the s-ATRP formed coating formation must be feasible at the lowest cost possible. This requires that aqueous reagents during all phases of coating deposition is the most economical option.

Previous investigators have produced polymer membrane coatings synthesized using aqueous functionalization and subsequent s-ATRP steps. [61] This approach used electrostatic adsorption to bond the initiator molecule to the membrane's surface. This type of bonding has certain advantages, notably the ability to perform all steps necessary to produce the coating in a few hours. Certain potential applications for membranes with either a surface coating or a gas permeable selective layer formed using s-ATRP may require covalent bonds between the porous membrane substrate and s-ATRP formed polymer layer.

The surfaces of saturated hydrocarbon polymers have been hydroxylated using a number of reagents in aqueous solutions including ammonium persulfate[28], Fenton type reagents[62] and potassium persulfate.[30, 31] Of these approaches, potassium persulfate appears to be the most promising. Ammonium persulfate tends to form carboxylic acids on the polymer surface while Fenton type reagents may have a range of side reactions other than hydroxyl formation.[63]

The emplacement of halogen atoms on the surface of membranes is a necessary step preceding the growth of ATRP formed polymers. The use of halide mineral acids may allow the halogenation of membrane surfaces in a more convenient, faster and cost effective manner. This may enable scaling the production of composite membranes formed using s-ATRP.

One of the most of the most attractive features of forming s-ATRP coatings on composite hollow membranes is the potential to form these coatings on the surface of fibers that are contained within membrane modules. This approach would allow very thin (~100 nm thick) coatings to be deposited on these fibers without the danger of damage to these delicate coatings during processing and handling.

For this technique to be feasible, the solvent must be aqueous. Various investigators have performed ATRP and s-ATRP reactions in aqueous solvents. To our knowledge hollow fiber membranes have not been modified by s-ATRP formed polymer coatings performed using water as the solvent.

In order to form a surface initiated atom transfer (s-ATRP) coating on a surface, that surface must be functionalized with halogen atoms, usually chlorine or bromine. When performing s-ATRP reactions from a polymer surface, this surface is typically functionalized with hydroxyl groups. A subsequent reaction with these hydroxyls produces a halogenated surface.

Previous investigators forming coatings on porous membranes using surface initiated atom transfer radical polymerization would expose the membrane to ozone gas.[23] Ozone would attack the surface of the membrane and produce peroxide groups.[64] The membrane surface was then reduced to form hydroxyl groups.

Hydroxylation with ozone has several disadvantages. The tensile strength of PP HFM decreases dramatically with increasing ozone treatment times. [65] Wang and colleagues found that to obtain the surface concentrations of functional groups necessary for further coating attachment by exposure to ozone for 5 min, the tensile strength decreased by 40%.[65]

As ozone reacts quickly with PP HFM, attempts to functionalize these fibers in large amounts or after potting into membrane modules will likely lead to non-uniformity of the surface density of the resulting hydroxyl groups. Portions of these bundles may receive excessive ozone exposure, resulting in reduced tensile strength while other areas may receive insufficient ozone exposure.

Hydroxylation of PP or other HFM with ozone is typically a two-step process. The first involves the exposure of the fibers to ozone itself. This procedure produces peroxide groups on the fiber surface. During the second stage these peroxides are reduced to hydroxyls, typically using sodium iodide.[23]

The potassium persulfate technique eliminates many of the issues occurring due to treatment of hollow fibers by ozone. This technique involves immersing the fibers in hot water with dissolved potassium persulfate.[30, 33] This technique is a one step process to produce hydroxyl functionalized membranes. Additionally, the reaction conditions can be easily controlled to produce uniformly hydroxyl functionalized hollow fiber bundles.

Hydroxylation of hollow fiber membranes using potassium persulfate has an added benefit in that extended reaction times do not cause dramatic decreases in mechanical strength.[66] Tensile testing of PP HFMs treated with potassium persulfate displayed a much smaller decrease in mechanical strength than comparative treatment of such fibers with ozone. For some short reaction times, the mechanical strength of the fibers is observed to increase.[30]

When exposed to temperatures above 80^{o}C, the persulfate ion degrades into sulfate radicals. These radicals form hydroxyl radicals upon reaction with water. Hydroxyl radicals are very reactive and are capable of homolitically breaking chemical bonds of the sp3 hybridized carbon forming the backbone of polypropylene. These carbon radicals will form hydroxyl groups upon exposure to hydroxyl radicals.

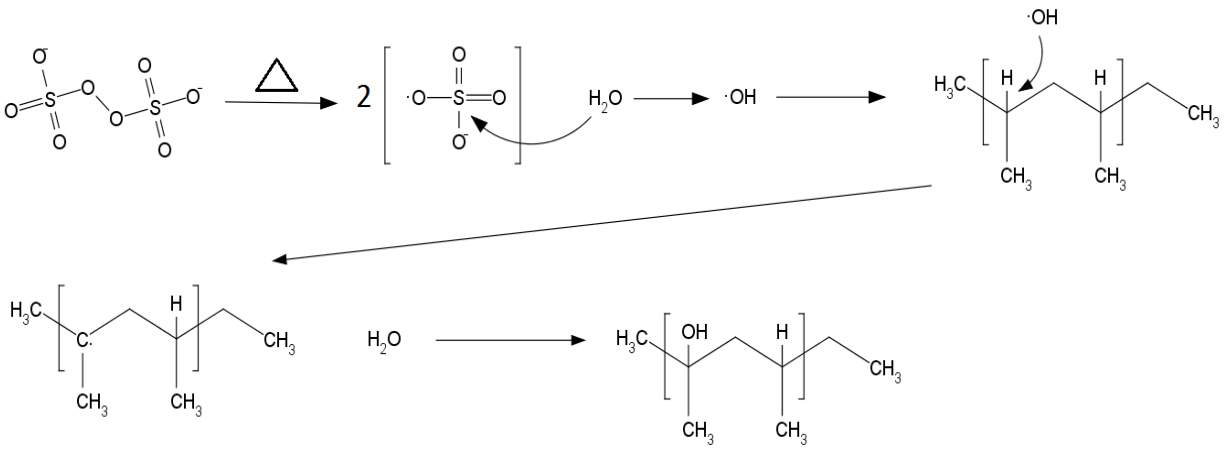

Figure 5.1; Reaction mechanism through which hydroxyl groups are formed on hydrocarbon polymer chains through aqueous potassium persulfate at temperatures above 80°C.

Previously explored techniques of producing s-ATRP coatings on porous polymer membranes involved the halogenation of these surfaces, after hydroxylation, through the use of acyl halide containing molecules. [22, 23] Halogenation with acyl halides necessarily involves the use of air and water sensitive reagents.

Treatment of hydroxyl functionalized hollow fiber membranes with halogen acids such as hydrochloric or hydrobromic acids allows these hydroxyls to be converted to the corresponding halogen.[67] This approach can be carried out at room temperature and does not use water or air sensitive reagents. Halogenation can be obtained simply by immersing the hydroxylated fibers into the mineral acid as opposed to the prolonged drop-wise addition of an acyl halide into a sealed flask over ice. This process may allow the scaled production of composite hollow fiber membranes using inexpensive reagents.

The halogenation of hydroxyl groups in the presence of halogen acid is driven to higher yields at lower pH and higher concentrations of the mineral acid.[68] Higher temperatures, in addition to increasing acid concentrations will cause faster halogenation of the hydroxyl. [69] The kinetic of this reaction may allow for rapid, inexpensive emplacement of bromine of chlorine on the surface of hydroxylated hollow fiber membranes in an aqueous solution at room temperature.

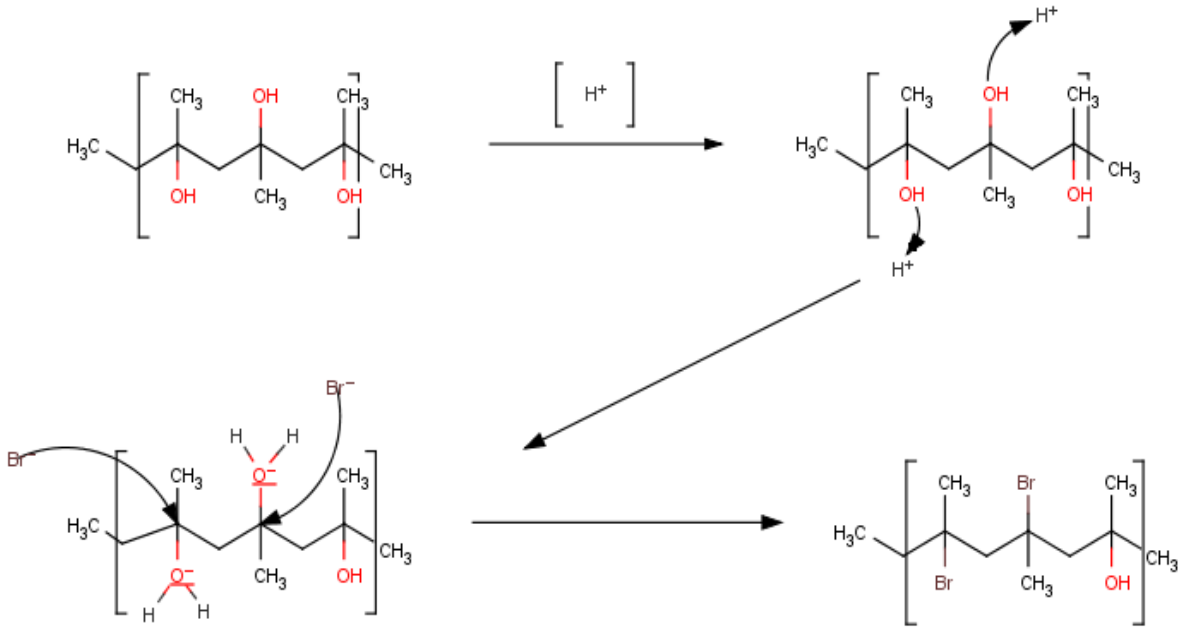

Figure 5.2; Bromination of hydroxylated polypropylene using concentrated hydrobromic acid.

Investigators such as Xu et. al[70] have polymerized poly(ethylene glycol) methacrylate from the surface of silicon using aqueous ATRP. Using the copper based ATRP recipe, PEGMA was polymerized from the surface of PP HFMs functionalized with bromine using water as the solvent of reaction.

In this work, a pathway to the fabrication of a membrane coating fabricated using s-ATRP with each reaction step using water as the solvent was explored. Bubble testing was done to measure the maximum porosity of the membrane coating. The permeability of the membrane to blood gases was measured and the durability of the coating was evaluated using a standardized method. Etching procedures proved that the s-ATRP formed polymer coating did not penetrate into the porosity of membrane wall.

5.3 Materials and Methods

5.3.1 Materials and Equipment

Commercially available polypropylene (PP) hollow fiber membrane (HFM) (X30-240) were purchased from Celgard™. The fiber was in the form of a single strand on a reel.
Polyethylene glycol methacrylate (PEGMA) (Mn 360) was purchased from Sigma Aldrich and purified by passing through chromatography columns containing aluminum oxide.
CuCl, CuCl2, 2-2’ bipyridine (bpy), hydrobromic acid, hydrochloric acid and potassium persulfate were purchased from Sigma Aldrich and used without further purification.

Deionized water was used as the solvent in all reactions and was purchased from Fischer Scientific. Reactive ion etching was performed using a Plasmalab 80 Plus manufactured by Oxford Instruments. Oxygen was used during operation as the etching gas.

5.3.2 S-ATRP Process

The persulfate ion has been used to functionalize the surface of polymers with hydroxyls.[30, 33, 37] This approach involves immersing the surface of the polymer to be treated in a de-oxygenated aqueous solution containing the persulfate ion at a temperature between 80 and 100^{o}C.

Clean PP HFM mats were immersed in 500 ml of water contained in a two necked reaction flask. One neck is connected to a reflux column. The other neck is sealed with a rubber septum. Through this septum a 6" needle is inserted and argon passed through to sparge the water. The water was heated to boiling under argon sparge and reflux.

After reaching boiling, the argon sparge was continued for twenty minutes. At this point, 50 mg of potassium persulfate was placed into a plunger type syringe. This syringe was then connected to a needle which was then inserted through the rubber septum. Water was then withdrawn into the syringe, dissolving the potassium persulfate. This solution was then inserted into the reaction flask. The persulfate solution was permitted to react with the PP HFM for ten minutes.

Afterwards, the fibers were withdrawn from the solution, washed with copious amounts of DI water and then dried under vacuum.

Hydroxyl functionalized PP HFMs were immersed into concentrated aqueous hydrobromic acid or hydrochloric acid to produce bromine or chlorine functionalized surfaces, respectively. The reaction was allowed to continue for 24 hours. Afterward, the fibers were cleaned with copious amounts of water and then dried under vacuum.

10 ml of DI water was mixed with 10 ml of PEGMA in a small flask and then sparged with argon for twenty minutes to remove oxygen. Afterward, 90 mg of CuCl, 24 mg of $CuCl_2$ and 168 mg of bpy were added to the flask. The solution was then sonicated with continuing argon sparge for 10 min.

A section of fiber mat functionalized with either bromine or chlorine was immersed in the above solution for twenty fours. Afterward, the fibers were removed from the solution, rinsed with copious amounts of DI water and then dried under vacuum.

5.3.3 Coating Evaluation

The surface of PP HFM was etched in such a manner that a sharp interface is formed between the coated and etched surface. This was done by placing a glass slide over a mat of HFM coated using s-ATRP in such a manner that the slide occludes approximately half of the fiber mat.

The glass slide covered mat was then placed into the reactive ion etch machine. An oxygen plasma was created in vacuum at 13.56 MHz and 100 W that was directed at the surface of the partially occluded membrane mat for five minutes.

Afterward the plasma reaction chamber was vented to atmosphere, the fiber mat was removed and stored until imaging using scanning electron microscopy

5.3.4 Imaging of Hollow Fiber Membrane Samples Using Scanning Electron Microscopy

Mats of hollow fiber membrane were fixed to aluminum support slugs using colloidal graphite. This technique allowed a grounded connected between the surface of the membrane and the aluminum support slug, preventing charging during the imaging procedure. Before imaging, the samples were coated with a layer of gold-palladium using RF sputtering to a thickness of 20 nm.

5.3.5 Bubble Testing of Coated HFM.

In order to determine the maximum pore size and size distribution, bubble testing was performed. This procedure was modified from ASTM F316-03. A cylindrical test cell was fabricated using polycarbonate. A long strand of X30-240 PP HFM coated using the s-ATRP method was embedded in a castable polyurethane resin in loop configuration to allow gas into the membrane's lumen and allowed it to cross the wall of the fiber.

The hollow fiber loop was immersed in a liquid within the vessel. Pressure was introduced and was raised until the first bubble was formed.

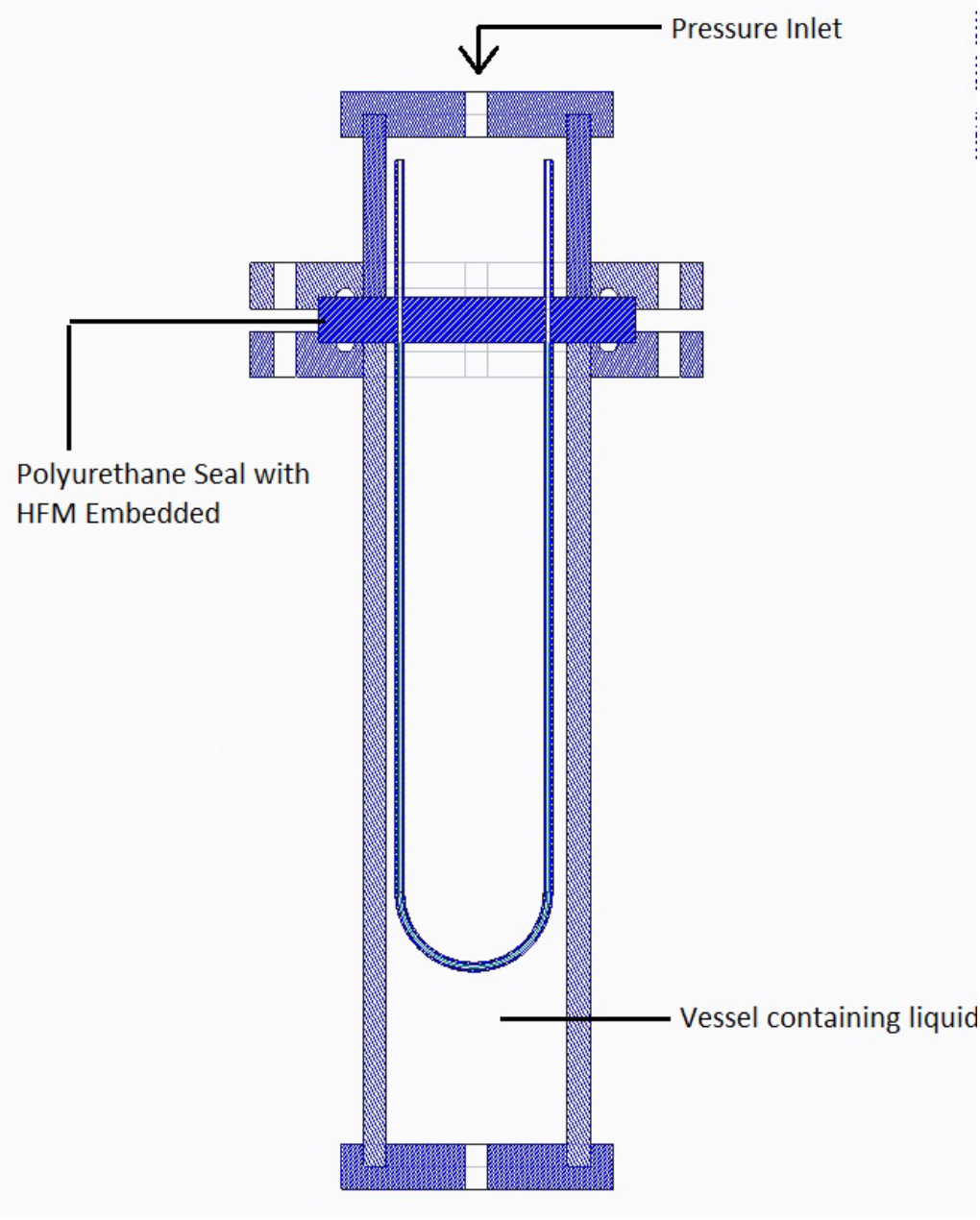

Figure 5.3; Pressure vessel for perform bubble testing, permeability and burst strength of hollow fiber membrane.

5.3.6 Pressure Testing of Coated HFM

Hollow fiber membranes embedded in polyurethane were placed in the pressure testing apparatus in figure 5.3. Using a preselected gas, the pressure to the bore of the fiber was raised to 10 psi. The amount of gas diffusing across the membrane was then measured using a mass flow controller connected to the bottom port. The gas pressure was then raised in increments of 10 psi and the flow correspondingly measured.

5.3.7 Durability/Delamination Resistance of S-ATRP Coating

Polypropylene hollow fiber membranes with an exterior, non-porous coating fabricated using s-ATRP were immersed into boiling saline as described in the technical standard ASTM D 3354-76. The coated fiber was immersed into the boiling saline for a period of eight hours and then removed. Afterward, these fibers were washed thoroughly with DI water and then dried under vacuum. SEM imaging was then performed to determine the integrity of the coated surface.

5.3.8 Porosity Determination

Bubble testing was used to determine to maximum pore size for a hollow fiber membrane coated via s-ATRP. The method used was modified from ASTM standard F316-03.[71] This technique involves applying pressure through the bore of the porous membrane and observing the onset of continuous bubbles. The bubble point is the pressure in which a stream of continuous bubbles is observed. At this pressure, the surface tension forces within the pore of the membrane are overcome, allowing the gas to escape.

As shown in figure 5.4, when a liquid filled pore is exposed to pressure two opposing forces are established at the liquid/gas interface. These forces are the pressure imposed by the gas applied to the bore and the capillary pressure formed from the action of the liquid within the pore.

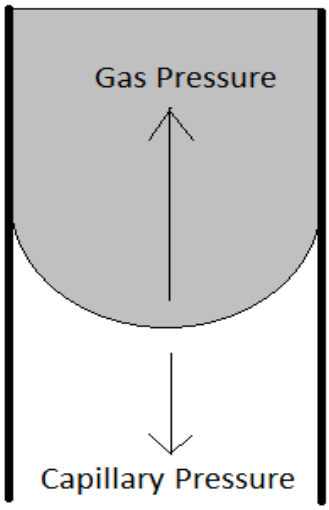

Figure 5.4; Diagram of opposing forces of capillary pressure and gas pressure formed within individual pore of a hollow fiber membrane during bubble testing. Gray area represents liquid within pore.

These forces at the liquid/gas interface are balanced in equation (5.1) shown below. The term on the left of the equation represents the force from the capillary action of the liquid. On the right, the force imposed on the liquid/gas interface due to the gas pressure.

$$2\pi r\gamma \cos\theta = \pi r^2 p \qquad (5.1)$$

$$r = radius\ of\ capillary$$

$$\gamma = surface\ tension\ of\ liquid$$

$$\theta = Angle\ of\ contact\ between\ surface\ of\ liquid\ and\ wall\ of\ capillary$$

$$p = Pressure\ of\ gas\ within\ capillary$$

Equation 5.1 can be simplified, equating the diameter of the pore, surface tension and gas pressure as shown in equation 5.2.

$$D = \frac{4\gamma}{P} \qquad (5.2)$$

$$D = Pore\ Diameter$$

5.3.9 Durability of Surface Coating

Previously investigated and developed coatings for membranes and medical purposes have failed due to delaminating or degradation of the coating from the surface. Such failures are unacceptable for medical coatings as the degradation products can cause serious injury to the patient. During early development of heparin coated blood circuits for example, several patients were injured or killed when the surface bound heparin leached into the bloodstream.

The s-ATRP formed outer coating on the outer surface of the hollow fiber is anchored via carbon-carbon covalent bonds. To ensure that this coating will not degrade or delaminate, the fibers were immersed

into boiling saline for a period of eight hours in accordance to ASTM Standard D 3354-76. Afterward, the fibers were dried and imaged using scanning electron microscopy.

5.4 Results and Discussion

The thickness of the coating was estimated using the data Xu et.[70] et. Al. developed, measuring the thickness of the s-ATRP fabricated PEGMA coating using ellipsometry. This data is plotted below in figure 5.4.

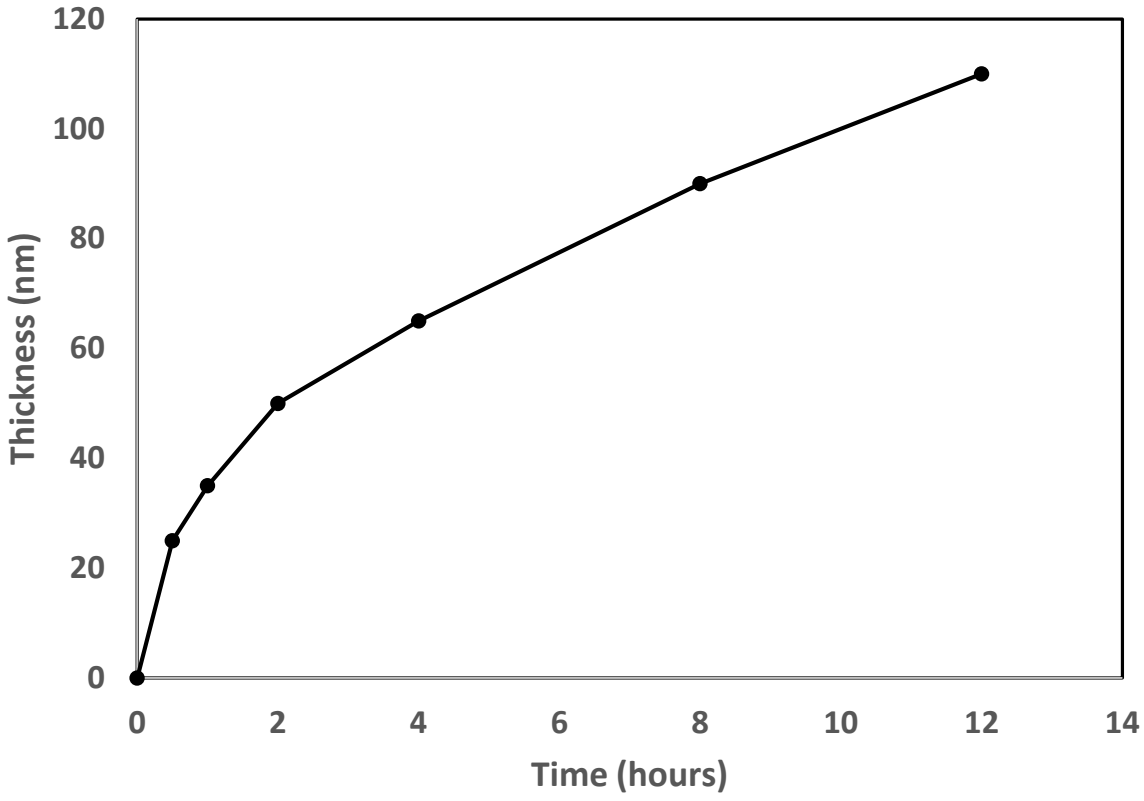

Figure 5.5 Thickness of PEGMA film grown from surface of silicon wafer using aqueous ATRP. [PEGMA]:[CuCl]:[CuCl2]:[bpy]=167:5:1:12. Same reaction conditions were used to fabricate s-ATRP membrane coating on surface of brominated PP HFMs.

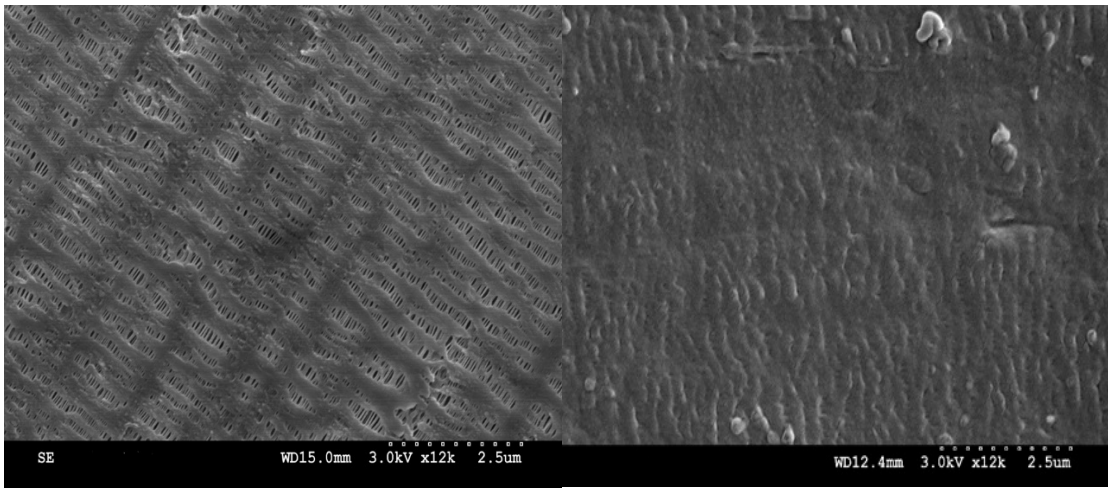

Figure 5.6; (*left*) Virgin PP HFM, (*right*) SEM image of surface of PP HFM after surface initiated atom transfer radical polymerization. Surface was hydroxylated using aqueous potassium persulfate and subsequently brominated using hydrobromic acid. Aqueous s-ATRP was then performed.

Successful formation of a non-porous exterior coating on PP HFMs was confirmed using scanning electron microscopy. This coating is continuous over the entirety of the hollow fiber membranes that were examined.

For s-ATRP to be an effective method of forming non-porous membrane coatings, the coating must not penetrate into the underlying porosity within the wall of the fiber. If this were to occur, the diffusion resistance of the membrane would be unacceptably high.

To determine the depth that the polymer coating formed via s-ATRP penetrated into the underlying porosity within the wall, the fiber was differentially etched. This produced a clean break between the etched and unetched portions of the fiber.

This procedure shows that with the protocol used within this study, the s-ATRP derived coating is confined to the exterior surface of the fiber. As a result, s-ATRP formed membrane coatings have the ability to act as the selective layer for gas separation applications or as a non-porous layer to prevent blood plasma leakage during blood oxygenation.

S-ATRP formed coatings may potentially be synthesized within the walls of a fiber through control of the surface tension of the reaction solution and the growth rate of s-ATRP reaction. In such a case, the reaction solution necessary to form the s-ATRP coating would need sufficiently low surface tension and viscosity to quickly penetrate into the pores of the hollow fiber. Additionally, the s-ATRP polymerization rate would necessarily be adjusted to be so low that free, unreacted monomer had sufficient time to diffuse into the wall of the fiber and reach an active polymerization site. A high polymerization rate would result in the consumption of available monomer molecules at the exterior surface before they reached the interior of the fiber.

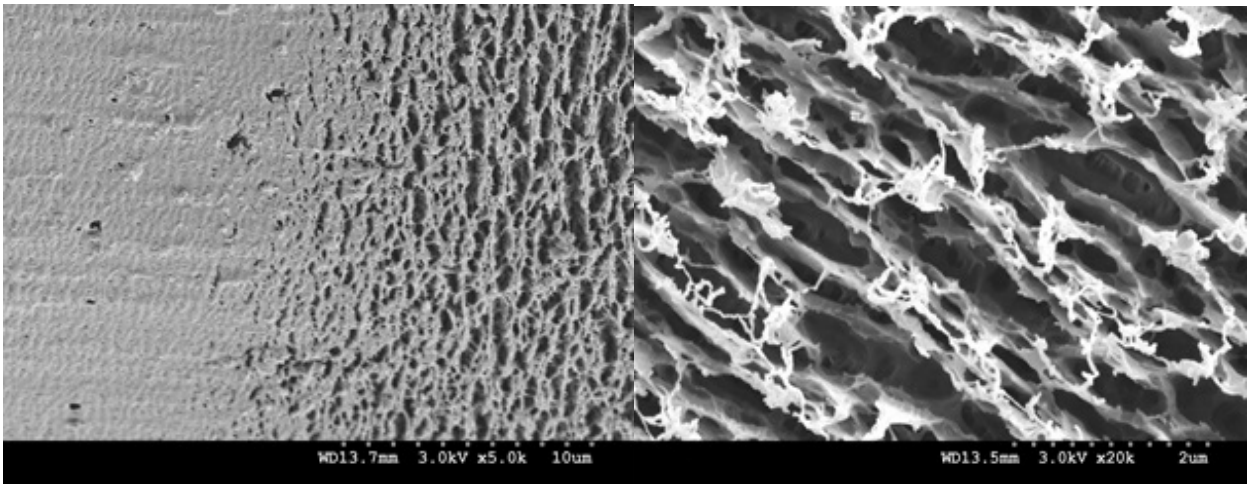

Figure 5.7; *(left)* SEM of interface between and unetched surface of composite PP HFM formed by s-ATRP. *(right)* Porosity within wall of fiber, underneath outer coating after directed plasma etching.

Table 5.1. Bubble pressure of polypropylene hollow fiber membranes before and after deposition of PEGMA coating using s-ATRP. Coating thickness is approximately 120 nm.

Fiber Type	Bubble Pressure in water (psi)	Maximum Pore Size (μm)
Virgin X30-240	25	1.67
Composite PP HFM with S-ATRP Coating	>160 (maximum range of regulator)	<0.26

To determine the extent of exposed porosity on the surface of composite HFMs fabricated using s-ATRP, bubble testing was performed on these fibers. The apparatus in figure 5.3 was used.

The pore sizes of the hollow fiber are diminished as the s-ATRP formed coating polymerizes across the entirety of the fiber. This result corresponds well to the result encountered by Husson et. Al.[26] These investigators found that the pore sizes on the surface of membranes not only decreased but became more uniform with increasing polymerization time. The results presented here indicate that the results found by the Husson group may be extended to membrane size scales that are industrially relevant. Furthermore, the process of forming this s-ATRP coating may be performed at atmospheric conditions using aqueous solvents and inexpensive, available reagents.

5.4.1 Durability of Surface Coating

No cracks, fissures or delaminated areas were found on the exterior surface of the coated fiber using SEM imaging after submersion in boiling saline for 8 hours.

The results of this test indicate that very strong bonds are present between the s-ATRP formed coating and the underlying porous support. Leaching or delamination of coatings in biomedical applications is an important concern. As it did not degrade or delaminate after an extended period immersed in boiling saline, the s-ATRP formed polymer coating would be expected to remain intact during use in harsh environments.

The ability of a coating to remain intact in harsh environments, such as prolonged contact with blood, is absolutely necessary if s-ATRP is going to be used to develop a long term blood oxygenation device or be employed in any other medical device.

5.4.2 Pressure Testing of S-ATRP Formed Composite Hollow Fiber Membrane

Pressure testing indicated that PP HFMs with an exterior s-ATRP formed coating did burst or fail at pressures up to 160 psi (g).

Mechanical durability of membranes is critical to their performance in most applications in which they are employed. In blood oxygenators, hollow fiber membranes must not burst or fail as the patient's life would be severely jeopardized. In separation applications, the maximum operating pressure often imposes a ceiling on the performance of these membranes.

These results show that forming an s-ATRP formed coating on the exterior surface of a PP HFM does not appreciably decrease its maximum operating pressure. Thus, s-ATRP formed coating techniques may be able to produce improved hollow fiber membranes for various applications without significantly changing the operational parameters of the process involved.

Table 5.2. Blood gas permeability across hollow fiber membranes for blood oxygenation.

	Permeability (ml/(s*cm^2*cmHg))			
Fiber Type	**O_2**		**CO_2**	
	Measured	**Literature[38]**	**Measured**	**Literature[38]**
PP	**$1.74 \pm 0.54 \times 10^{-2}$**	**$1.77 \pm 0.01 \times 10^{-2}$**	**$2.10 \pm 0.71 \times 10^{-2}$**	**$1.62 \pm 0.01 \times 10^{-2}$**
PMP	**$7.38 \pm 3.90 \times 10^{-3}$**	**$1.08 \pm 0.09 \times 10^{-3}$**	**$1.47 \pm 0.72 \times 10^{-3}$**	**$1.40 \pm 0.08 \times 10^{-3}$**
s-ATRP Formed Composite	**$9.40 \pm 2.17 \times 10^{-4}$**		**$9.83 \pm 2.65 \times 10^{-4}$**	

5.4.3 Permeability of HFM Functionalized with S-ATRP Formed PEGMA Coating

Table 5.2 describes the permeability of PP HFMs coated via s-ATRP to carbon dioxide and oxygen.

As shown in table 5.2 the two orders of magnitude decrease of the permeability through the s-ATRP formed PP composite HFM compared to the virgin PP HFM indicates that the s-ATRP formed coating was uniformly deposited. This finding, coupled with the bubble point data indicates that no large areas of porosity was exposed. The nearly identical permeability of carbon dioxide and oxygen through the s-ATRP formed composite membrane indicates that small pinholes are present in the membrane.

Pinholes of this nature should not cause blood plasma leakage or gas emboli formation due to their very small diameter and thus very high pressure needed to force liquid through them as determined by bubble point testing. These pinholes would prevent membranes formed using this approach from applications in gas separation. For this to be possible, the membrane coating would need to be formed in such as manner as to occlude and eliminate these pinholes, possibly by increasing the thickness of the coating or using a basement fiber with much smaller pores.

Due to the persistent radical effect, surface initiated radical polymerizations will ultimately reach a maximum thickness. The persistent radical effect involves the formation of a non-polymerizable specie when two adjacent radicals interact with each other. The persistent radical effect can be minimized, and the maximum thickness of the polymer coating can be maximized by decreasing the polymerization rate while minimizing the number of actively growing polymer chains.

Minimization of the persistent radical effect in the s-ATRP reactions performed in this work may be accomplished by reducing the concentration of Cu(I) and Cu(II) while decreasing the Cu(I)/Cu(II) ratio. Future work will involve the formation of coatings using these experimental parameters. The use of porous supports with much smaller porosity should allow the pores to be completely occluded, allowing the formation of selectively permeable membranes.

5.5 Conclusions

S-ATRP is capable of coating extended, porous hollow fiber membrane surfaces with a continuous polymer coating to form a composite membrane using only aqueous solutions in relatively mild conditions. These coatings are durable, and do not penetrate into the underlying porous wall of the HFM. The blood gas permeability of these composite membranes, coupled with the ability to synthesize these membrane coatings indicates that they would be excellent candidates for use in blood oxygenation. This aqueous process could be used to retrofit existing oxygenators incorporating polypropylene hollow fiber membranes. The fibers could be functionalized using persulfate and hydrobromic acid before or after potting. The s-ATRP formed coating would then be synthesized on the exterior surface of the PP HFM in-situ of the oxygenator, preventing damage during handling and processing.

CHAPTER 6 MODULES FABRICATED USING COMPOSITE S-ATRP HOLLOW FIBER MEMBRANES

Keywords: S-ATRP, Composite Membrane, Hollow Fiber Membrane, Membrane Module

6.0 Abstract

Hollow fiber membrane modules incorporating polypropylene hollow fibers were coated *in-situ* using surface initiated atom transfer radical polymerization. These modules did not leak when exposed to a powerful surfactant. The uncoated, control module leaked out completely in under five seconds. The membrane modules were shown to be capable of exchanging adequate oxygen to function in a blood oxygenation role.

6.1 Highlights

- Surface initiated atom transfer radical polymerization (s-ATRP) allows for the deposition of polymer coatings that are non-porous with very accurately defined thicknesses.
- This technique allows for the deposition of these coatings on the surface of membranes while they are contained within a membrane module.
- Modules containing composite membranes were resistant to blood plasma leakage that affects porous membranes in blood oxygenators.
- Membrane modules incorporating s-ATRP formed membranes were able to adequately oxygenate blood and were shown to be resistant to fluid leakage.

6.2. Introduction

Polymeric hollow fiber membranes (HFMs) are widely used due to their low cost and high surface area per unit volume, when compared to spiral wound membranes. Their current uses include industrial filtration, water treatment, blood oxygenation, hemodialysis, and gas separation.

The processes used to manufacture these fibers typically involve one of two methods, thermally-induced phase separation (TIPS) and melt spinning cold stretching (MSCS). TIPS begins with mixing a polymer and a suitable solvent at an elevated temperature to generate a miscible solution. The solution is extruded through a hollow die and solidified by cooling. As the temperature of the fiber decreases, the solvent and polymer demix , the solvent forms a separate phase (creating solvent-filled voids), and the polymer crystallizes. The solvent is then removed, leaving open pores. Polypropylene hollow fiber membranes can be produced by a TIPS process using soybean oil as the solvent. [72] MSCS involves extruding a molten polymer through a die, followed by high extension (drawing) to crystallize the polymer, and then heat treating the fiber. Micropore formation occurs as crystalline lamellae spread during cold stretching.[73] Both processes usually result in HFMs with high porosity. The morphology of the HFM is open and sponge-like. At the outer surface of the fiber, the porosity is lower and is characterized by regularly spaced holes.

Coatings are being developed for desired for HFMs used in long term blood oxygenation as a way to eliminate blood plasma leakage and gas emboli formation. Blood plasma leakage occurs from open

pores when phospholipids in the blood act as surfactants. The phospholipids diminish the surface tension at the blood plasma/gas interface, resulting in plasma intrusion into the membrane pores. When it reaches the inner wall of the fiber, the plasma is carried out through the bore, producing foam. When foaming occurs, blood oxygenators must be replaced, as they can no longer exchange sufficient blood gas. Conversely, pressure variations across the HFM lumen can allow the formation of gas bubbles on the blood side of the membrane if there are open pores on the exterior surface. Gas emboli can severely injure or kill a patient quickly.

Various methods of applying surface coatings to HFMs have been explored. Unfortunately, all encounter serious drawbacks. These coatings are highly susceptible to damage before sealing into modules. A 15% and 34% increase in carbon dioxide and oxygen permeation rate was found in these fibers after they were knitted into mats for ease of handling.[38]

Prior fiber coating approaches limited the range of polymer chemistries that could be used for coating. Plasma polymerization can only form a polymer coating if a suitable precursor gas is available. To date, the most widely explored coatings are based on fluorocarbon, hydrocarbon, siloxane or a combination of these chemistries.

Surface-initiated polymerization provides several advantages over previously explored methods. The presence of covalent bonds between the coating and the substrate prevents leaching, delamination or degradation of the coating. Additionally, a wider variety of coating chemistries may be used with this process.

With the discovery of atom transfer radical polymerization (ATRP), controlled radical polymerizations can now be carried out in mild environments and solvents. These polymerizations may be initiated at the surface of HFMs and may be performed within a module. This aspect is particularly attractive as it would prevent damage to the very thin coating during module fabrication.

Within the last decade, s-ATRP has been explored to produce gas separation membranes on a limited basis.[22, 74, 75] However, these membranes were of an investigatory nature and were formed on a limited surface area. To achieve commercial success in various applications of membranes such as blood oxygenation and gas separations s-ATRP formed membranes must be efficiently formed on large surface areas.

Prior work has demonstrated the feasibility of coating hollow fibers via s-ATRP polymerizations. In this work, hollow fiber in membrane modules were coated, *in situ*, using s-ATRP. These modules were then evaluated to determine the functionality, durability and consistency of the membrane coating.

6.3 Materials and Methods

Polypropylene hollow fiber membrane (X30-240) reels were purchased from Celgard™ USA. Reagent grade potassium peroxydisulfate and poly(ethylene glycol) methacrylate (PEGMA) (Average MW 360) were purchased from Sigma Aldrich. Ultra high purity argon was purchased from Scott-Gross Co. Ozone was produced with an A2Z Ozone generator (model# A2ZS-6G). Hydrobromic acid was purified by distillation at 125oC. [76] Copper (I) chloride, copper (II) chloride, 2-2’ bipyridine, α-bromoisobutyryl bromide, tetrahydrofuran (THF), acetone and triethylamine (TEA) were purchased from Sigma and used without further purification. Stainless steel tubing of 3/4” diameter and stainless steel Swage-lock™

fittings were used to fabricate the laboratory scale membrane modules. Castable polyurethane resin (WC-781) from BJ Industries was used to the seal the hollow fiber membranes into the module.

6.3.1 Fiber Bundle Fabrication and Cleaning

Propylene hollow fibers were wound around two dowels set at a distance of 30 inches apart. Fifty wraps produced bundles containing 100 parallel fibers each (~76 m of hollow fiber). The bundles were secured by wrapping them with a thin tantalum wire. The fibers were then placed into a Soxhlet extractor with acetone. The fibers were extracted continuously for 36 hours and then dried under vacuum overnight after removal.

6.3.2 Fabrication of Hollow Fiber Membrane Module

Eight of the hollow fiber membrane bundles were incorporated into a laboratory scale membrane module using protocol developed by Li et. Al.[77] The tantalum wire, which prevented unravelling of the bundles, was removed before insertion into the tube. The module was comprised of ¾ inch diameter stainless tubing with stainless steel Yor-lock™ fittings. WC-781 castable polyurethane resin was used to seal the hollow fibers into the ends of the module. After this resin had hardened for 24 hours, the module was heated to 80^{o}C, removed from the oven and the ends of the protruding resin were cut with a razor to expose the hollow fibers.

6.3.3 Functionalization of fiber exterior surfaces

6.3.3.1 Exterior surface hydroxylation

PP HF bundles were then placed into a 500 ml two-necked reaction flask and filled with deionized water until the fibers were completely submerged (600 ml). A condenser was attached to one of the necks and the other was fitted with a rubber septum. A 6” needle was then inserted into the rubber septum to sparge the water with argon. The reaction flask was heated until reflux while under argon sparge.

60 mg of potassium peroxydisulfate was placed into a syringe. This syringe was attached to a needle that was then inserted through the rubber septum. To minimize contact with oxygen, after the needle was below the waterline, the plunger of the syringe was withdrawn slightly to allow the sparged water in the flask to enter the syringe barrel and dissolve the potassium peroxydisulfate. The plunger was then pushed back to add the potassium peroxydisulfate into the reaction flask.

The polypropylene hollow fiber membrane bundles were permitted to react for 10 min. Afterward they were removed, washed thoroughly with deionized (DI) water and then dried under vacuum overnight.

6.3.3.2 Exterior surface bromination

Two of these bundles were placed it a 500 ml reaction flask fitted with a bubbling type air lock. 400 ml of dry THF and 40 ml TEA was placed in the flask. A 6” needle was then used to sparge the solution with argon. During this time, the reaction flask was placed over ice and cooled. In a graduated cylinder 10 ml of bromoisobutryl bromide and 60 ml of dry THF were added, and the flask was quickly sealed with a rubber septum.

Using the argon feed and double tipped needle, the contents of the graduated cylinder were then transferred to the reaction flask dropwise, over the course of one hour. After this transfer was completed, the contents of the reaction flask was allowed to react overnight. The fibers were removed, cleaned with copious amounts of water and acetone, and dried under vacuum.

6.3.4 s-ATRP coating protocols

Eight of the brominated bundles were encased in a stainless steel module and potted at each end. After the polyurethane resin hardened, the HFMs were exposed by slicing with a sharp razor. The aqueous solution previously used to synthesize the surface-initiated atom transfer radical polymerization coating (Chapter 3) was placed into contact with the exterior surface of the fibers for a period of 24 hours. Afterward DI water was flushed through the membrane module overnight. The module was the dried by flushing with compressed air for 24 hours.

The HFMs were exposed to a solution of 15 mmol PEGMA, 1.08 mmol bipyridine, 0.45 mmol CuCl, 0.09 mmol $CuCl_2$ and 37.04 mol of water to form membrane coating via s-ATRP. The water and PEGMA were mixed and sparged with argon for 20 min before addition of the remaining components. After sparging, the CuCl, $CuCl_2$, and bipyridine were added to the water/PEGMA solution. This solution was then sonicated under an argon sparge for ten minutes. The fibers were allowed to remain in this ATRP solution for 24 hours, then cleaned thoroughly with DI water and dried under vacuum.

6.3.5 Fabrication of PMP Module

PMP hollow fiber bundles containing one hundred fibers each were fabricated, then cleaned with acetone and dried under vacuum. Eight of these virgin PMP hollow fiber bundles were then potted into stainless steel modules as described previously (6.3.2). These fiber were not functionalized and were evaluated as received.

6.3.6 Gas Permeation of s-ATRP formed Composite PP HFM Module

The blood gas permeability of HFM modules containing composite PP HFMs formed by s-ATRP was determined by exposing one of the tube side openings to a pure gas supply while the other tube opening was sealed. The gas permeating across the membrane was then measured in an immersed graduated cylinder.

6.3.7 Leak Testing of Membrane Modules

The shell sides of hollow fiber membrane modules (Li et al [77]) were connected to a closed circuit of a liquid reservoir, pump, and tubing to connect them. 1 liter of deionized water was the circulated through the shell side of the membrane module while compressed air at 50 psi was pumped through the tube side. Water was permitted to recirculate through the module for a period of one hour. At this point, 10 ml of Triton X-100 was added to the fluid reservoir without interrupting circulation. Sweep gas exiting the module was carefully observed for the presence of fluid or bubbles.

6.3.8 Gas Transfer to Blood

Bovine blood was collected from a local slaughterhouse and was immediately treated with an acid-citrate-dextrose (ACD) solution as described by Strumia et al.[78] This citrated blood was then refrigerated and used within a few hours of collection. A mock circulatory loop was made using the protocol described by “Guidance for Cardiopulmonary Bypass Oxygenators 510(k) Submissions; Final Guidance for Industry and FDA Staff.”[79] This loop consisted of the membrane module connected in a closed loop to a blood reservoir, pump and commercially available oxygenator. This loop was connected to the shell side of the membrane module allowing blood to enter and leave the unit. The commercially available oxygenator used carbon dioxide as a sweep gas to remove oxygen from the blood and saturate it with CO_2, mimicking the action of the body. Ports were attached at the entrance and exit of the membrane module to allow for collection of blood samples. Blood samples were taken prior to and after

the membrane module. These samples were then analyzed with the blood gas analyzer and the blood gas exchange rate across the membrane unit was determined.

6.3.9 Apparent Porosity Determination

Modules incorporating s-ATRP formed composite HFMs connected to separate, closed loops of recirculating DI water through both the exterior and bore surfaces. One liter of DI water was circulated through the shell side of the module using a centrifugal pump with a maximum output pressure of 5 psi. 500 ml of DI water was recirculated through the tube side at 60 psi at a rate of 70 ml/min. The pressure of the water entering each compartment of the membrane unit was recorded. Additionally, the volume of each fluid reservoir was recorded with time.

6.4 Results and Discussion

6.4.1 Gas permeability

The permeability of the three membrane types to pure gases is displayed in Table 6.1. As expected, the s-ATRP PP HFM have a slightly lower permeance to blood gases due to the presence of a coating, and therefore significantly lower surface porosity than either the PP or PMP HFMs. The permeance values of the s-ATRP formed composite PP HFMs are on the same order of magnitude as the virgin PP or PMP fibers. It is therefore expected that the s-ATRP formed composite HFMs may be used in blood oxygenators of similar size to those currently in existence. The coating reduces the oxygen permeance to 30% of that for the untreated PP HFM, while reducing the carbon dioxide permeance to 75% of that for the untreated PP HFM. The coated PMP membrane has higher oxygen and carbon dioxide permeances.

Table 6.1. Gas permeance of hollow fibers

	Permeance (ml/min-m^2-kPa)		
Blood gas	**PP**	**s-ATRP PMP**	**s-ATRP PP**
Oxygen	**830 ± 39**	**486 ± 40**	**234 ± 97**
Carbon dioxide	**603 ± 22**	**661 ± 324**	**442± 119**

6.4.2 Susceptibility to Blood Plasma Leakage

This test simulated the effect of blood plasma leakage by exposing the porous surface of the HFMs to an aqueous solution containing an effective surfactant – Triton X-100. The surfactant accelerates the wetting process that would occur when exposed to blood. Modules with three different membrane types were evaluated for gas leakage: uncoated PP HFM, S-ATRP coated PP HFM, and virgin PMP fibers. A timer was initiated when the Triton X-100 was added to the water in order to measure the time between surfactant addition and wetting out of the fiber.

The modules containing virgin PP HFMs immediately wetted out and began producing large amounts of foam from the bores of the HFMs. The modules containing s-ATRP coated PP or PMP HFMs did not produce foam after one hour of continuous exposure to the Triton X-100 solution. This solution was permitted to remain in contact with the HFM overnight. However, no foam was observed for either the PMP or PP coated HFM modules.

A critical pore size equation (ASTM E128-99) [11] was used to estimate of the pore size of the membrane if leaks had been observed during leak testing. Using the applied pressure (50 psig), the surface tension values of PP and the pore size equation from ASTM E128-99, the critical pore size of the coated membrane would be 0.226 µm. No leaking was observed during exposure of the PMP and s-ATRP formed modules to the 1% aqueous Triton X-100 solutions, which, according the manufacturer, has a surface tension of 30 dynes/cm. Therefore, the presence of pores of 0.23 µm or larger are absent from these modules.

6.4.3 Gas Transfer to Blood

In order for a leak-proof membrane technology to be feasible, it must be capable of removing carbon dioxide from the blood at the rate at which it is produced through metabolism, while supplying oxygen at a rate equal to or above the body's need. This gas exchange must occur with sufficient efficiency that the membrane surface area is not overly large to allow for ambulation and minimize priming volume.

The mass transfer coefficients of the blood side boundary layer as well as through the coated membrane itself are displayed in Table 6.2. The coefficient for each blood gas's diffusion through the boundary layer is approximately an order of magnitude higher than the coefficient through the membrane. The major barrier to blood gas diffusion in modern membrane oxygenators is permeation through the blood side boundary layer.[80, 81] These mass transfer coefficients are dependent upon the flow rate and orientation of the fibers. The literature reports values of between 10^{-5} and 10^{-4} m/s.[82] These values correspond well to the liquid side boundary layer mass transfer coefficients calculated using the methods described by Taskin[83] et al., using the Sherwood number correction factors derived by Wickramasinghe et al.[80, 84, 85] for the laboratory scale hollow fiber membrane module.

The s-ATRP PP HFM mass transfer coefficient across the membrane to blood gas is nearly an order of magnitude less than the blood side boundary layer. Thus, this membrane should be suitable for blood oxygenation use with oxygenators using current membrane capacities and configurations.

During testing of the membrane unit with bovine blood, no blood was observed leaking through the membrane and flowing out of the membrane bores.

Table 6.2. Convective mass transfer coefficients for gas transfer across coated PP hollow fibers

	Convective Mass Transfer Coefficient (m/s)	
Blood Gas	**Blood Side Boundary Layer**	**Through S-ATRP PP HFM**
Oxygen	$1x10^{-4}$	$4.77x10^{-3}$
Carbon Dioxide	$1x10^{-4}$	$3.47x10^{-3}$

6.4.4 Apparent Porosity of Coated PP Modules

When DI water was recirculated through separate circuits attached to both the shell and lumen side of the membrane module, the volume of the water circulating through the shell side of the module began increasing at regular rate.

Assuming Poiseuille flow within the pores spanning the walls of the hollow fiber, the maximum porosity of the membrane module was determined. This was accomplished by calculating the flux across a pore with a maximum size of 0.23 μm at a pressure of 55 psi and length of 30 μm, corresponding to the membrane's wall thickness. This value was then divided into the flux rate of water across the membrane module to determine the number of pores with diameter of 0.23 μm. The total area of these pores was then determined as a percentage of the total membrane surface area of the module. The porosity of the hollow fiber membrane modules decreased from 45% to at least 0.26% or below after the formation of an s-ATRP film. This represents at least a 99.4% decrease in the porosity of the membrane unit.

6.5 Conclusions

Surface-initiated atom transfer radical polymerization may be used to form very thin (~100 nm) polymer coatings on the exterior surface of polymer hollow fiber membranes after these membranes have been potted into membrane modules. These composite membranes are leak proof at modest applied pressures, do not produce gas emboli and are capable of adequate blood gas exchange to function as oxygenators.

CHAPTER 7 ALGORITHM TO DETERMINE PROPORTIONAL LIMIT FROM TENSILE TESTING DATA

7.0 Abstract

A method was developed which allows determination of the proportional limit of a sample from tensile testing data. This technique calculates the cumulative moving average at each successive measurement point in the data and then calculates the difference between this value and the value of the modulus at that point. A minimum value in this difference when the linear elastic region of deformation transitions to plastic deformation. This method can be implemented in software for rapid analysis of large sets of tensile testing data. This method has the potential to non-destructively test mechanical parts.

7.1 Highlights

- Proportional limit of sample is determined by determining minimum difference of modulus at each point and the cumulative modulus at that point
- Method allows for determination of proportional limit without human intervention
- Method is easily incorporated into data analysis programs, allowing for efficient analysis of large numbers of specimens
- Method allows real-time determination of proportional limit, potentially allowing for "minimally destructive" testing of parts and components to determine maximum service load
- This algorithm may produce errors in the following instances
    - Elastic region of deformation is non-linear and the stress is not directly related to the strain by the Young's Modulus
    - Tensile testing data with large amounts of noise
    - Tensile testing with a sampling rate high enough to allow consecutive data to be identical will need to be smoothed with a moving average before analysis

7.2 Introduction

Tensile testing is widely used in academia and industry to determine the mechanical properties of solid materials. This procedure involves the measurement of an applied force and corresponding extension. These data point are then normalized and plotted against one another to produce the familiar stress-strain diagram.

During the initial stages of extension, the stress and strain will directly related by a constant – the Young's modulus. During this linear region in which elastic deformation occurs, if the force applied to the sample were to be released, the sample's dimensions would return to their initial values.

Application of force beyond a certain point results in permanent deformation of the sample. Deformation beyond this point is non-linear and permanent. This point of permanent deformation is known as the yield point. In practice, the yield point is described by two different locations on the stress strain diagram.

The proportional limit is the point at which stress and strain on a sample reach the end of their linear relationship and deformation becomes non-linear. At this point, a small increase in the stress creates a much larger increase in strain.

The elastic limit is slightly (in some cases much larger as in the case of elastomers) larger than the proportional limit. This is the minimum point at which permanent deformation may be measured.

During service, failure is most often defined as permanent deformation of a component. For this reason, accurate determination of the yield point of a given material is critical to the design of component constructed from it.[86] Additionally, accurate knowledge of the forces necessary to cause yielding are critical to the successful use of a component.

As important as yield point determination is, the current, widely accepted method of determining this value is the 0.2% offset method. A point is offset on the x axis (denoting strain) by an amount equal to 0.2% strain. A straight line is then constructed with slope equal to that of the elastic region. The yielding point is defined as the point at which these two lines intersect.

There are important problems with this approach. The 0.2% offset method does not identify the exact yielding point; thus a component exposed to forces at the yielding point, as determined by the 0.2% offset method, has already undergone permanent deformation and has failed. The second drawback with this approach is the reliance on human interaction to determine the point of intersection. As a result, significant differences in yielding points from the same data could be reached by different investigators.

The need to have human interaction in the 0.2% offset method of yielding determination prevents automation of the analysis process. This prevents rapid analysis of many samples via computer programs.

The mechanical analysis of treated hollow fiber is critical as structural failure could potentially lead to catastrophic results in blood oxygenator applications. Additionally, membrane separation processes are more efficient at high pressures, placing an upper bound on performance due to membrane mechanical properties.

The development of an algorithm to determine the yield point of tensile testing data that does not require human interaction would significantly increase the accuracy this data. This approach would remove human error and allow for much faster analysis when incorporated into data analysis software.

7.3 Algorithm to Determine Proportional Limit

The proportional limit of force vs. elongation data from tensile testing information was identified by determining the point of inflection occurring at the end of the linear elastic region of deformation. This algorithm consists of the following steps:

1. The modulus at each measurement point is first calculated.
2. The cumulative moving average of the modulus at each measurement point was then determined, with the initial point of measurement serving as the first point in the cumulative moving average determination.
3. The absolute value of the difference between the cumulative moving average of the modulus and the modulus itself was determined at each point of measurement.
4. The minimum value of the difference between the modulus moving average and the modulus at each point was determined. This minimum value point is the point of inflection occurring at the end of the elastic region and is the proportional limit.

The cumulative moving average of the modulus at each point, i, was determined by averaging the modulus at that point, i, with the modulus at each of the preceding points. This is described by equation 7.1.

$$CA_i = \frac{\sum_1^i E_i}{i} \qquad \text{Equation 7.1}$$

The index, i, of the point of inflection is determined by the minimum value of the difference between the cumulative moving average of the modulus and the modulus at each point as described by equation 6.2.

$$i_{yield} \cong min\left\{\sqrt{(CA_i - E_i)^2}\right\} \qquad \text{Equation 7.2}$$

7.4 Precautions Necessary for Implementation of Algorithm

7.4.1 Removal of Initial Portions of Measurement from Consideration of Minimum Value

The use of equation 7.2 to determine the index of the data point corresponding to the point of inflection must be used with caution as the first few data points will produce values near zero as shown in figure 7.3. This is due to the cumulative moving average of one point will be equal to the value of that point. Therefore, the difference between the cumulative moving average of the modulus and the value of the modulus at only one point will be zero. As the number of points increases from this first point, the difference between the cumulative moving average and the actual value at each point will increase until a normalization occurs. This value of the difference will then begin to decrease until a minimum is reached, corresponding to the yield point.

7.4.2 Smoothing of Data

The stress-strain data may need to be smoothed using a moving average if one or both of the following conditions are met;

1. If the data are acquired with a sampling rate that is very high in relation to the elongation rate, consecutive data points may be identical. In this case, the algorithm presented here would indicate a point of inflection at each occurrence of identical consecutive measurements.
2. If the data are sufficiently noisy as to not be consistently monotonically increasing through the elastic region of deformation, errors will be produced. In such a case, each point in which the data decreased, a point of inflection would be determined by the algorithm presented here.

The preferred manner of smoothing the data is to use a moving average function that replaces the value at each point by the average of n preceding and n succeeding values where n is an integer. The ideal value of n is the smallest possible integer which allows for the stress-strain data to be monotonically increasing during the region of elastic deformation.

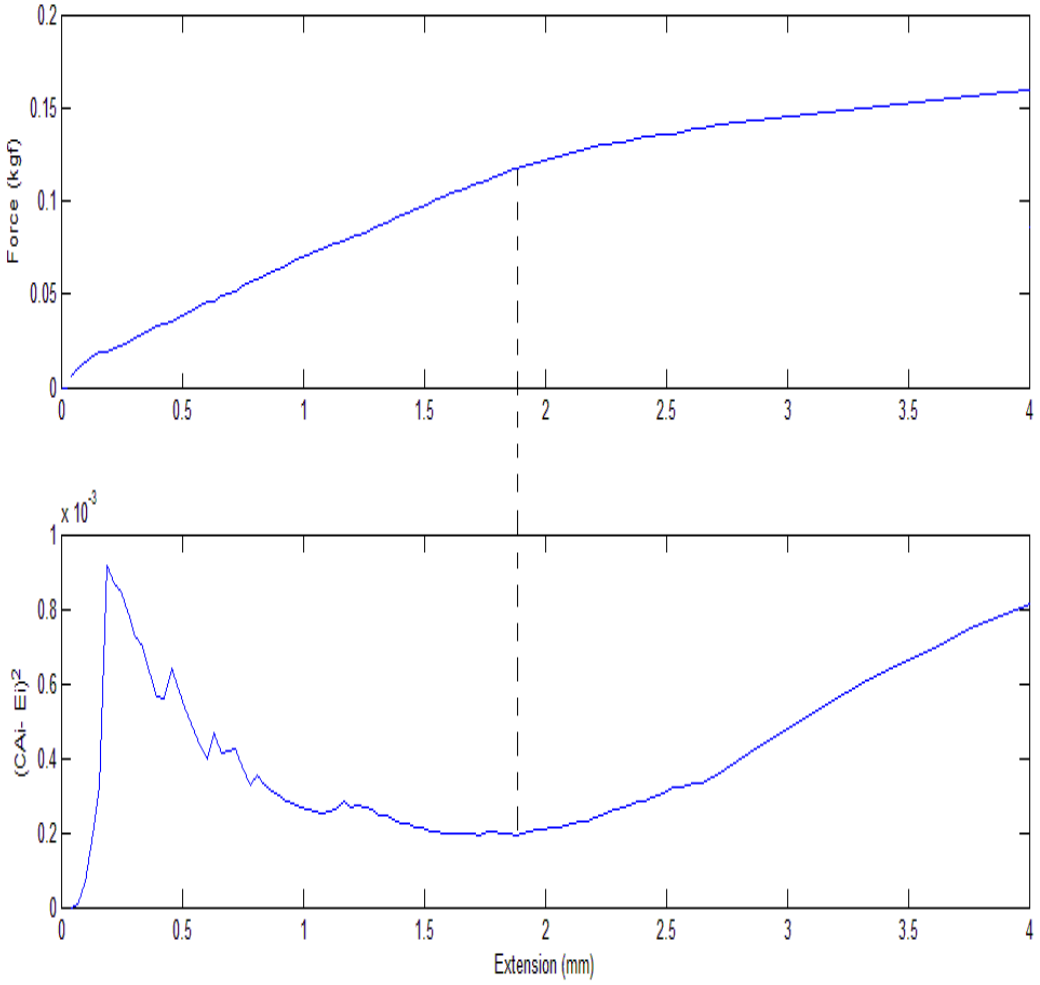

Figure 7.1; (top) Force vs. elongation data for polypropylene hollow fiber membranes after testing. (bottom) Difference between modulus at each point and cumulative moving average of modulus at each point. The dashed line is used to indicate correspondence between minimum value of equation 8.2 and point of inflection.

7.5 Effect of Linearity in Elastic Region of Deformation

The algorithm presented here was used to determine the yielding point of polypropylene HFMs. As the linearity of the elastic region decreases, the minimum value of the difference between the modulus cumulative moving average and the value of the modulus at each point becomes less defined.

Tensile testing data with a curved elastic region of deformation may not be able to be analyzed using the method presented here.

7.6 Comparison of Minimum Value Algorithm and 0.2% Offset Method

The yield point as determined by the minimum value of the difference in the cumulative moving average of the modulus at each point will have a lower value by definition than that produced by the 0.2% offset method. This is due to the algorithm selecting the proportionality limit at the point of yielding. This is illustrated in figure 7.6.

7.6.1 Experimental

Polypropylene HFMs were cleaned using Soxhlet extraction with acetone and then treated with either ammonium persulfate, potassium persulfate or ozone and then analyzed with tensile testing as described in chapter 3.

7.6.2 Analysis of Tensile Testing Data

The tensile testing data were analyzed using the MATLAB program available in Appendix A. This program used the difference of the cumulative moving average and actual value of the modulus algorithm to determine proportion limit.

The yield point of the tensile testing data was then manually analyzed using the 0.2% offset method. A line was created with slope equal to that of the stress-strain during the elastic region of deformation. This line was offset by 0.2% of the strain. The yielding point for this analysis was found where this offset line intersected with the stress-strain data as shown in figure 6.6.

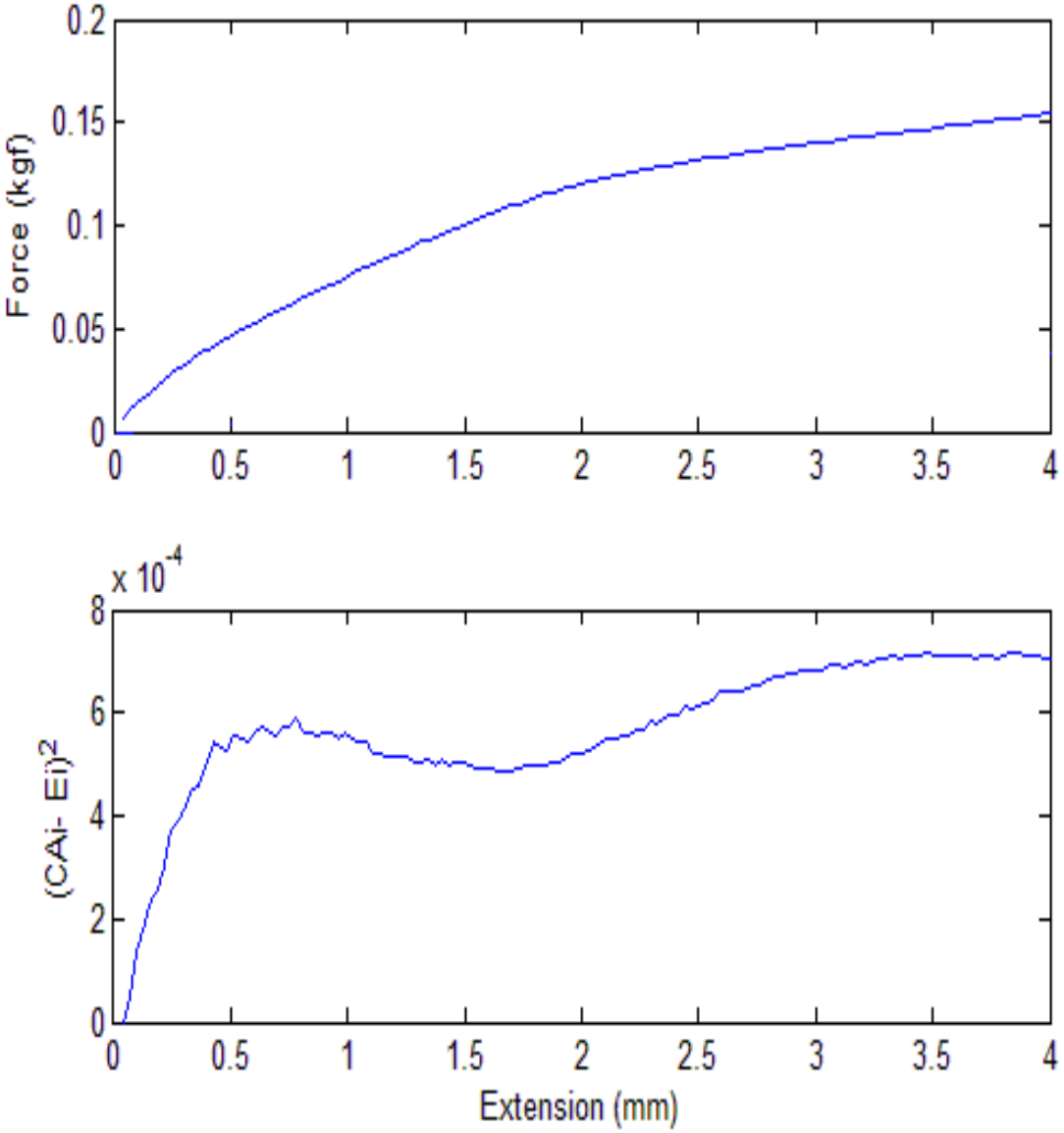

Figure 7.2 (top) Force vs elongation data of polypropylene HFM. (Bottom) Square of the difference between the cumulative moving average and the value of the modulus at each point. Note minimum value corresponding to point of inflection – proportional limit. The data here are relatively curved in the elastic region, resulting in a less well defined minimum value.

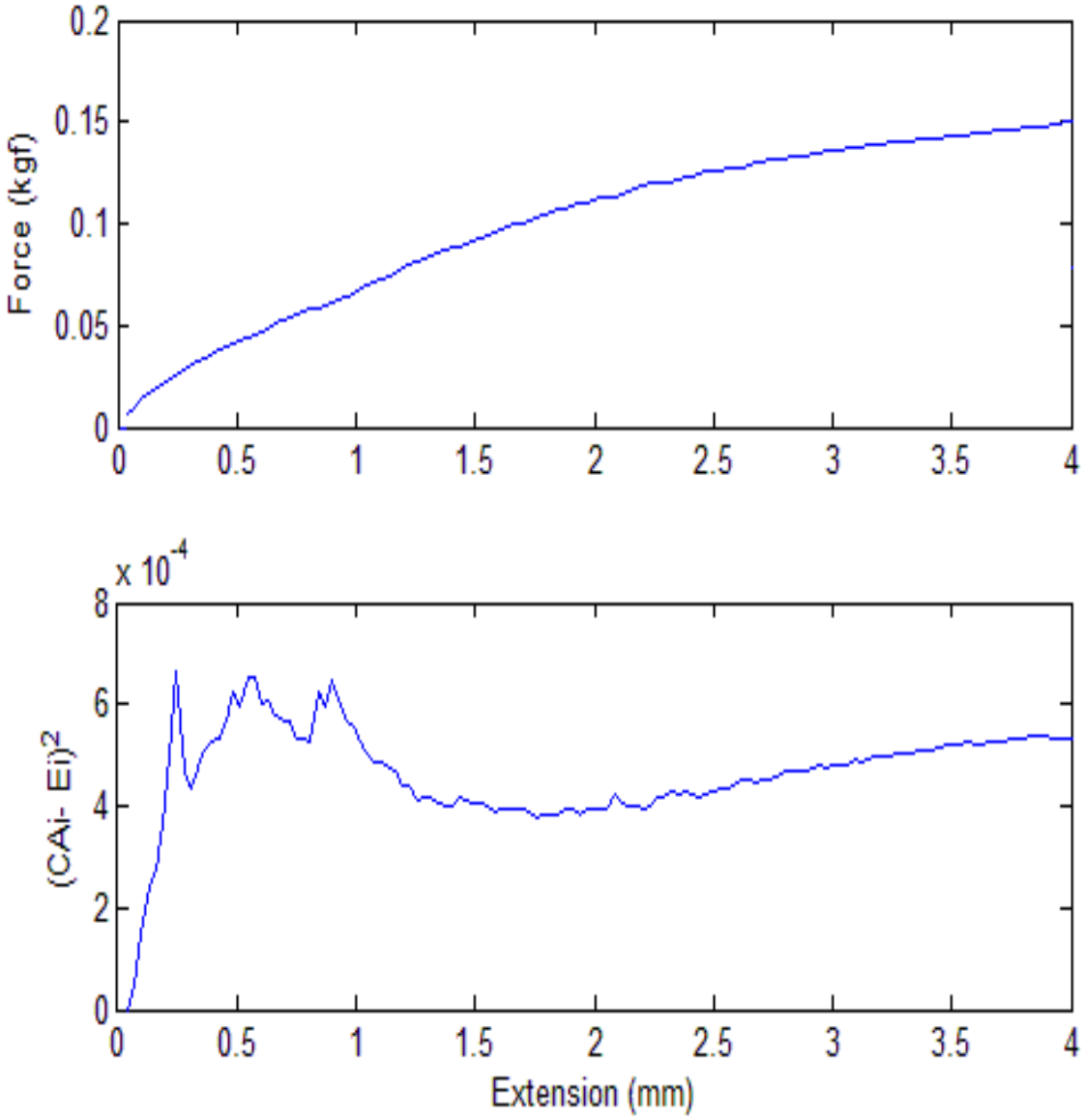

Figure 7.3 (top) Force vs elongation data of polypropylene HFM. (Bottom) Square of the difference between the cumulative moving average and the value of the modulus at each point. The data here are highly curved in the elastic region, resulting in a minimally defined minimum value.

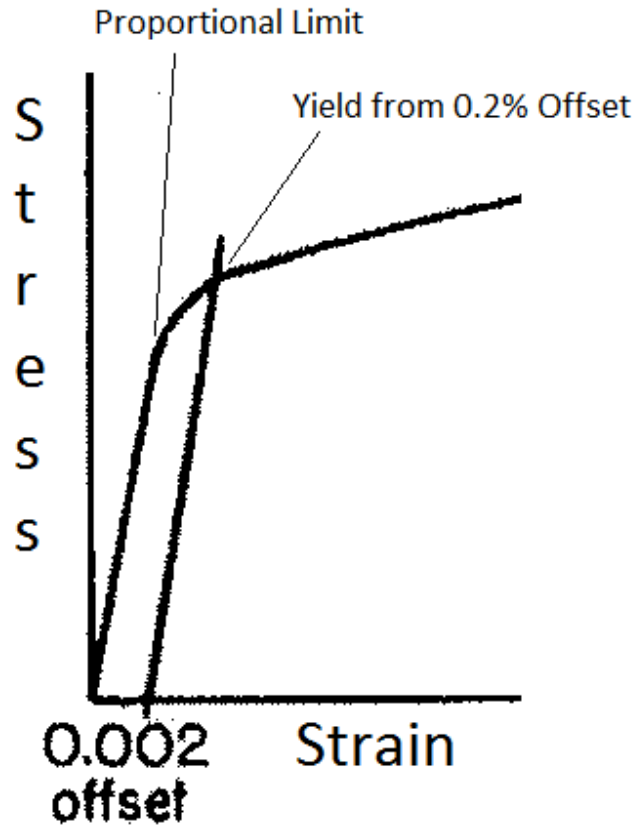

Figure 7.4. Yielding point on typical stress-strain diagram. Proportional limit and yield point determined by 0.25 offset method are described.

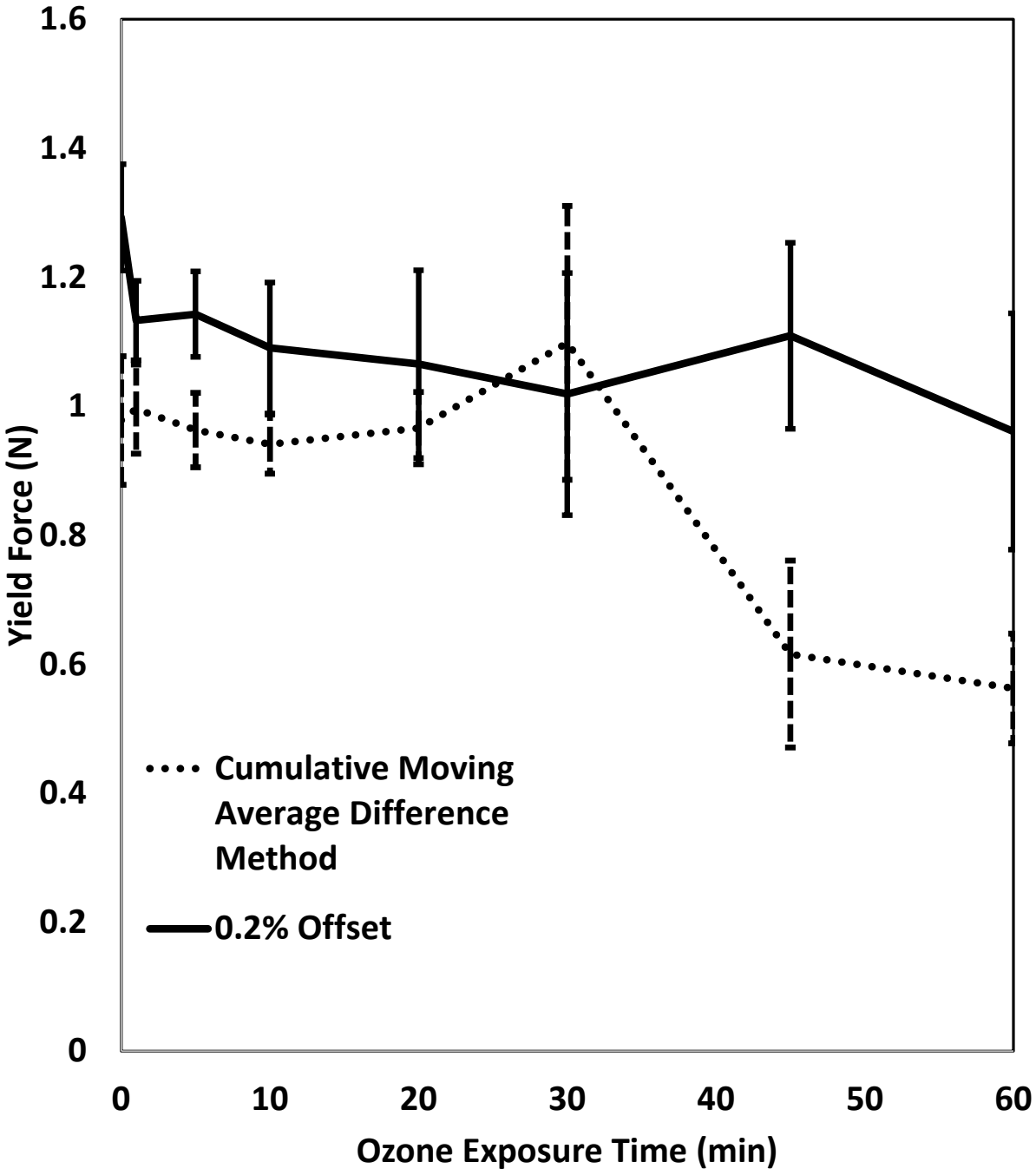

Figure 7.5 Yield point of polypropylene HFMs treated by ozone. Comparison of 0.2% offset and cumulative moving average difference methods.

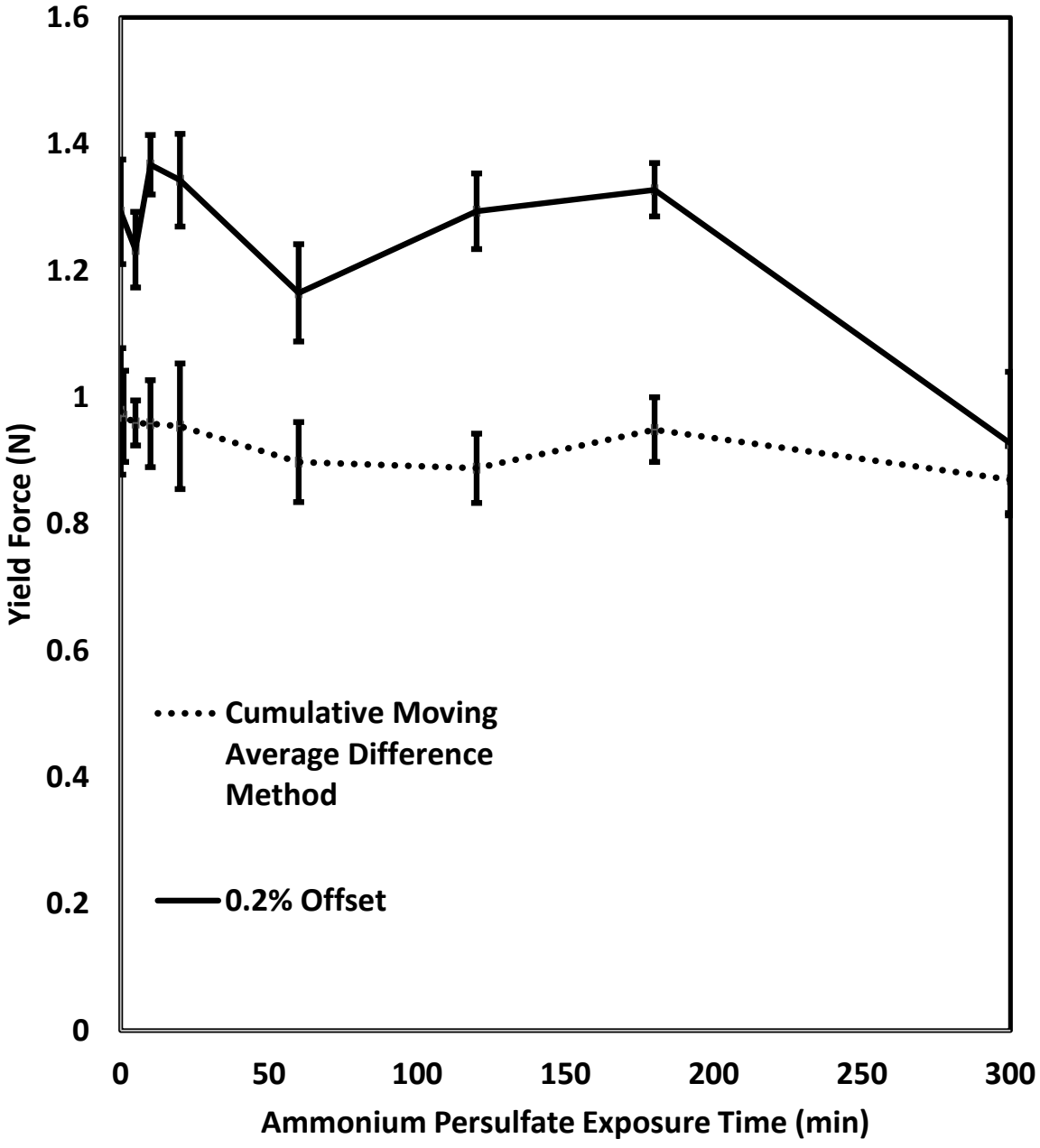

Figure 7.6 Yield point of polypropylene HFMs treated by ammonium persulfate impregnated before immersion in ammonium persulfate. Comparison of 0.2% offset and cumulative moving average difference methods.

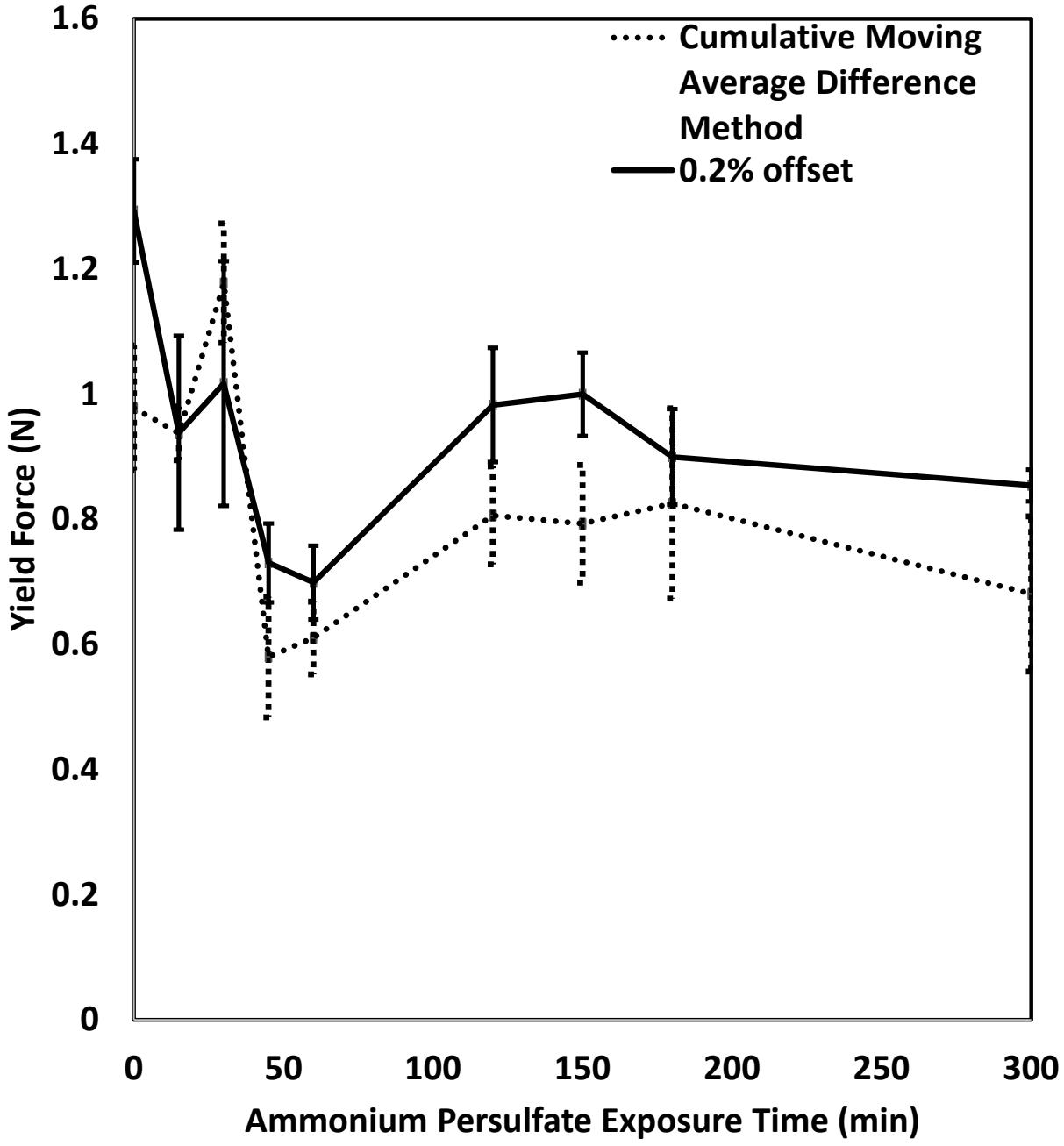

Figure 7.7 Yield point of polypropylene HFMs treated by ammonium persulfate that were dry before immersion. Comparison of 0.2% offset and cumulative moving average difference methods.

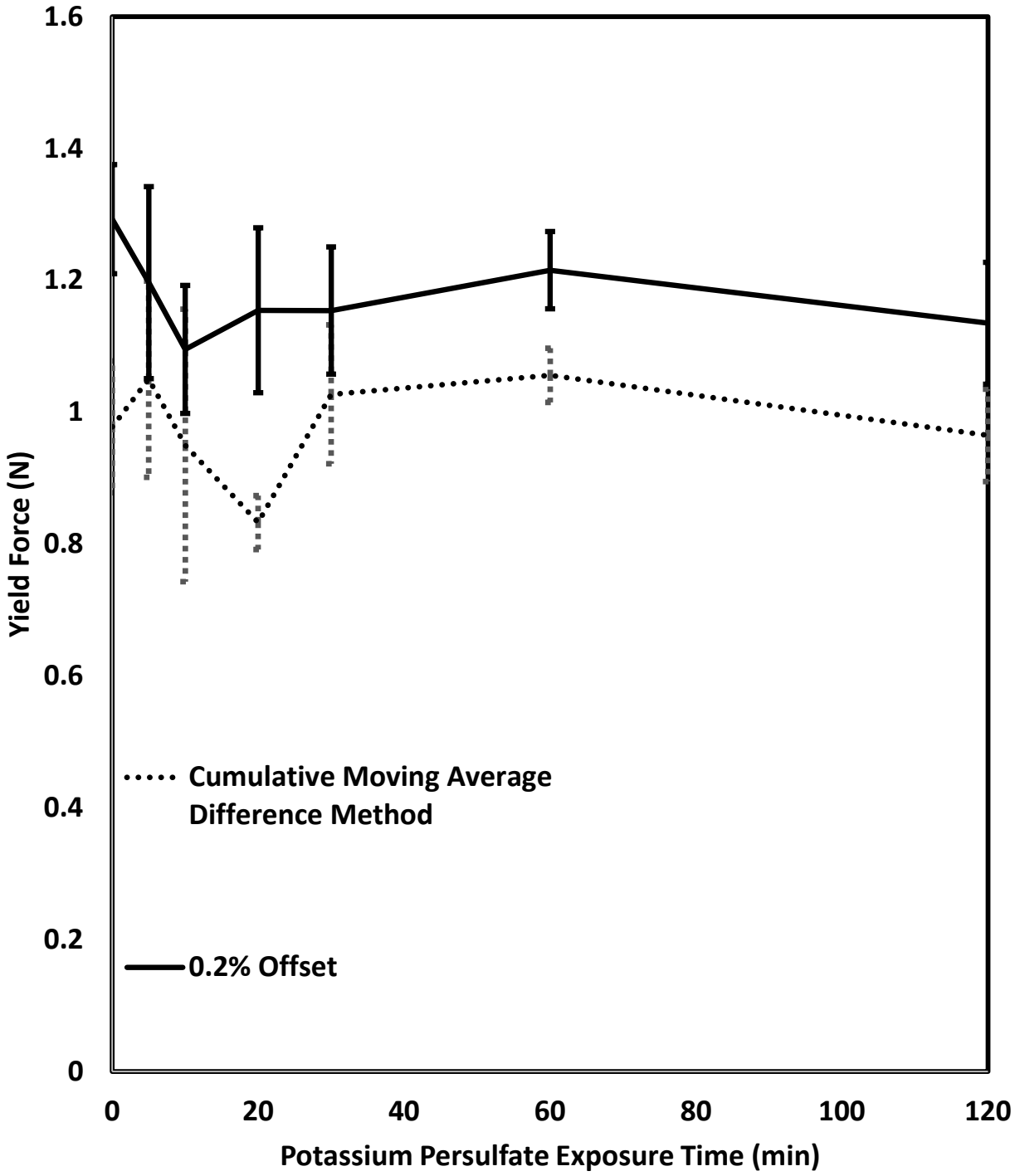

Figure 7.8 Yield point of polypropylene HFMs treated by potassium persulfate that were impregnated before immersion. Comparison of 0.2% offset and cumulative moving average difference methods.

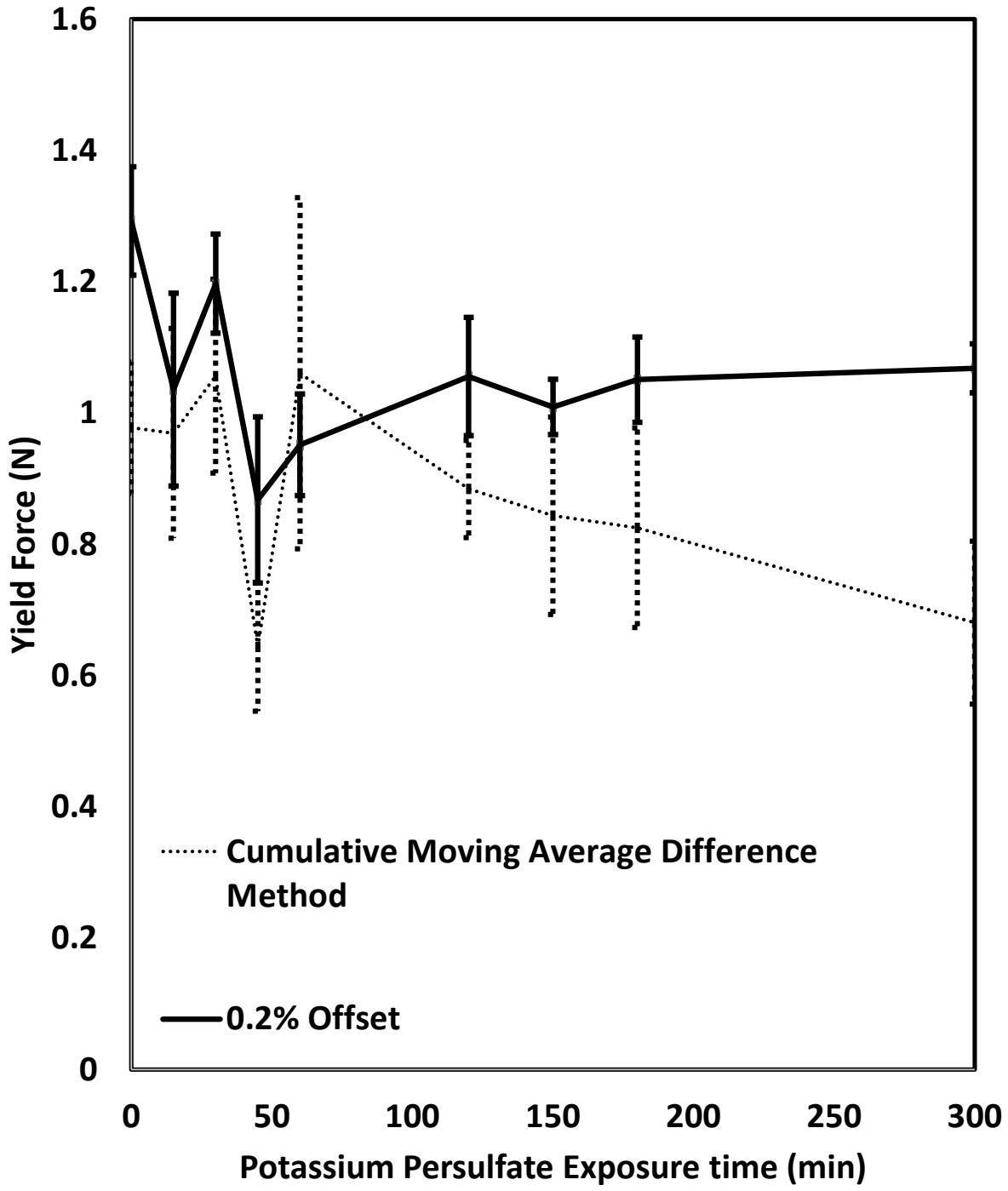

Figure 7.9 Yield point of polypropylene HFMs treated by potassium persulfate that were dry before immersion. Comparison of 0.2% offset and cumulative moving average difference methods.

Table 7.1 Difference in yield point between 0.2% offset and CADM method.

	Average Percent Difference in Modulus at Yield Value Between 0.2% Offset and CADM Method	**Standard Deviation**
Ozone	12.82%	16.29%
APS Immersed	34.63%	20.14%
APS non-immersed	7.93%	10.77%
KPS Immersed	8.44%	4.60%
KPS Non-Immersed	15.45%	17.21%
Average	**15.85%**	**13.80%**

Polypropylene HFM Treatment Type	Percent Difference in Yield Force Between 0.2% Offset and CADM Method using Modulus	Standard Deviation
Ozone	29.33%	30.60%
APS Immersed	37.07%	12.49%
APS non-immersed	15.73%	14.86%
KPS Immersed	20.76%	10.32%
KPS Non-Immersed	17.90%	14.73%
Average	**24.16%**	**16.60%**

Table 7.2. Difference between 0.2% offset method and CADM to determine yield force.

As displayed in table 7.12, the yield force calculated by the 0.2% offset method is typically 24.16% greater than that calculated by the CADM method. The error in this measurement is ±16.60%. This result generally matches the results found in charts 7.6 through 7.10, in which tensile testing data of polypropylene hollow fibers are displayed after various treatments. This corresponds well to theory as shown in figure 7.6. The proportional limit (calculated in the CADM) should always have a yield force and yield strain less than that calculated with the 0.2% offset method.

7.7 Sources of Error in CADM Measurement

In order for data to be analyzed using the CADM it must meet certain general criteria. The data must be smooth and free of significant noise, it must be monotonically increasing in the region of elastic elongation and the shape of the stress-strain or force-elongation line must be linear during the elastic region of deformation. If the data does not meet the first two criteria- smooth and monotonically increasing in the elastic deformation region, data conditioning may be able to make the data fit for CADM analysis. The lack of a linear and strain region of elastic deformation prevents use of the CADM.

7.7.1 Error Due to Significant Noise

The CAD method of determining the yield point finds the point of inflection at which point the linear stress-strain portion of deformation transforms to the non-linear region initiating plastic deformation. The presence of noise which causes the data to not satisfy the condition of monotonically increasing during the elastic region of deformation will cause areas of local minimums to develop. These could potentially be misread as the inflection point denoting the proportional limit.

This situation can be corrected through the use of a smoothing function if significant noise is present. The most straightforward method involves the use of a moving average function. This function replaces the value at a data point with an average of the preceding n and succeeding n points. The optimum value of n for a given set of noisy data is the minimum integer which allows the data to be monotonically increasing.

7.7.2 Error Due to Repeated Sequential Values

As with errors incurred due to the presence of noise, the presence of identical sequential values will cause false identification of the proportional limit due to the condition of monotonically increasing data not being satisfied. These repeated values are due to a data acquisition rate that is too fast in relation to the extension rate. The ideal data acquisition interval is the smallest that allows the data to be monotonically increasing during the elastic region of deformation for a given elongation rate.

As the data acquisition interval increases, the probability of recording repeated, identical values increases. However, fine detail is lost and the accuracy of the yield point measurement may be harmed.

Data acquired with a sufficiently small recording interval to produce repeated identical values may be processed to allow for analysis using CADM. Two such approaches are discussed below

1. Smoothing average: The data at a given point is replaced by the average of the original preceding n and succeeding n points. The integer n is the smallest value which permits removal of the sequential identical data points. If the value of n is too large, fine detail will be lost. If this value is too small, the sequential identical data points may not be removed.
2. Sequential mapping: The entire data set is divided into sequential groups, with each group containing m data points. A new data set is then developed with each successive data point equal to the average of the m data points in each sequential group. The effect of sequential mapping is to produce data that would be similar to that gathered at a slower sampling rate.

The use of data filtering may prevent real time analysis of the data while it is being gathered.

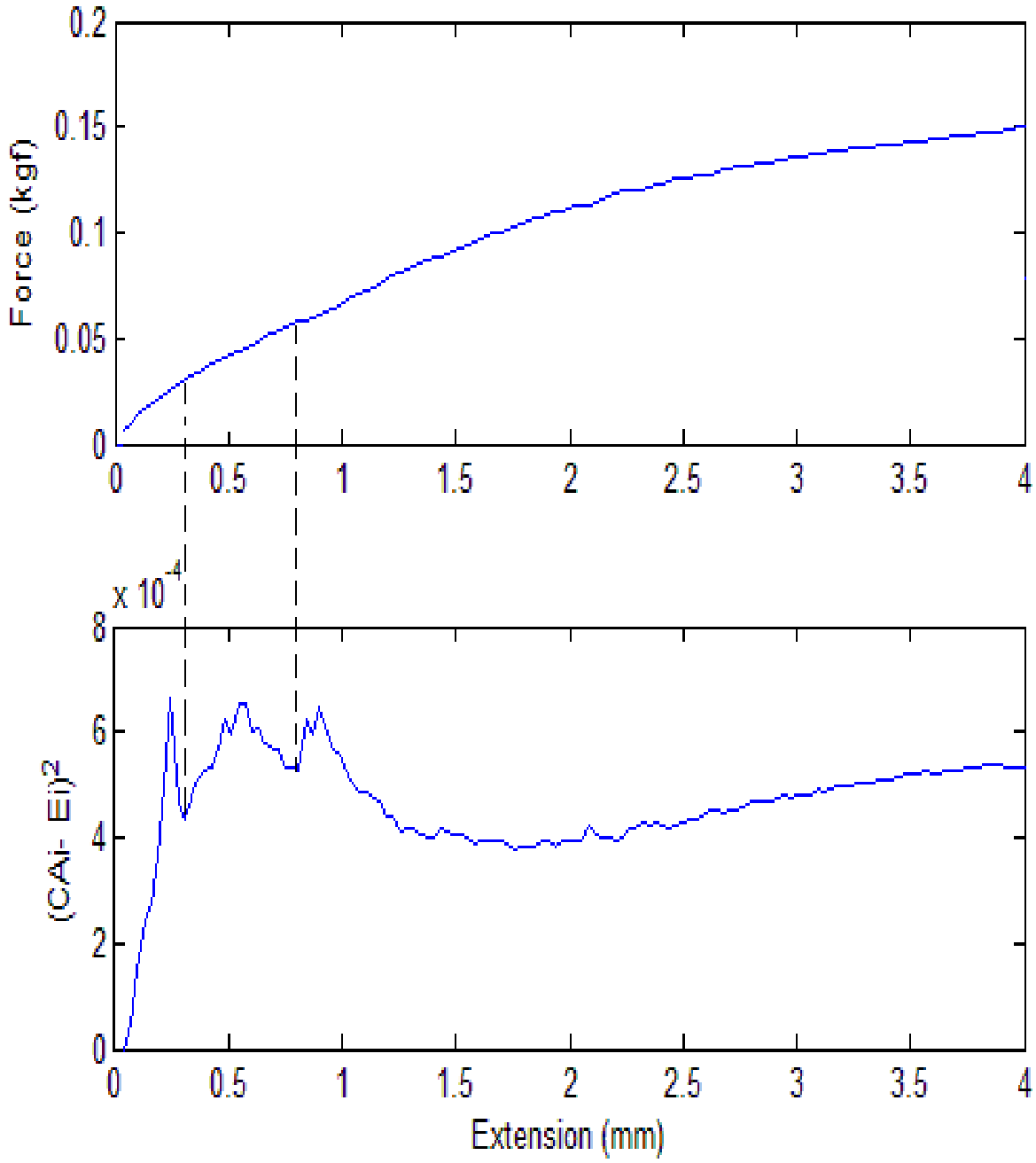

Figure 7.10 (top) Force/extension data for virgin polypropylene HFM. (bottom) Graph of difference between cumulative average of modulus at each point and the modulus at that point. Note local minimum points, denoted by dashed lines corresponding to segments of repeated identical data points.

7.8 Potential Uses of the CAD Method

The CAD method allows for determination of the proportional limit – the point at which further deformation is permanent. As a result, this approach may be applied during real time mechanical tests. Failure of load bearing components is typically defined as that imparting permanent deformation. Therefore, the CAD method would allow for determination of the maximum load that may be applied to a part in a non-destructive manner. The CAD method is able to be easily coded in software and electronic machine controls; thus it may allow for real time testing of the mechanical integrity of every component in a production environment.

The ability of the CAD method to be used in software would allow for the rapid determination of yielding points of the mechanical testing data through computational analysis. The traditional 0.2% offset approach is not easily digitized and requires extensive human intervention, making this process slow and subject to variation between operators.

7.9 Conclusions

The CAD method of determining the proportional limit allows for the rapid determination of the yield point from mechanical testing data. This approach, unlike the 0.2% offset method of determining mechanical yield, is able to be programmed into software easily and eliminates human interaction during the measuring process – preventing variation from different operators. The CAD method allows for fast analysis of the yielding points of tensile testing data in a large amount of data sets.

This method allows for the real time determination of the proportional limit during mechanical testing. As the proportional limit is the point at which further deformation would not be recoverable, the CAD method allows for accurate determination of the maximum load that a component may be subjected to without failure. Typically, the force or load that causes failure in a part is that which causes plastic, non-recoverable deformation. Therefore, the CAD method could easily be incorporated into a manufacturing setting to determine the maximum load that each part or component could endure in a non-destructive manner.

APPENDIX 1 MATLAB PROGRAM TO DETERMINE MEMBRANE PROPERTIES FROM TENSILE TEST DATA

```
%Joseph V. Alexander 21FEB2013
%%Program to analyze tensile testing data acquired from hollow fiber
%%membranes. Each Excel file must be named with the number of minutes
%%elapsed at the point of test.
%%Excel files for each sample must be arranged so that each
%%fiber run is contained in a worksheet that has two columns. The first is
%%the extension data (mm) the second column is the force (kgf). This
%%program will determine the .xls files present, analyze them and present
%%the graphed data for each xls file and the overall data.

%%The yield point will be found by determining the moving average of the
%%modulus during the elastic region of deformation. The yield point is
%%determined when the modules varies more than a predetermined fraction of
%%the moving average.

m=5 %Number of points to include in smoothing average
filename='5 hr.xlsx'
yield_percent_variance=5 %Percent variance of moving average of modulus that
%will be used to determine yield strength.
number_of_initial_points_to_ignore=20
fiber_outer_diameter=360 %Fiber dimensions in microns
fiber_inner_diameter=244
%Insert code to determine the names of files present
original_length=25 %Original fiber length in mm
fiber_outer_diameter_meters=fiber_outer_diameter*(0.000001)
fiber_inner_diameter_meters=fiber_inner_diameter*(0.000001)
```

```
Ao=pi*((fiber_outer_diameter_meters/2)^2-(fiber_inner_diameter_meters/2)^2)

[STATUS,SHEETS] = xlsfinfo(filename)
number_of_samples=length(SHEETS)
combined_mechanical_data=zeros(6,number_of_samples)
for j=1:number_of_samples
   sheet=SHEETS(1,j)
   sheet=char(sheet)
   num=xlsread(filename,sheet)
   extension=num(:,1)
   force=num(:,2)

   number_of_points=length(extension)

   %Determination of modulus

   modulus=(force)./(extension)
  %Forming smoothed average
  number_of_new_points=number_of_points/m
  smoothed_extension=zeros(1,number_of_new_points)
  smoothed_force=zeros(1,number_of_new_points)

  for z=1:(number_of_new_points-1)
     smoothed_extension(z)=mean(extension(m.*z:m.*(z+1)))
     smoothed_force(z)=mean(force(m.*z:m.*(z+1)))
     z=z+1
  end
```

```
 smoothed_modulus=(smoothed_force)./(smoothed_extension)

  %Determination of moving average
  modulus_moving_average=zeros(1,length(smoothed_modulus));

 for k=1:(number_of_new_points);

 modulus_moving_average(1,k)=mean(smoothed_modulus(1,1:k));
 k=k+1;
end

 %Determination of difference in modulus to moving average
 modulus_difference=smoothed_modulus-modulus_moving_average
x=length(modulus_difference);
plot(smoothed_extension, modulus_difference);

%Determination of yeild point by finding smallest difference between
%modulus and cumulative average of modulus.

[C, I]=max(modulus_difference(number_of_initial_points_to_ignore:length(modulus_difference)))
indices_of_min_difference=I+number_of_initial_points_to_ignore

yield_force=smoothed_force(1,indices_of_min_difference)
yield_extension=smoothed_extension(1,indices_of_min_difference)
[Ultimate_force, indices_UTF]=max(force)
max_elongation=extension(indices_UTF,1)

%Computed data is then stored in columns of matrix containing data for all
%samples.
```

```
combined_mechanical_data(1,j)=j
combined_mechanical_data(2,j)=yield_force
combined_mechanical_data(3,j)=yield_extension
combined_mechanical_data(4,j)=yield_force/yeild_extension
combined_mechanical_data(5,j)=Ultimate_force
combined_mechanical_data(6,j)=max_elongation
  j=j+1
end

%Computing average and standard deviation for data collected across all
%samples

sample_wide_statistics=zeros(6,3)
sample_wide_statistics(2,2)=mean(combined_mechanical_data(2,:))
sample_wide_statistics(2,3)=std(combined_mechanical_data(2,:))
sample_wide_statistics(3,2)=mean(combined_mechanical_data(3,:))
sample_wide_statistics(3,3)=std(combined_mechanical_data(3,:))
sample_wide_statistics(4,2)=mean(combined_mechanical_data(4,:))
sample_wide_statistics(4,3)=std(combined_mechanical_data(4,:))
sample_wide_statistics(5,2)=mean(combined_mechanical_data(5,:))
sample_wide_statistics(5,3)=std(combined_mechanical_data(5,:))
sample_wide_statistics(6,2)=mean(combined_mechanical_data(6,:))
sample_wide_statistics(6,3)=std(combined_mechanical_data(6,:))
```

REFERENCES

1. MONTOYA, J.P., et al., *Plasma Leakage through Microporous Membranes: Role of Phospholipids.* ASAIO Journal, 1992. **38**(3): p. M399-M405.
2. Melsrose, D.A., I, *Mechanical Heat-Lung Use In Man.* British Medical Journal 1953. **2**(4827): p. 57-62.
3. Lim, M.W., *The history of extracorporeal oxygenators*.* Anaesthesia, 2006. **61**(10): p. 984-995.
4. Galletti, P. and C. Mora, *Cardiopulmonary Bypass: The Historical Foundation, the Future Promise*, in *Cardiopulmonary Bypass*, C. Mora, et al., Editors. 1995, Springer New York. p. 3-18.
5. Hewitt, R.L., O. Creech, and Jr, *HIstory of the pump oxygenator.* Archives of Surgery, 1966. **93**(4): p. 680-696.
6. JD, H., *Acute Pulmonary Failure: Treatment with Extracorporeal Oxygenation.* Medical Instrumentation, 1977. **11**: p. 198-201.
7. Bartlett, R.H., et al., *Extracorporeal membrane oxygenation (ECMO) cardiopulmonary support in infancy.* Trans Am Soc Artif Intern Organs, 1976. **22**: p. 80-93.
8. Agati, S., et al., *DIDECMO: a new polymethylpentene oxygenator for pediatric extracorporeal membrane oxygenation.* ASAIO J, 2006. **52**(5): p. 509-12.
9. Hoopes, C.W., et al., *Extracorporeal membrane oxygenation as a bridge to pulmonary transplantation.* J Thorac Cardiovasc Surg, 2013. **145**(3): p. 862-7; discussion 867-8.
10. *Registries - Heart/Lung*, 2013, The International Society for Heart Lung Transplantation.
11. Callahan, L.A. and G.S. Supinski, *Hyperglycemia and acquired weakness in critically ill patients: potential mechanisms.* Crit Care, 2009. **13**(2): p. 125.
12. Mendez-Tellez, P.A. and D.M. Needham, *Early physical rehabilitation in the ICU and ventilator liberation.* Respir Care, 2012. **57**(10): p. 1663-9.
13. Krzysztof Matyjaszewski, T.P.D., *HANDBOOK OF RADICAL POLYMERIZATION*. 2002: Wiley Interscience.
14. Matyjaszewski, K., *Atom Transfer Radical Polymerization (ATRP): Current Status and Future Perspectives.* Macromolecules, 2012. **45**(10): p. 4015-4039.
15. Matyjaszewski, K., Tsarevsky, Nicolay V., *Macromolecular Engineering by Atom Transfer Radical Polymerization.* Journal of the American Chemical Society, 2014. **136**(18): p. 6513-6533.
16. Leibfarth, F.A., et al., *External Regulation of Controlled Polymerizations.* Angewandte Chemie International Edition, 2013. **52**(1): p. 199-210.
17. Sankhe, A.Y., S.M. Husson, and S.M. Kilbey, *Effect of Catalyst Deactivation on Polymerization of Electrolytes by Surface-Confined Atom Transfer Radical Polymerization in Aqueous Solutions.* Macromolecules, 2006. **39**(4): p. 1376-1383.
18. Tsujii, Y., et al., *Structure and Properties of High-Density Polymer Brushes Prepared by Surface-Initiated Living Radical Polymerization*, in *Surface-Initiated Polymerization I*, R. Jordan, Editor. 2006, Springer Berlin Heidelberg. p. 1-45.
19. Fischer, H., *The Persistent Radical Effect In "Living" Radical Polymerization.* Macromolecules, 1997. **30**(19): p. 5666-5672.
20. Fischer, H., *The persistent radical effect in controlled radical polymerizations.* Journal of Polymer Science Part A: Polymer Chemistry, 1999. **37**(13): p. 1885-1901.
21. Kim, J.-B., et al., *Kinetics of surface-initiated atom transfer radical polymerization.* Journal of Polymer Science Part A: Polymer Chemistry, 2003. **41**(3): p. 386-394.
22. Balachandra, A.M., G.L. Baker, and M.L. Bruening, *Preparation of composite membranes by atom transfer radical polymerization initiated from a porous support.* Journal of Membrane Science, 2003. **227**(1–2): p. 1-14.

23. Yao, F., et al., *Antibacterial effect of surface-functionalized polypropylene hollow fiber membrane from surface-initiated atom transfer radical polymerization.* Journal of Membrane Science, 2008. **319**(1-2): p. 149-157.
24. Khulbe, K.C., C. Feng, and T. Matsuura, *The art of surface modification of synthetic polymeric membranes.* Journal of Applied Polymer Science, 2010. **115**(2): p. 855-895.
25. Wan, L.-S., Z.-M. Liu, and Z.-K. Xu, *Surface engineering of macroporous polypropylene membranes.* Soft Matter, 2009. **5**(9): p. 1775-1785.
26. Singh, N., et al., *Surface modification of microporous PVDF membranes by ATRP.* Journal of Membrane Science, 2005. **262**(1–2): p. 81-90.
27. Bhut, B.V. and S.M. Husson, *Dramatic performance improvement of weak anion-exchange membranes for chromatographic bioseparations.* Journal of Membrane Science, 2009. **337**(1–2): p. 215-223.
28. Zhang, Y., et al., *A novel method to immobilize collagen on polypropylene film as substrate for hepatocyte culture.* Materials Science and Engineering: C, 2006. **26**(4): p. 657-663.
29. Kuhn, H. and D. Medlin, *ASM Handbook, Volume 08 - Mechanical Testing and Evaluation*, ASM International.
30. Bamford, C.H. and K.G. Al-Lamee, *Studies in polymer surface functionalization and grafting for biomedical and other applications.* Polymer, 1994. **35**(13): p. 2844-2852.
31. Clement H. Bamford, K.G.A.-L., *Polymer Surface Functionalisation and grafting by a simple and inexpensive method.* Macromolecular Rapid Communications, 1994. **15**: p. 379-384.
32. Schneider, K. and T.J. van Gassel, *Membrandestillation.* Chemie Ingenieur Technik, 1984. **56**(7): p. 514-521.
33. Bamford, C.H. and K.G. Al-Lamee, *Studies in polymer surface modification and grafting for biomedical uses: 2. Application to arterial blood filters and oxygenators.* Polymer, 1996. **37**(22): p. 4885-4889.
34. Aurther J. Kidnay, W.R.P., *Fundamentals of Natural Gas Processing*. 2006: CRC Press.
35. Wandera, D., S.R. Wickramasinghe, and S.M. Husson, *Stimuli-responsive membranes.* Journal of Membrane Science, 2010. **357**(1–2): p. 6-35.
36. Bhardwaj, V., et al., *Polysulfone Hollow Fiber Gas Separation Membranes Filled with Submicron Particles.* Annals of the New York Academy of Sciences, 2003. **984**(1): p. 318-328.
37. Amornsakchai, T., N. Liewcharoen, and P. Phinyocheep, *Surface modification of low density polyethylene using accelerated decomposition of potassium persulfate and ceric ion induced acrylamide grafting.* Journal of Materials Science Letters, 2002. **21**(13): p. 1035-1038.
38. Eash, H.J., et al., *Evaluation of Plasma Resistant Hollow Fiber Membranes For Artificial Lungs.* ASAIO Journal, 2004. **50**(5): p. 491-497 10.1097/01.MAT.0000138078.04558.FE.
39. Kang, G.-d. and Y.-m. Cao, *Application and modification of poly(vinylidene fluoride) (PVDF) membranes - A review.* J. Membr. Sci., 2014. **463**: p. 145-165.
40. Lau, W.J., et al., *A recent progress in thin film composite membrane: A review.* Desalination, 2012. **287**: p. 190-199.
41. Rana, D. and T. Matsuura, *Surface Modifications for Antifouling Membranes.* Chem. Rev. (Washington, DC, U. S.), 2010. **110**(4): p. 2448-2471.
42. Khulbe, K.C., C. Feng, and T. Matsuura, *The art of surface modification of synthetic polymeric membranes.* J. Appl. Polym. Sci., 2010. **115**(2): p. 855-895.
43. Lloyd, D.R., K.E. Kinzer, and H.S. Tseng, *Microporous membrane formation via thermally induced phase separation. I. Solid-liquid phase separation.* J. Membr. Sci., 1990. **52**(3): p. 239-61.
44. Matsuyama, H., M.-m. Kim, and D.R. Lloyd, *Effect of extraction and drying on the structure of microporous polyethylene membranes prepared via thermally induced phase separation.* Journal of Membrane Science, 2002. **204**(1–2): p. 413-419.

45. Kim, J.-J., et al., *Operation parameters of melt spinning of polypropylene hollow fiber membranes.* Journal of Membrane Science, 1995. **108**(1–2): p. 25-36.
46. Cury-Boaventura, M.F., C. Pompeia, and R. Curi, *Comparative toxicity of oleic acid and linoleic acid on Jurkat cells.* Clin. Nutr., 2004. **23**(4): p. 721-732.
47. Cury-Boaventura, M.F., et al., *Comparative toxicity of oleic and linoleic acid on human lymphocytes.* Life Sci., 2006. **78**(13): p. 1448-1456.
48. Jaselskis, B., N.L. Stemm, and W.D. Johnston, *Determination of the fatty-acid composition of soybean oil by high-pressure liquid chromatography.* Talanta, 1982. **29**(1): p. 54-56.
49. Herslöf, B. and G. Kindmark, *HPLC of triglycerides with gradient elution and mass detection.* Lipids, 1985. **20**(11): p. 783-790.
50. Yao, F., et al., *Antibacterial effect of surface-functionalized polypropylene hollow fiber membrane from surface-initiated atom transfer radical polymerization.* J. Membr. Sci., 2008. **319**(1+2): p. 149-157.
51. ASTM, *Standard test method for maximum pore diameter and permeability of rigid porous filters for laboratory use*, 2011.
52. Grulke, E.A., *Solubility parameter values*, in *Polymer Handbook*, E.I. J. Brandrupt, and E. Grulke, Editor. 2000, John Wiley: New York. p. VII/519-560.
53. Jaselskis, B., N.L. Stemm, and W.D. Johnston, *Determination of the fatty acid composition of soybean oil by high-pressure liquid chromatography.* Talanta, 1982. **29**(1): p. 54-6.
54. Feng, R., et al., *Highly effective antifouling performance of N-vinyl-2-pyrrolidone modified polypropylene non-woven fabric membranes by ATRP method.* Journal of Membrane Science, 2011. **369**(1–2): p. 233-242.
55. Li, L., G. Yan, and J. Wu, *Modification of polysulfone membranes via surface-initiated atom transfer radical polymerization and their antifouling properties.* Journal of Applied Polymer Science, 2009. **111**(4): p. 1942-1946.
56. Liu, F., et al., *Preparation of hydrophilic and fouling resistant poly(vinylidene fluoride) hollow fiber membranes.* Journal of Membrane Science, 2009. **345**(1–2): p. 331-339.
57. Kim, D.-G., et al., *Dual Effective Organic/Inorganic Hybrid Star-Shaped Polymer Coatings on Ultrafiltration Membrane for Bio- and Oil-Fouling Resistance.* ACS Applied Materials & Interfaces, 2012. **4**(11): p. 5898-5906.
58. Li, C.Y., et al., *Preparation of pH-sensitive membranes via dopamine-initiated atom transfer radical polymerization.* Journal of Membrane Science, 2011. **367**(1–2): p. 7-13.
59. Yue, W.-W., et al., *Grafting of zwitterion from polysulfone membrane via surface-initiated ATRP with enhanced antifouling property and biocompatibility.* Journal of Membrane Science, 2013. **446**(0): p. 79-91.
60. Yuan, B., et al., *Copolymer Coatings Consisting of 2-Methacryloyloxyethyl Phosphorylcholine and 3-Methacryloxypropyl Trimethoxysilane via ATRP To Improve Cellulose Biocompatibility.* ACS Applied Materials & Interfaces, 2012. **4**(8): p. 4031-4039.
61. Jain, P., et al., *Completely Aqueous Procedure for the Growth of Polymer Brushes on Polymeric Substrates.* Langmuir, 2007. **23**(23): p. 11360-11365.
62. Bhattacharya, A. and B.N. Misra, *Grafting: a versatile means to modify polymers: Techniques, factors and applications.* Progress in Polymer Science, 2004. **29**(8): p. 767-814.
63. Neyens, E. and J. Baeyens, *A review of classic Fenton's peroxidation as an advanced oxidation technique.* Journal of Hazardous Materials, 2003. **98**(1–3): p. 33-50.
64. Gatenholm, P., T. Ashida, and A.S. Hoffman, *Hybrid biomaterials prepared by ozone-induced polymerization. I. Ozonation of microporous polypropylene.* Journal of Polymer Science Part A: Polymer Chemistry, 1997. **35**(8): p. 1461-1467.

65. Wang, Y., et al., *Hydrophilic modification of polypropylene microfiltration membranes by ozone-induced graft polymerization.* Journal of Membrane Science, 2000. **169**(2): p. 269-276.
66. Alexander, J.V., J.W. Neely, and E.A. Grulke, *Effect of chemical functionalization on the mechanical properties of polypropylene hollow fiber membranes.* Journal of Polymer Science Part B: Polymer Physics, 2014. **52**(20): p. 1366-1373.
67. Grunwald, E. and S. Winstein, *Kinetics and Mechanism of the Reaction of Hydrogen Bromide with Ethanol.* Journal of the American Chemical Society, 1947. **69**(8): p. 2051-2053.
68. Kamm, O. and C.S. Marvel, *ORGANIC CHEMICAL REAGENTS. V.1 THE PREPARATION OF ALKYL AND ALKYLENE BROMIDES.* Journal of the American Chemical Society, 1920. **42**(2): p. 299-309.
69. Skakun, S.A., I.G. Tribrat, and M.I. Vinnik, *Kinetics and mechanism of the hydrobromination of propyl alcohol by HBr in aqueous H2SO4 solution.* Bulletin of the Academy of Sciences of the USSR, Division of chemical science, 1982. **31**(11): p. 2148-2154.
70. Xu, D., et al., *Functionalization of hydrogen-terminated silicon via surface-initiated atom-transfer radical polymerization and derivatization of the polymer brushes.* Journal of Colloid and Interface Science, 2004. **279**(1): p. 78-87.
71. *Pore Size Characteristics of Membrane Filters by Bubble Point and Mean Flow Pore Test*, 2011.
72. Lloyd, D.R., K.E. Kinzer, and H.S. Tseng, *Microporous membrane formation via thermally induced phase separation. I. Solid-liquid phase separation.* Journal of Membrane Science, 1990. **52**(3): p. 239-261.
73. Kim, J.-J., et al., *Structural study of microporous polypropylene hollow fiber membranes made by the melt-spinning and cold-stretching method.* Journal of Membrane Science, 1994. **93**(3): p. 209-215.
74. Sullivan, D.M. and M.L. Bruening, *Ultrathin, Gas-Selective Polyimide Membranes Prepared from Multilayer Polyelectrolyte Films.* Chemistry of Materials, 2002. **15**(1): p. 281-287.
75. Nagale, M., B.Y. Kim, and M.L. Bruening, *Ultrathin, Hyperbranched Poly(acrylic acid) Membranes on Porous Alumina Supports.* Journal of the American Chemical Society, 2000. **122**(47): p. 11670-11678.
76. W. Armarego , C.C., *Purification of Laboratory Chemicals, Seventh Edition*. 2012: Butterworth-Heinemann.
77. Li, D., R. Wang, and T.-S. Chung, *Fabrication of lab-scale hollow fiber membrane modules with high packing density.* Separation and Purification Technology, 2004. **40**(1): p. 15-30.
78. Max M. Strumia, A.B., John McGraw, Margaret Dolan, and Louise Colwell, *An Acid Citrate-Dextose Solution with Low Water Volume and Low Dextrose Concentration.* Journal of clinical Investigation, 1947. **26**(4): p. 678-686.
79. Services, U.S.D.o.H.a.H., *Guidance for Cardiopulmonary Bypass Oxygenators 510(k) Submissions; Final Guidance for Industry and FDA Staff*, F.a.D. Administration, Editor 2000.
80. Wickramasinghe, S.R. and B. Han, *Designing Microporous Hollow Fibre Blood Oxygenators.* Chemical Engineering Research and Design, 2005. **83**(3): p. 256-267.
81. Malek, A., K. Li, and W.K. Teo, *Modeling of Microporous Hollow Fiber Membrane Modules Operated under Partially Wetted Conditions.* Industrial & Engineering Chemistry Research, 1997. **36**(3): p. 784-793.
82. Litt, M., *Gas-liquid reactions, P. V. Danckwerts, McGraw-Hill Book Co., New York (1970). 276 pages.* AIChE Journal, 1971. **17**(2): p. 509-510.
83. M. Ertan Taskin, K.H.F., Tao Zhang, Bartley P. Griffith, and Zhongjun J. Wu, *Micro-scale Modeling of Flow and Oxygen Transfer in Hollow Fiber Membrane Bundle.* Journal of Membrane Science, 2010. **15**(362): p. 172-183.
84. Wickramasinghe, S.R., et al., *Designing Blood Oxygenators.* Annals of the New York Academy of Sciences, 2003. **984**(1): p. 502-514.

85. Wickramasinghe, S.R., M.J. Semmens, and E.L. Cussler, *Mass transfer in various hollow fiber geometries.* Journal of Membrane Science, 1992. **69**(3): p. 235-250.
86. Kuhn, H.A., *Overview of Mechanical Properties and Testing for Design*, in *ASME Handbook Volume 8: Mechanical Testing and Evaluation*. 1990.

VITA

Name	Joseph Victor Alexander
Bachelor of Science in Mechanical Engineering	University of Kentucky, 2008
Bachelor of Science in Materials Science and Engineering	University of Kentucky, 2008
Certification in Nanotechnology	University of Kentucky, 2008

Peer Reviewed Journal Publications (Ph.D. Work)

1. 'Effect of Chemical Functionalization on the Mechanical Properties of Polypropylene Hollow Fiber Membranes', *Joseph V. Alexander*, James W. Neely, Eric A. Grulke, Under Review, Thin Solid Films